REPUBLIQUE ALGERIENNE DEMOCRATIQUE ET POPULAIRE
MINISTERE DE L'ENSEIGNEMENT SUPERIEUR ET DE LA RECHERCHE SCIENTIFIQUE
UNIVERSITE ECHAHID HAMMA LAKHDAR D'EL OUED

Faculté de la Technologie

Laboratoire de Valorisation des Technologies des Ressources Sahariennes (VTRS)

Thèse de Doctorat

Présentée par :

TOUMI Djaafar

En vue de l'obtention du diplôme de **DOCTORAT LMD** en **:**

Option : Réseaux électriques

Optimisation d'un système photovoltaïque adapté par une commande MPPT basée sur les algorithmes intelligents

Soutenue le …./ …./ ……., devant le jury composé de :

MED TOUFIK Ben Chouia	*Professeur*	*Université de Biskra*	*Président*
DJILANI Ben Attous	*Professeur*	*Université d'El-Oued*	*Rapporteur*
YACINE Labbi	*MCA*	*Université d'El-Oued*	*Co- Rapporteur*
BOUALAGA RABHI	*Professeur*	*Université de Biskra*	*Examinateur*
ZELOUMA LAID	*Professeur*	*Université d'El-Oued*	*Examinateur*
HICHAM Serhoud	*MCA*	*Université d'El-Oued*	*Examinateur*

Année Universitaire 2022/2023

Acknowledgment

First of all I would like to introduce my greatly indebted in my work and success to my Merciful GOD who supported me with patience and strength to complete this thesis.

Cordial thanks and deep gratitude are offered to my ***PROF. DR. Djiliani Benattous****, Professor in Faculty of Engineering, University of El-Oued, for his valuable guidance and supervision.*

I would also like to give my sincere gratitude to ***DR. Yacine Labbi****, PhD in Faculty of Engineering, University of El-Oued, for her support and encouragement.*

Special appreciation goes to ***DR. Ahmed Ibrahim****, Post-doctoral Research at Zagazig University of Egypt , for his constant support, his invaluable help, and his constructive comments and suggestions.*

Special thanks to staff members and instructors of my department for their exerted efforts to facilitate the difficulties during the work.

I thank all members of the jury who agree to judge my work and for the interest they have shown in this last.

Thanks to my parents for always loving and supporting me and for giving me all I needed to do this work.

To my family, ***my only love****, "You are my reason for living; you are the source of all my happiness. I love you with all my heart."*

Djaafar Toumi

Dedication

I dedicate this work to

My mother and my father

My sisters and my brothers

My teachers and my friends

And all my family

Djaafar Toumi

ABSTRACT

Solar PV systems are considered in this study and exhibited cost-effectiveness and better efficiency. For controlling the photovoltaic power, DC-DC buck converter has utilized in this thesis. Further, the Maximum Power Point Tracking (MPPT) mechanism is used in order to attain maximum efficiency. The main energy characteristics are analyzed and the mathematical models of the components of an autonomous PV system are developed to study the modes of tracking the MPP. The necessary conditions for matching the parameters of the PV and the DC-DC buck converter are evaluated to track the MPP.

This thesis aims to create an original method and algorithm for calculating and selecting parameters of the main elements of a PV stations. The optimal value of the sampling time of the MPP controller is obtained for different schemes of the PV system. This research aims to increase the efficiency of the PV system by applying the improved particle swarm optimization (IPSO), perturb and observe (P&O), and incremental conductance algorithm in different cases of the operations.

The simulation of dynamic modes of an autonomous photovoltaic (PV) station is performed in the MATLAB/SIMULINK software package. The simulation results of dynamic operations of the PV system show that the voltage converter and the MPP controller with the selected parameters according to the proposed method provide reliable and effective tracking of the MPP in all different connections of the PV systems.

Keywords: Fuzzy logic contro, lMATLAB/Simulink, Maximum power point tracking, Perturb and observe, Photovoltaic array, DC–DC buck converter sampling time

Résumé

Les systèmes solaires photovoltaïques sont pris en compte dans cette étude et ont présenté une rentabilité et une meilleure efficacité. Pour contrôler la puissance photovoltaïque, un convertisseur abaisseur DC-DC a été utilisé dans cette thèse. De plus, le mécanisme de suivi du point de puissance maximale (MPPT) est utilisé afin d'atteindre une efficacité maximale. Les principales caractéristiques énergétiques sont analysées et les modèles mathématiques des composants d'un système PV autonome sont développés, Nous avons étudier les modes de suivi du MPP les conditions nécessaires pour faire répondre les paramètres du PV et du convertisseur abaisseur DC-DC .

Cette thèse vise à créer une méthode et un algorithme originaux de calcul et de sélection des paramètres des principaux éléments d'une n système PV. La valeur optimale du temps d'échantillonnage du contrôleur MPP est obtenue pour différents schémas du système PV. As vise également à augmenter l'efficacité du système PV en appliquant l'algorithme l'optimisation par l'essaim de particules (IPSO), la perturbation et l'observation (P&O) et l'algorithme d'Incrément de conductance dans différences conditions de fonctionnement.

La simulation du système photovoltaïque autonome est effectuée dans l'environnement MATLAB/SIMULINK. Les résultats de simulation et opérations dynamiques du système PV montrent que le convertisseur de tension et le contrôleur MPP avec les paramètres sélectionnés selon la méthode proposée fournissent un suivi fiable et efficace du MPP dans tous les différents comportements dynamiques des systèmes photovoltaïques.

Mots clés: Contrôle de logique floue, lMATLAB/Simulink, suivi du point de puissance maximale, perturbation et observation, photovoltaïque, convertisseur abaisseur, temps d'échantillonnage

الـملخص

في هذه الدراسة تم النظر في أنظمة الطاقة الشمسية الكهروضوئية والتي أظهرت فعالية من حيث التكلفة وكفاءة أفضل. للتحكم في الطاقة الكهروضوئية، تم استخدام محول باك **DC-DC** . علاوة على ذلك يتم استخدام آلية تتبع نقطة الطاقة القصوى **(MPPT)** من أجل تحقيق أقصى قدر من الكفاءة ، ويتم تحليل خصائص الطاقة الرئيسية وتطوير النماذج الرياضية لمكونات النظام الكهروضوئي المستقل لدراسة طرق تتبع نقطة الاستطاعة العظمى **(MPP)** . يتم تقييم الشروط اللازمة لمطابقة معلمات **PV** و محول باك **DC-DC** لتحديد و تتبع نقطة الطاقة القصوى **(MPP)** .

تهدف هذه الأطروحة إلى إنشاء طريقة وخوارزمية أصلية لحساب واختيار معلمات العناصر الرئيسية لمحطات الكهروضوئية. يتم الحصول على القيمة المثلى لوقت أخذ العينات لوحدة التحكم **MPP** لمخططات مختلفة من نظام .**PV** كما يهدف أيضًا إلى زيادة كفاءة النظام الكهروضوئي من خلال تطبيق تحسين سرب الجسيمات **(IPSO)** والاضطراب والمراقبة **(P&O)** وخوارزمية التوصيل الإضافي **(InC)** في حالات مختلفة من العمليات. يتم إجراء محاكاة للأنماط الديناميكية لمحطة كهروضوئية مستقلة **(PV)** في حزمة برامج.**MATLAB / SIMULINK**

تظهر نتائج محاكاة العمليات الديناميكية للنظام الكهروضوئي أن محول الجهد ووحدة التحكم **MPP** مع المعلمات المحددة وفقًا للطريقة المقترحة توفر تتبعًا موثوقًا وفعالًا لـ**MPP** في جميع التوصيلات المختلفة للأنظمة الكهروضوئية

الـكـلـمـات الـمـفـتـاحية : محطات كهروضوئية ، **DC – DC** محول باك، ماتلاب / سيمولينك ، وقت الحصول على العينات، التحكم المنطقي الضبابي **(FLC)** ، تتبع الحد الأقصى لنقطة الطاقة **(MPPT)** ، القلق والمراقبة **(P&O)** ، المصفوفة الكهروضوئية **(PV)**

Contents

Chapter (3) Methodology

Chapter (4) Data Analysis

Chapter (5) Results And Discussion

Chapter (6) Conclusions

List Of Figures

List Of Tables

List Of Symbols

N	Number of particles
W	The inertia weight
v_i	The velocity of each particle
x_i	Position of each particle
k_{max}	The maximum iteration times
d	Duty cycle
c_1 ,c_2	The acceleration factor
L	inductance
c	capacitance
R	Load resistance
η	Tracking Efficiency
p_o	The output power of the PV panel
Pmax	The value of the maximum real power
T	Temperature
G	The solar irradiance
f	The switching frequency
t_s	Sampling time
V	Tracked voltage
I	Tracked current

List Of Abbreviations

IPSO	Improved particle swarm optimization
IC	Incremental conductance
PV	Photovoltaic
PSC	Partial shading conditions
MPP	Maximum power point
MPPT	Maximum power point tracking
GMPP	Global maximum power point
CFPSO	Constriction factor particle swarm optimization
PO	Perturb and observe
GA	Genetic algorithm
ANN	Artificial neural network
PSO	Particle swarm optimization
FLC	Fuzzy Logic

Chapter (1)

Introduction

1.1 Introduction

The increasing demand for energy around the globe and the predicted end of resources of energy has emphasized on the need for renewable energy resources. Despite the abundant resources of renewable energy present in nature, over 80% of the world's energy needs are satisfied by fossil fuels such as petroleum and gas, which has long-term effects in the form of greenhouse effect [1] [2] [4].

Solar energy is the energy derived from the sun through the form of solar radiation. Solar powered electrical generation relies on Photovoltaic (PV).

The major challenge when using PV energy is its strong dependence upon the weather conditions. In addition, it is more difficult to extract the extrem power point (MPP) from its nonlinear characteristics (i.e., power-voltage (P-V) characteristics) [3]. To solve these problems, numerous of maximum power point tracking (MPPT) techniques have been proposed to catch the optimal operating point of the PV power generation system.

1.2 Aim of the work

This thesis is aimed to perform the MPPT process in the PV system combined with the buck converter using the proposed novel improved particle swarm optimization (IPSO). And using fuzzy logic control with the boost converter. The purpose of the research was to develop a methodology for selecting the parameters of the main components of an autonomous PV, providing the most efficient conversion of solar energy. To test and verify the results obtained, simulation modeling of the dynamic regimes of the PV was used in the MATLAB / Simulink® software package. Furthermore, a comprehensive assessment is carried out against the conventional incremental conductance algorithm (IC) and perturb and observe (P&O) algorithm in MATLAB/Simulink. To select the optimal sampling time for the digital MPPT; providing their maximum performance has been determined based on a new methodology. To validate the efficiency of the proposed methodology by comparing it with the classical methods in terms of, tracking accuracy, tracking speed, peak power, tracked power and efficiency.

1.3 Motivation of the work

The huge potential and widespread availability of solar energy determine the good prospects for the use of PV plants in our world, especially in the micro generation sector [5] [7], which is strongly stimulated by the measures taken by the state support. The major challenge when using PV energy is its strong dependence upon the weather conditions [6]. In addition, it is more difficult to extract the maximum power point from its nonlinear characteristics (i.e., power-voltage (P-V) characteristics). To solve these problems, numerous of maximum power point tracking techniques have been proposed to catch the optimal operating point of the PV power generation system. A variety of conventional techniques such as P&O, IC , constant voltage and some others have been introduced to extract the MPP of the solar array under uniform solar irradiance of the PV system. For autonomous PV system, the solution to this problem is complicated by the fact that they can significantly vary in topology, types of DC-DC converters and the uses of MPPT controllers[8] [10]. Moreover, the well-known methods for selecting the parameters of DC-DC converters with the subsequent synthesis of control systems [2] [3], which are widely used in the design of traditional power sources, are unacceptable for solving this problem. Recently, a large number of scientific works devoted to the development and study of new evolutionary algorithms for searching for MPP PV have been published annually in scientific periodicals, which confirms the high relevance of this problem for PV[11] [13].

1.4 Scientific background

PV system has received a great attention as it appears to be one of the most promising renewable energy sources. Photovoltaic power generation has an important role to play due to the fact that it is a green source [9]. The only emissions associated with PV power generation are those from the production of its components [12]. PV generation of power is caused by electromagnetic radiation separating positive and negative charge carriers in absorbing material. If an electric field is present, these charges can produce a current for use in an external circuit. Such fields exist permanently at junctions in PV cells as ‘built-in’ electrostatic fields and provide the electromotive force for useful power production [2]. In cases for which large amounts of energy are required, multiple solar panels will be placed in long connected series called solar farms that span several acres. Solar panels can also be assembled on tops of roofs

to provide power for individual homes. The advantages of the PV solar energy can be summarized as follows:

- No noise, no moving parts, no emissions and no use of fuels and water,
- Minimal maintenance requirements,
- PV operates even in cloudy weather conditions,

However the main drawback of the PV solar energy is high initial costs that overshadow the low maintenance costs [13] [14]. The development for improving the efficiency of the PV system is still a challenging field of research [15]. Unfortunately, PV power generation circuits have two major problems: the conversion efficiency of electric power generation is low, especially under low irradiation conditions, and the amount of electric power generated by solar arrays changes continuously with weather conditions [4]. In general, there is unique point on the I-V or P-V curve that is called the MPP, at which the entire PV module operates with maximum efficiency and produces its maximum power

1.5 Thesis Outline

The general outline of this thesis is as follows. Chapter 1 treats the introduction, the aim of this research and the motivation of this work within literature in the same field. Chapter 2 focuses on the literature review and key prior findings necessary for conducting the methodological framework in this study. Chapter 3 outlines the used methodology with regard to the modeling procedure. The focus lies on the determination of the input variables required for the modeling procedure and its individual steps. Chapter 5 discusses the results, approximations within the chosen methodology and the implications of the results. Chapter 6 of this work delivers the research conclusions. Finally mentions the key recommendations for future research.

References

[1] Boyle, G. (ed.) (2004, 2nd edn), “Renewable Energy", Oxford University Press.

[2] John Twidell and Tony Weir, “Renewable Energy Resources”, Taylor & Francis Second edition published 2006.

[3] Demirbas, A., "Political, economic and environmental impacts of biofuels: A review", Applied Energy, Vol. 86, 2009, pp. 108-117.

[4] R. Faranda, S. Leva, “Energy Comparison of MPPT techniques for PV Systems”, WSEAS Transactions on Power Systems, Vol. 3, Issue 6, 2008, pp. 446-455.

[5] U. Yilmaz, Ali Kircay, S. Borekci, “PV system fuzzy logic MPPT method and PI control as a charge controller,” Renewable and Sustainable Energy Reviews, vol. 81, pp 994–1001, 2018.

[6] H. M. Abd Alhussain, N. Yasin, “Modeling and simulation of solar PV module for comparison of two MPPT algorithms (P&O & INC) in MATLAB/Simulink,’’ Indonesian Journal of Electrical Engineering and Computer Science (IJEECS), vol. 18, 2020.

[7] G. A. Madrigal, K. G. Cuevas, V. Hora, K. M. Jimenez, J. N. Manato, M. J. Porlaje, B. Fortaleza, “Fuzzy logic-based maximum power point tracking solar battery charge controller with backup stand-by AC generator,” Indonesian Journal of Electrical Engineering and Computer Science (IJEECS), vol. 16, pp.136–146, 2019.

[8] M. Kermadi, and El M. Berkouk, “Artificial intelligence-based Maximum Power Point Tracking Controllers for Photovoltaic Systems: Comparative study,” Renewable and Sustainable Energy Reviews, vol. 69, pp. 369-386, 2017.

[9] T. Esram and P. L. Chapman, “Comparison of Photovoltaic Array Maximum Power Point Tracking Techniques,” in IEEE Transactions on Energy Conversion, vol. 22, no. 2, pp. 439-449, 2007. doi: 10.1109/TEC.2006.874230.

[10] B. Tarek, D. Said and M. E. H. Benbouzid, “Maximum Power Point Tracking Control for Photovoltaic System Using Adaptive Neuro- Fuzzy “ANFIS”,” 2013 Eighth International Conference and Exhibition on Ecological Vehicles and Renewable Energies (EVER), Monte Carlo, pp. 1 -7, 2013. doi: 10.1109/EVER.2013.6521559.

[11] E. Irmak and N. Güler, “A model predictive control-based hybrid MPPT method for boost converters,” International Journal of Electronics, Taylor & Francis, 2019.

[12] Salam J. Yaqoob, and Adel A. Obed, “Modeling, Simulation and Implementation ofPhotovoltaic Panel Model by Proteus Software Based on High Accuracy Two-diode Model,” Journal ofTechniques, vol. 1, no. 1. pp. 39-51, 2019.

[13] R. Wai, S. Member, and W. Wang, “Grid-Connected Photovoltaic Generation System,” IEEE Trans. Circuits Syst. , vol. 55, no. 3, pp. 953–964, 2008.

[14] J. Ahmed and Z. Salam, "A modified P&O maximum power point tracking method with reduced steady state oscillation and improved tracking efficiency," IEEE Trans. Sustain. Energy, vol. 7, no. 4, pp. 1506–1515, Oct. 2016.

[15] A. Gupta, P. Kumar, R. K. Pachauri, Y. K. Chauhan, "Performance analysis of neural network and fuzzy logic based MPPT techniques for solar PV systems," 6th IEEE Power India, International Conference (PIICON), pp. 1-6, 2014.

Chapter (2)

Literature Review

2.1 Introduction

An efficient maximum power point tracking (MPPT) method plays an important role to improve the efficiency of a photovoltaic (PV) generation system [2] [3]. This study provides an extensive review of the current status of MPPT methods for PV systems which are classified into several categories. The categorisation is based on the tracking characteristics of the discussed methods. The novelty of this study is that it focuses on the key characteristics and selection parameters of the methods, to make a comprehensive analysis, which is not considered together in any review works so far. Again, the pros and cons, classification and immense comparison among them described in this study can be used as a reference to address the gaps for further research in this field. A comparative review in tabular form is also presented at the end of the discussion of each category to evaluate the performance of these methods, which will help in selecting the appropriate technique for any specific application.

2.2 Literature Review

A new method for the MPPT control of PV systems, which uses one estimate process between every two perturb processes in search for the maximum PV output is presented in [1]. In this method, the perturb process conducts the search over the highly nonlinear PV characteristic, and the estimate process compensates the perturb process for irradiance-changing conditions [4] [5]. The EPP method significantly improves the tracking accuracy and speed of the MPPT control compared to available methods. The authors stated that the main technical requirements in developing a practical PV system include a) an optimal control that can extract the maximum output power from the PV arrays under all operating and weather conditions, and b) a high performance-to-cost ratio to facilitate commercialization of developed PV technologies [6].

Ref. [7] presented an intelligent approach for the improvement and optimization of the PV control performances. A PV system topology incorporating maximum power point tracking controller (MPPT) is studied. In order to perform this goal a special interest was focused on the well known P&O algorithm and compared to a designed fuzzy logic controller (FLC) [10]. A detailed study of the MPPT controller to insure a high PV system performance which can be

selected for practical implementation issue is presented. A simulation work dealing with MPPT controller, a DC/DC Boost converter feeding a load is achieved.

Ref. [8] presented a comparative study of two type of maximum power point tracking (MPPT). The optimization of energy generation in a PV system is necessary to let the PV cells operate at the maximum power point corresponding to the maximum efficiency. Since the MPP varies, based on the irradiation and cell temperature, appropriate algorithms must be utilized to track the MPP. This is known as MPPT. Different MPPT algorithms, each with its own specific performance, have been proposed in the literature [9] [11]. A so-called perturb and observe (P&O) as well as incremental conductance method is considered here and both are compared. This two method is widely diffused because of its low-cost and ease of implementation. When atmospheric conditions are constant or change slowly, the P&O method oscillates close to MPP. However, when these change rapidly, this method fails to track MPP and gives rise to a waste of part of the available energy [12]. A comparative study has been done on both the methods by using MATLAB environment. The MPPT algorithm was set up and validated by means of MATLAB simulations and experimental tests, confirming the effectiveness of the method.

Ref. [13] presented an Artificial Intelligence based perturbation and observation method. The proposed modified tracking algorithm uses an Artificial Neural Networks to detect the atmospheric conditions variations in order to adjust the perturbation step for the next perturbation cycle. The improved tracking performance of this presented method was verified trough simulation. The presented tracking algorithm shows better steady state and dynamical performance than traditional P&O.

Ref. [14] proposed the implementation of fuzzy logic based on the change of power and change of power with respect to change of voltage, fuzzy determines the size of the perturbed voltage. The performance of fuzzy logic with various membership functions (MFs) is tested to optimize the MPPT. Fuzzy logic can facilitate the tracking of maximum power faster and minimize the voltage variation [16].

Ref. [15] presented an application of the neural networks for identification of the maximum power (MP) and the normal operating power (NOP) of a PV module. Two neural networks are developed; the first is the maximum power neural network (MPNN) and the second is the normal

operating power neural network (NOPNN). The two neural networks receive the solar radiation and the PV module surface temperature as inputs, and estimate the MP and the NOP of a PV module as outputs. The training process for the two neural networks used a series of input/output data pairs. The training inputs are the solar radiation and the PV module surface temperature, while the outputs are the PV module MP for the MPNN and the PV module NOP for the NOPNN [17] [20].

Ref. [18] proposed an integrated PSO and ANN algorithms to track the solar power optimally based on various operation conditions due to the uncertain climate change. The proposed approach has the capability to estimate the amount of generated PV power at a specific time. The Levenberg-Marquardt ANN algorithm based solar insolation forecast has shown satisfactory results with minimal error and the generated PV power has been optimized significantly with the aids of the PSO algorithm [22].

A novel intelligent fuzzy logic controller for MPPT in grid-connected photovoltaic systems based on boost converter and single phase grid-connected inverter is introduced in [19]. This is simple to be implemented on MCU chip and needs no memory space to save fuzzy rules, and that optimizing factor in the fuzzy inference equation can adjust fuzzy rules on-line automatically to improve system control effect, which provides the system with an intelligent characteristic [21].

An intelligent control method for MPPT of a photovoltaic system under variable temperature and insolation conditions which uses a fuzzy logic controller applied to a DC-DC converter device is proposed in [23]. Results of this simulation are compared to those obtained by the perturbation and observation controller.

A fuzzy logic control (FLC) is proposed in [24] to control MPPT for a photovoltaic (PV) system; this technique uses the fuzzy logic control to specify the size of incremental current in the current command of MPPT. Most of the performed works in the literature reviews in this point is based on assumed not actual solar radiation data [27]

To sum, a variety of conventional techniques such as perturb and observe (P&O) [23], incremental conductance [25], constant voltage [26] and some others [30] have been introduced to extract the MPP of the solar array under uniform solar irradiance of the PV system. Although

these approaches show good performance in detecting this maxima, they failed to catch the global maximum power point (GMPP) under partial shading conditions (PSC) of the PV panels [28]. Under PSC of the PV panel, the P-V characteristics get more complex with multiple local peaks (LPs) and one global MPP due to the use of the bypass diodes to withstand the hot spot effect [29].

Recently, several evolutionary optimization techniques have been proposed to mitigate the effect of PSC on the PV arrays. Moreover, they have been utilized to detect the global maximum power point (GMPP) of the PV panels where the conventional methods fail to converge [31], [32]. For instance, the genetic algorithm (GA) [31], [33], artificial intelligence methods using fuzzy logic and neural networks have been applied to find the GMMP [32], [34]. A detailed review, classification, and comparative analysis of the GMPP algorithms are given in [35], [36][40], [38]. The criteria for comparative evaluation of the effectiveness of different GMPP techniques use the simple hardware implementation, cost, speed, and accuracy of tracking GMPP in various operating conditions of the PV [39].

The main contribution of this research is to propose a new methodology to select the optimal parameters of the MPP controller of the PV system based on the basic principles of the MPPT algorithm. Moreover, this work considers the designing and selecting the parameters of the buck DC-DC power converter, which connected to battery charge by taking into consideration the topology and configuration of the PV panel.

Moreover, this thesis introduces a new technique for determining the optimal value of the sampling time for the digital MPPT controller, providing their maximum performance.

2.3 Conclusions

Improvements in the efficiency of the solar PV system by extracting maximum power is presently one of the key challenges in research sectors of renewable energy. In that sense, the concept of the MPPT controller is found to be a valuable concept as it maximises the output power delivered by the solar PV module. A lot of articles have been already published for presenting the detailed analysis of several MPPT methods. In this review work, the discussed methods are classified based on the nature of the algorithm. The MPPT methods are detailed in this study along with their pros and cons, which signify that the selection of the MPPT technique should be based on the specific application and requirement of the utility. A tabular comparison is also presented at the end of each category, which may be a striking apparatus to the utility of choosing the most productive and perfect kind of MPPT to satisfy the prerequisites of both operators and consumers. This data may find an alluring source to help the engineers in setting with the predominant mechanical scenario.

References.

[1] Guohui Zeng, Xiubin Zhang, Junhao Ying,Changan Ji, " A Novel Intelligent Fuzzy Controller for MPPT in Grid-connected Photovoltaic Systems", Proc. of the 5th WSEAS/IASME Int. Conf. on Electric Power Systems, High Voltages, Electric Machines, Tenerife, Spain, December 16-18, 2005, pp. 515-519.

[2] M.S. Aït Cheikh, C. Larbes, G.F. Tchoketch Kebir and A. Zerguerras, " Maximum power point tracking using a fuzzy logic control scheme", Revue des Energies Renouvelables, Vol. 10, No 3, 2007, pp. 387 – 395.

[3] M.S. Aït Cheikh, C. Larbes, G.F. Tchoketch Kebir and A. Zerguerras, " Maximum power point tracking using a fuzzy logic control scheme", Revue des Energies Renouvelables, Vol. 10, No 3, 2007, pp. 387 – 395.

[4] Pongsakor Takun, Somyot Kaitwanidvilai and Chaiyan Jettanasen, " Maximum Power Point Tracking using Fuzzy Logic Control for Photovoltaic Systems", Proceedings of the International MultiConference of Engineers and Computer Scientists 2011, Vol. II, IMECS 2011, March 16-18, 2011, Hong Kong.

[5] A. Jäger-Waldau, European Commission, and Joint Research Centre, {PV} status report 2018 study. 2018.

[6] T. H. Kwan and X. Wu, "High performance P&O based lock-on mechanism MPPT algorithm with smooth tracking," Sol. Energy, vol. 155, pp. 816–828, Oct. 2017.

[7] N. A. Kamarzaman and C. W. Tan, "A comprehensive review of maximum power point tracking algorithms for photovoltaic systems," Renew. Sustain. Energy Rev., vol. 37, pp. 585–598, Sep. 2014.

[8] S. G. Obukhov, I. A. Plotnikov, and S. K. Sheryazov, "Methods of effective use of solar power system," in 2016 2nd International Conference on Industrial Engineering, Applications and Manufacturing (ICIEAM), 2016, pp. 1–6.

[9] M. A. Husain, A. Tariq, S. Hameed, M. S. Bin Arif, and A. Jain, "Comparative assessment of maximum power point tracking procedures for photovoltaic systems," Green Energy Environ., vol. 2, no. 1, pp. 5–17, Jan. 2017.

[10] G. Shankar and V. Mukherjee, "MPP detection of a partially shaded PV array by continuous GA and hybrid PSO," Ain Shams Eng. J., vol. 6, no. 2, pp. 471–479, Jun. 2015.

[11] S. G. Obukhov, I. A. Plotnikov, and S. K. Sheryazov, "Methods of effective use of solar power system," in 2016 2nd International Conference on Industrial Engineering, Applications and Manufacturing (ICIEAM), 2016, pp. 1–6.

[12] Mirhassaniet SM, Golroodbari SZ, Golroodbari SM, Mekhilef S. An improved particle swarm optimization based maximum power point tracking strategy with variable sampling time. Electr Power Energy Syst 2015; 64:761–70.

[13] Rezk H, Fathy A. Simulation of global MPPT based on teaching–learning-based optimization technique for partially shaded PV system. Electr Eng 2016. http://dx.doi.org/10.1007/s00202-016-0449-3, (Oct).

[14] Ahmed J, Salam Z. A Maximum Power Point Tracking (MPPT) for PV system using Cuckoo Search with partial shading capability. Appl Energy 2014;119:118–30.

[15] Kofinas P, Dounis AI, Papadakis G, Assimakopoulos MN. An Intelligent MPPT controller based on direct neural control for partially shaded PV system. Energy Build 2015; 90:51–64.

[16] A. Ibrahim, R. Aboelsaud, and S. Obukhov, ``Improved particle swarm optimization for global maximum power point tracking of partially shaded PV array," Electr. Eng, vol. 101, no. 2, pp. 443455, Jun. 2019.

[17] Fathabadi H. Novel highly accurate universal maximum power point tracker for maximum power extraction from hybrid fuel cell/photovoltaic/wind power generation systems. Energy 2016; 116:402–16.

[18] Fathy A, Rezk H. A novel methodology for simulating maximum power point trackers using mine blast optimization and teaching learning based optimization algorithms for partially shaded photovoltaic system. J Renew Sustain Energy 2016;8:023503. http://dx.doi.org/10.1063/1.4944971.

[19] X. S. Li, H. Q. Wen, L. Jiang, W. Xiao, Y. Du, and C. Zhao, "Animproved MPPT method for PV system with fast-converging speed and zero oscillation," IEEE Transactions on Industry Applications, vol. 52, no. 6, pp. 5051–5064, 2016.

[20] R. Ayop, C. W. Tan, "A comprehensive review on photovoltaic emulator," Renew. Sustain. Energy Rev., vol. 80, pp. 430–452, December 2017.

[21] J. I. Corcau and L. Dinca, "Modeling and Analysis of a Fuzzy Type MPPT Algorithm," 2019 International Conference on Electrical Drives & Power Electronics (EDPE), The High Tatras, Slovakia, pp. 230-234, 2019.

[22] M. Mosa, M. B. Shadmand, R. S. Balog and H. A. Rub, "Efficient maximum power point tracking using model predictive control for photovoltaic systems under dynamic weather conditions," IET Renewable Power Generation, vol. 11, no. 11, pp. 1401 -1409, 2017.

[23] RI. Putri, S.Wibowo and M.Rifa'i," Maximum power point tracking for photovoltaic using incremental conductance method," Energy Procedia. ,Vol.68 pp.22-30, Apr.2015.

[24] Haripriya T, Alivelu M, Rao UM, Performance evaluation of DC grid connected solar PV system for hybrid control of DC–DC boost converter. In: 10th international conference on intelligent systems and control (ISCO), pp 1–6, ISSN: 1868-5145, 7–8 Jan 2061.

[25] K. S. Tey and S. Mekhilef, "Modified incremental conductance MPPT algorithm to mitigate inaccurate responses under fast-changing solar irradiation level," Solar Energy, vol. 101, pp. 333–342, 2014.

[26] M. Rolevski, Z. Zecevic, MPPT controller based on the neural network model of the photovoltaic panel. In Proceedings of the 2020 24th International Conference on Information Technology (IT), Zabljak, Montenegro, 18–22, pp. 1–4, February 2020.

[27] N. Kumar, I. Hussain, B. Singh, B. Panigrahi, "Self-Adaptive Incremental Conductance Algorithm for Swift and Ripple Free Maximum Power Harvesting from PV Array", IEEE Trans. Industrial Informatics, vol. 14, no. 5, May. 2018.

[28] F.Awolusi, O. L.Oke, O. O.Akinkurolere, A. O. Sojobi, & O. G Aluko "Performance comparison of neural network training algorithms in the modelling properties of steel fibre reinforced concrete," Heliyon, Vol.5.no.1, pp.01115. 2019.

[29] A Mohapatra, B. Nayak, P. Das, & K. B. Mohanty, "A review on MPPT techniques of PV system under partial shading condition,". Renewable and Sustainable Energy Reviews. , Vol.80, pp.854-867,Dec.2017.

[30] Gomathi.B, and Sivakami.P, "An Incremental Conductance Algorithm based solar maximum power point tracking system", International Journal of Electrical Engineering. ISSN0974-2158 Volume 9, pp. 15-24. 2016.

[31] M. S. Shadlu, "Comparison of maximum power point tracking (MPPT) algorithms to control DC-DC converters in photovoltaic systems," Rec. Adv. Electric. & Electron. Eng., vol. 12, no. 4. pp. 355-367, 2019.

[32] R. Wai, S. Member, and W. Wang, "Grid-Connected Photovoltaic Generation System," IEEE Trans. Circuits Syst. , vol. 55, no. 3, pp. 953–964, 2008.

[33] E. Romero-cadaval, G. Spagnuolo, and L. G. Franquelo, "Grid-Connected Photovoltaic Generation Plants," Ieee Ind. Electron. Mag., no. September, pp. 6–20, 2013.

[34] H. Boumaaraf, A. Talha, and O. Bouhali, "A three-phase NPC grid-connected inverter for photovoltaic applications using neural network MPPT," Renew. Sustain. Energy Rev., vol. 49, pp. 1171–1179, 2015, doi: 10.1016/j.rser.2015.04.066.

[35] A. Islam, N. Mohammad, and P. K. S. Khan, "Modeling and Performance Analysis of a Generalized Photovoltaic Array in Matlab," 2010 Jt. Int. Conf. Power Electron. Drives Energy Syst. 2010 Power India, no. December 2017, 2010.

[36] M. G. Villalva, J. R. Gazoli, and E. R. Filho, "Comprehensive Approach to Modeling and Simulation of Photovoltaic Arrays," vol. 24, no. 5, pp. 1198–1208, 2009.

[37] T. Esram and P. L. Chapman, "Comparison of Photovoltaic Array Maximum Power Point Tracking Techniques," IEEE Trans. Energy Convers., vol. 22, no. 2, pp. 439–449, 2007.

[38] M. A. Elgendy, B. Zahawi, S. Member, and D. J. Atkinson, "Assessment of Perturb and Observe MPPT Algorithm Implementation Techniques for PV Pumping Applications," IEEE Trans. Sustain. Energy, vol. 3, no. 1, pp. 21 –33, 2012.

[39] D. P. Hohm, "Comparative Study of Maximum Power Point Tracking Algorithms Using an Experimental, Programmable, Maximum Power Point Tracking Test Bed," Conf. Rec. Twenty-Eighth IEEE Photovolt. Spec. Conf. - 2000 (Cat. No.00CH37036), 2000.

[40] H. A. Sher et al., "A New Sensorless Hybrid MPPT Algorithm Based on Fractional Short-Circuit Current Measurement," IEEE Trans. Sustain. Energy, vol. 6, no. 4, pp. 1426–1434, 2015.

Chapter (3)

Methodology

3.1 Introduction

This chapter develops a mathematical model of a photovoltaic (PV) system. A PV system is one that converts solar energy into electricity using one or more solar panels.It is made up of several components, including as PV modules, a battery bank, mechanical and electrical connections, and devices for regulating and controlling system functioning. A photon of sufficient wavelength and energy can induce an electron in a PV material to break loose from the atom that is holding it. Those electrons can be swept toward a metallic contact and become an electric current if there is an electric field nearby. It's interesting to note that the sun provides the power for PVs, and that the earth receives it. Numerous photovoltaic systems can operate independently. As depicted in Figure3.1 , such systems include a PV generator, energy storage (such as a battery), AC and DC consumers, and components for power conditioning.

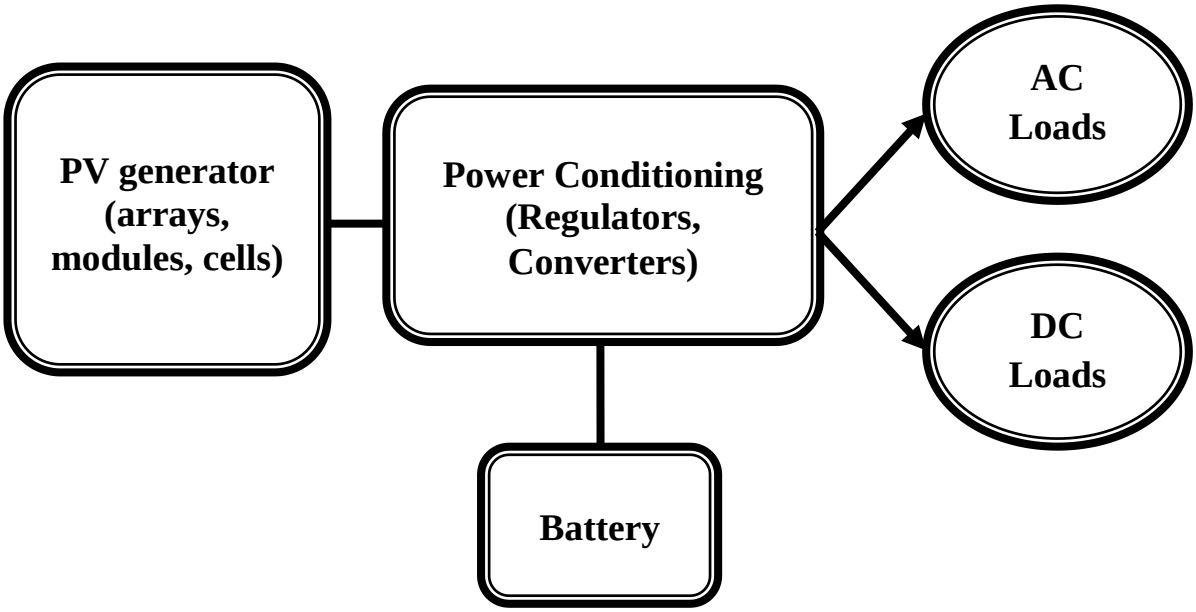

Fig. 3.1 The components of a stand-alone photovoltaic system

3.2 Component models for stand-alone PV system

The system of research of this work is the PV system which is designed to provide the electric power to the consumers in isolation from the central electrical network. From the point of view of the basic architecture, three main option scan be distinguished for constructing autonomous PV (Fig. 3.2).

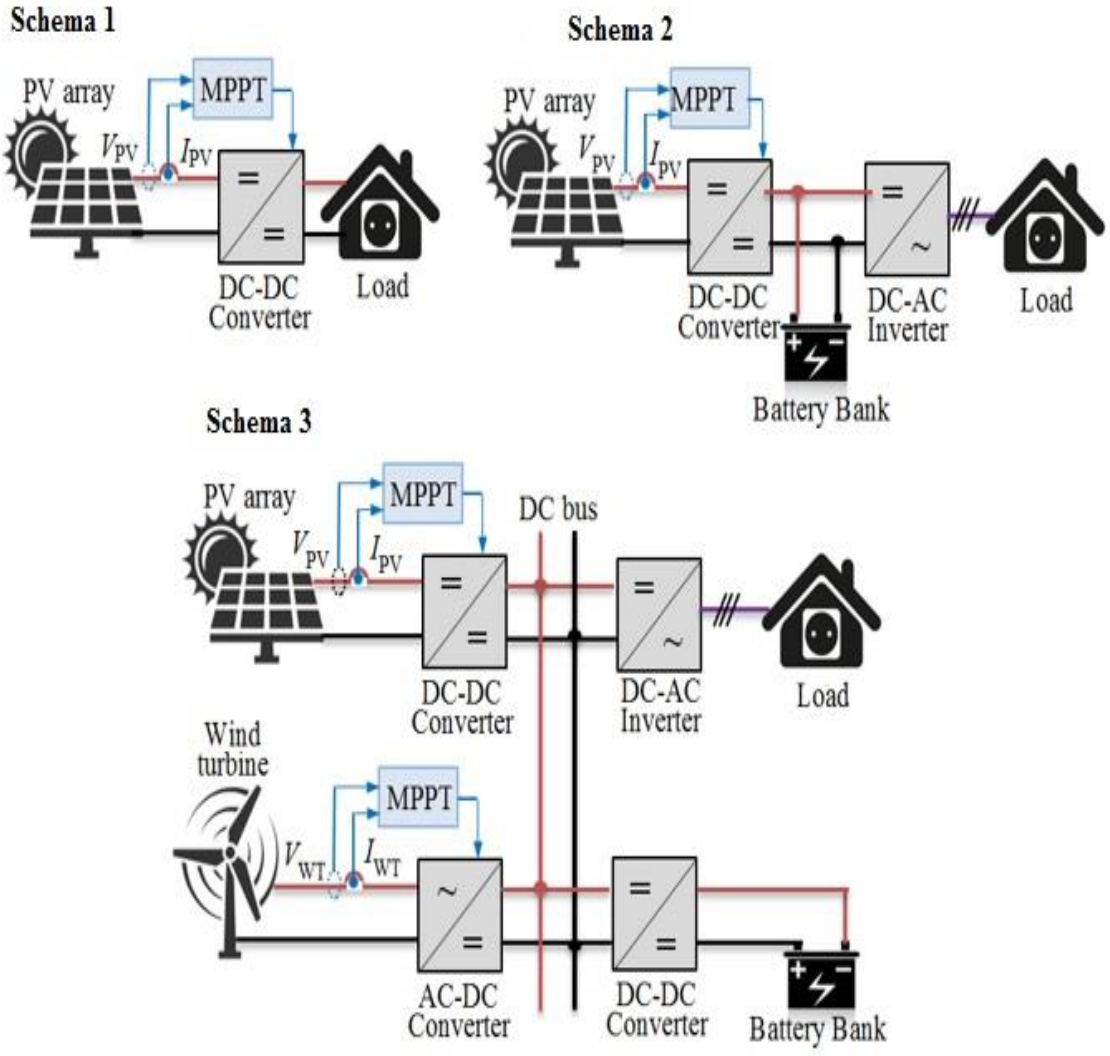

Fig. 3.2. A typical block diagram of the construction of autonomous photovoltaic stations

In the simplest configuration (Schema 1), the PV includes only the PV array and a DC-DC converter operating under the control of the MPPT point search controller. The advantages of this type of PV are maximum simplicity and low cost, an obvious disadvantage is the low reliability of power supply to consumers [2] [3]. The area of the practical application of such stations is heating, cooking and pumping water systems that are not critical to the supply voltage parameters [1]. The main function of the control system of such a PV is to maximize the use of available solar energy without the need to control the output voltage and current of the DC-DC converter.

Autonomous PV systems with energy storage devices, which mainly use rechargeable batteries (Battery Bank), are more widely used [4]. The use of battery bank can significantly increase the reliability of the PV and provide consumers with the electricity of the required quality, but the cost of the PV and the complexity of the control system increase [5]. Depending on the purpose, in practice, two main options are used to build autonomous PV power plants with energy storage: energy systems with a single generating source (Schema 2) and hybrid energy complexes, in addition to photomultiplier stations, other plants are also used as generation sources, for example, wind energy (Schema 3).

Note that there are other ways to build autonomous PV and hybrid energy systems [6] [7]. The choice for analysis of the three presented in Fig. 3.2, the topologies are explained by the fact that they differ from each other in the nature of the electric load of the DC-DC converter, which has a direct effect on its dynamic characteristics, and, accordingly, on the selection of parameters of all the main elements of the PV. For all other PV topologies not considered in this paper, the operation modes of the DC-DC converter will be similar to one of the above cases.

It should also be noted that various types of voltage converters are used as part of autonomous PV, a detailed review and comparative analysis of which are presented in [8] [10]. In these studies, autonomous PV based on a buck DC-DC converter, which is mainly used in low-power energy systems, is considered as an object of analysis. Also, in this paper, we do not consider modes of partial shading of PV panels, which are especially critical for high-power photovoltaics, requiring the use of specialized MPPT controllers [6] [11].

The primary objective of this section is to provide a description of the models for the components of an independent PV system: load, converter, controller, PV generator, and battery The PV system's modeling is based on modular blocks, as shown in Fig. 3.3.

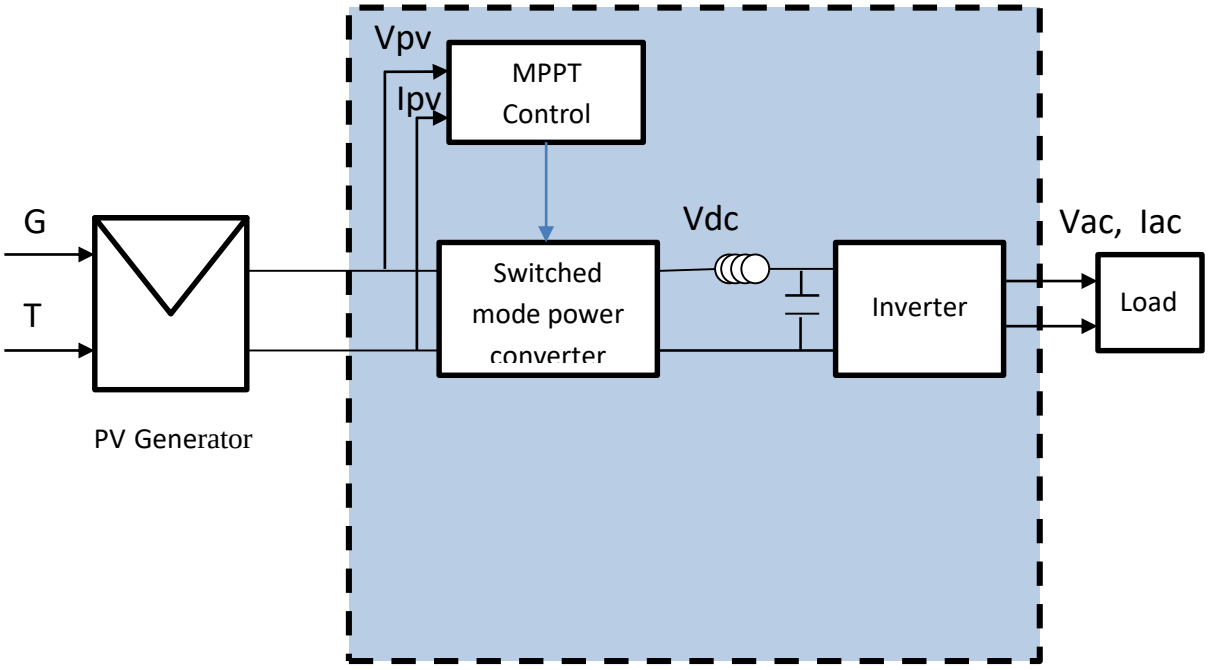

Fig. 3.3 Block diagram for the stand-alone PV system

3.2.1 PV generator (cell, module, array)

A PV generator is the entire collection of solar cells, connectors, protective components, supports, and so on [12]. The current modelling focuses only on cell, module, and array. When electrical contacts are connected to cell terminals, electrons flow from the n-side into the connecting wire, via the load, and back to the p-side, as illustrated in Fig. 3.4. They recombine with holes on the p-side, completing the circuit. Positive current flows in the opposite direction of electron flow, hence the current arrow in the image depicts current flowing from the p-side to the load and back into the n-side[11] [13].

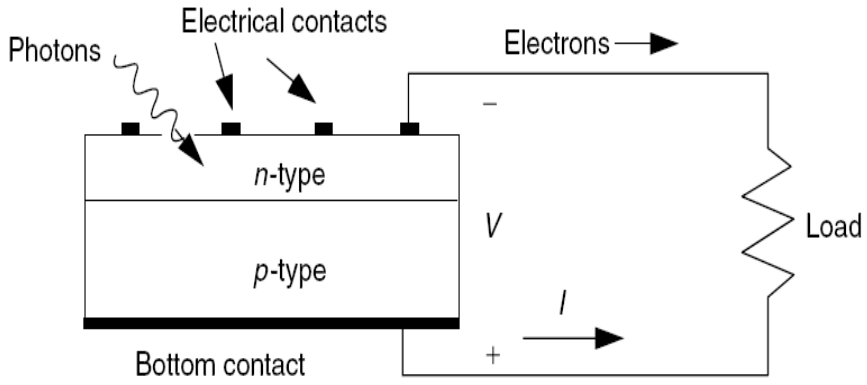

Fig. 3.4 The configuration of the PV cell electric current

3.2.2 The Simplest Equivalent Circuit for a Photovoltaic Cell

As illustrated in Fig. 3.5, a simple equivalent circuit model for a photovoltaic cell consists of a real diode in parallel with an ideal current source. The ideal current source produces a current proportional to the amount of solar flux to which it is exposed.

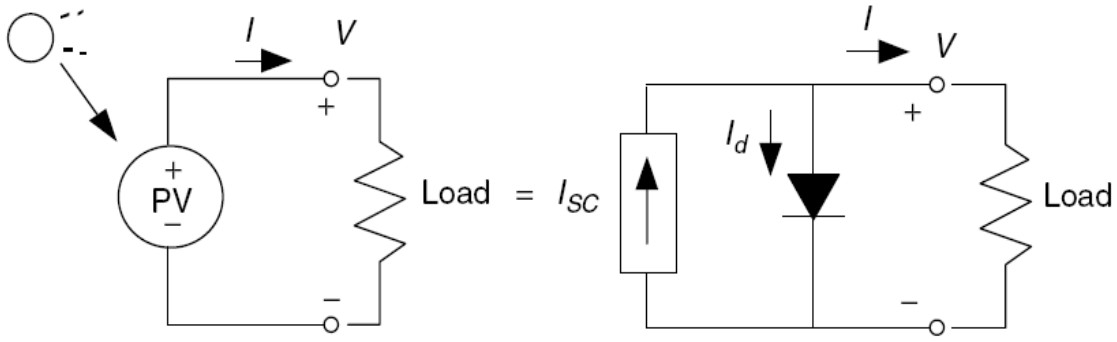

Fig. 3.5 A simple equivalent circuit for a photovoltaic cell

There are two criteria that are particularly interesting for both, the real PV and its equivalent circuit. As seen in Fig. 3.6, (a) The current flowing when the terminals are shorted together (the short-circuit current, I_{SC}.), and (b) the voltage across the terminals when the leads are left open (the open-circuit voltage, V_{OC}). When the leads of the equivalent circuit for the PV cell are shorted together, no current flows in the diode because V is equal to zero, so all of the current

from the ideal source flows through the shorted leads. Because the short-circuit current must equal ISC, the magnitude of the ideal current source must also equal I_{SC}.

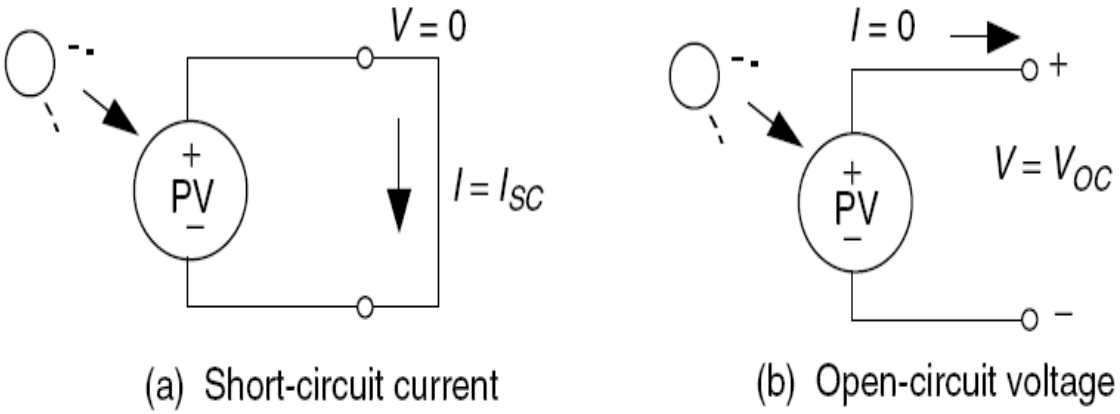

Fig. 3.6 The short circuit current and open circuit voltage of photovoltaic cell

Now one. May develop a voltage and current equation for the PV cell equivalent circuit shown in Fig. 3.6b. Begin with

$$I = I_{SC} - I_d \tag{3.1}$$

$$I = I_{SC} - I_0(e^{\frac{qV}{nk_bT}} - 1) \tag{3.2}$$

Where I_{SC} is the short circuit current, I is the Cell current, I_0 is the Reverse saturation current, V is the Cell voltage, The ideality factor, also known as the quality factor or emission coefficient, is denoted by n. The ideality factor ranges from 1 to 2 depending on the production technique and semiconductor material used, and is frequently thought to be about equal to 1. k_b is the Boltzmann constant (k_b=1.38×10-23 (j/K)), T is the cell Temperature in Kelvin, q is the Charge of an electron (q=1.6×10-19 (coul)). Fig. 3.7 shows the current–voltage relationship for a PV cell when it is dark, no illumination, and light, illuminated, based on eqn. (3.2).: When the PV cell leads are left open, I = 0, then eqn. (3.2) for the open-circuit voltage V_{OC} may be solved as follows:

$$V_{OC} = \frac{nk_bT}{q}\ln(\frac{I_{SC}}{I_0} + 1) \tag{3.3}$$

And at 25˚C, eqns. (3.2) and (3.3) become

$$I = I_{SC} - I_0(e^{38.9} - 1) \tag{3.4}$$

$$V_{OC} = 0.0257 \ln(\frac{I_{SC}}{I_0} + 1) \tag{3.5}$$

Inpboth of pthese equations, short-circuit current, I_{SC}, is directly proportional to solar insolation, which means that we can now quite easily plot sets of PV current–voltage curves for varying sunlight.

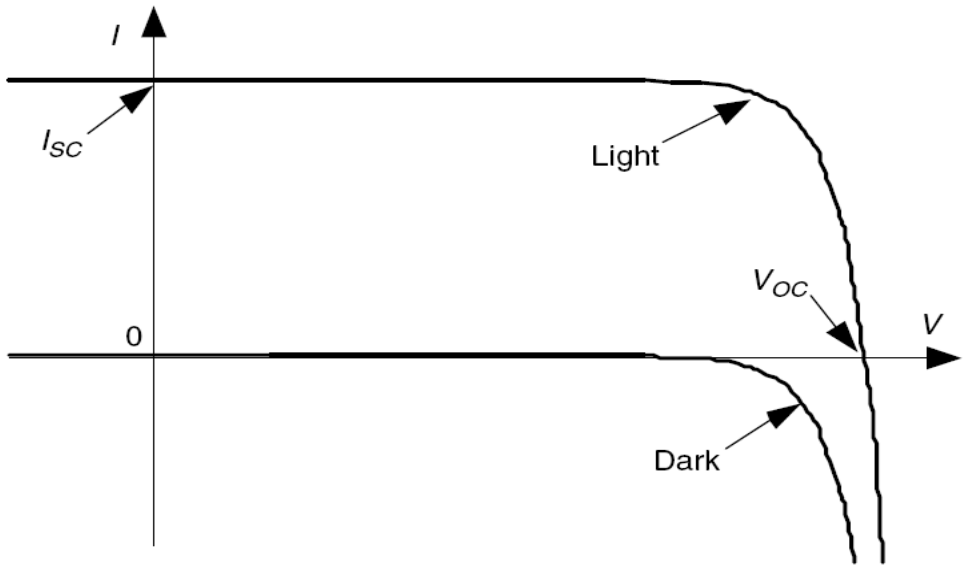

Fig. 3.7 Photovoltaic cell voltage–current relationship for dark and light

3.2.3 A more Accurate Equivalent Circuit for a PV Cell

There are times when a more complex PV equivalent circuit than that shown in Fig. 3.5 is needed [14]. For example, consider the impact of shading on a string of cells wired in series as shown in Fig. 3.8. If any cell in the string is in the dark, shaded, it produces no current. In our simplified equivalent circuit for the shaded cell, the current through that cell's current source is zero and its diode is back biased so it doesn't pass any current either [16]. This means that the simple equivalent circuit suggests that no power will be delivered to a load in this case. So, we need a more complex model if we are going to be able to deal with realities such as the shading problem. Fig. 3.9 shows a PV equivalent circuit that

includes some parallel leakage resistance R_p. The ideal current source I_{SC} in this case delivers current to the diode, the parallel resistance, and the load:

$$I = I_{SC} - I_d - \frac{V}{R_P} \tag{3.6}$$

For a cell to have losses of less than 1% due to its parallel resistance, R_P should be greater than about $R_P > \frac{100V_{OC}}{I_{SC}}$ [15]. Modifying the idealized PV equivalent circuit by adding parallel resistance causes the current at any given voltage to drop by V/R_P as shown in Fig. 3.10.

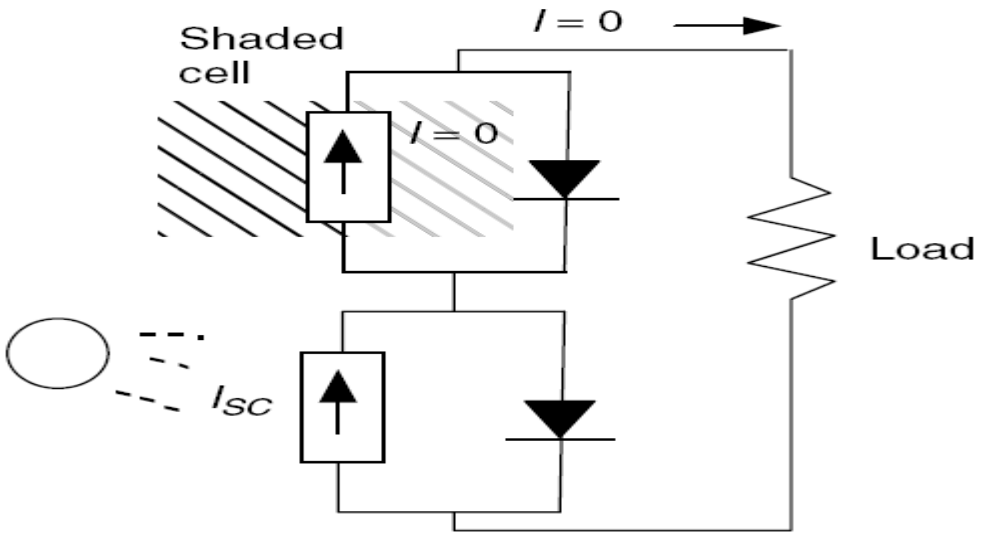

Fig. 3.8 A simple equivalent circuit of a string of cells in series for shaded case

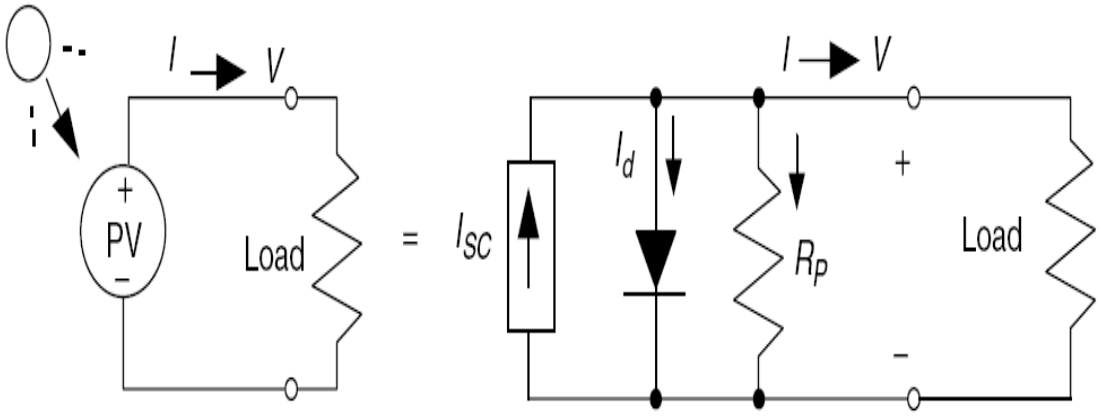

Fig. 3.9 A PV cell equivalent circuit with parallel resistance

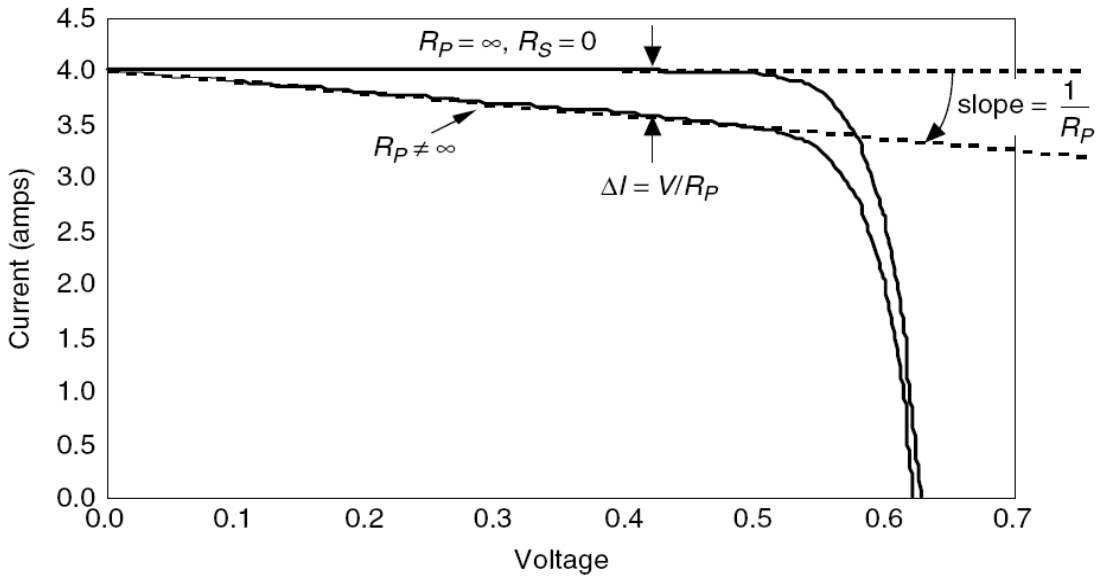

Fig. 3.10 The voltage-current characteristic for PV cell circuit with parallel resistance

A better equivalent circuit for the PV cell will include series resistance as well as parallel resistance as shown in Fig. 3.11 [17] [19]. The original PV equivalent circuit has been simplified by adding some series resistance, RS. Some of this might be due to contact resistance caused by the link between the cell and its wire leads, while some could be due to semiconductor resistance [18].

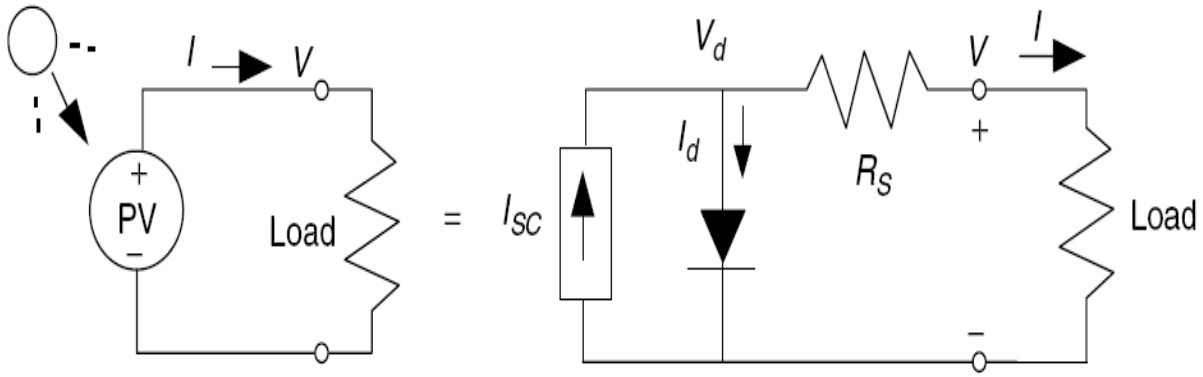

Fig. 3.11 A PV cell equivalent circuit with series resistance

Referring to the circuit shown in Fig. 3.11, one can get,

$$V_d = V + I.R_S \tag{3.7}$$

$$I = I_{SC} - I_0 \left\{ \exp\left[\frac{q(V+I.R_S}{nk_bT} \right] - 1 \right\} \tag{3.8}$$

For a cell to have less than 1% losses due to the series resistance, R_S will need to be less than about $R_P < \frac{0.01V_{OC}}{I_{SC}}$ [15]. Eqn. (3.8) can be interpreted as the original PV current-voltage curve with the voltage at any given current shifted to the left by $\Delta V = IR_S$ as shown in Fig. 3.12.

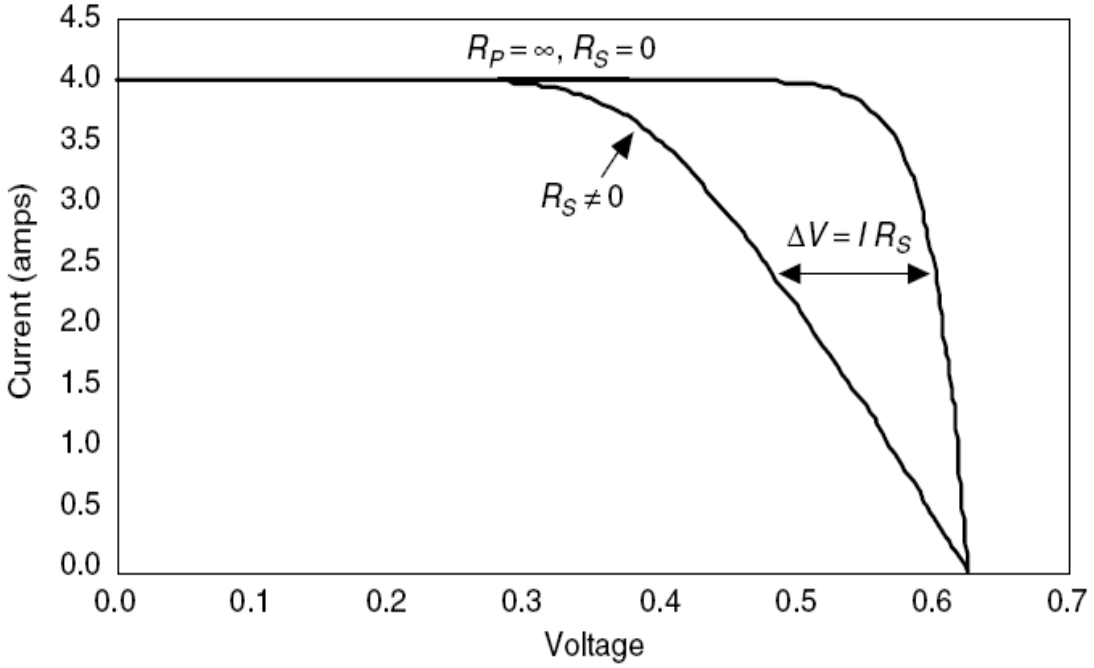

Fig. 3.12 The voltage-current characteristic for PV cell circuit with series resistance

Finally, as illustrated in Fig. 3.13, we may generalise the PV equivalent circuit by incorporating both series and parallel resistances. The equation for current and voltage is as follows:

$$I_{SC} = I + I_d + I_P \tag{3.9}$$

$$I = I_{SC} - I_0 \left\{ \exp\left[\frac{q(V+I.R_S}{nk_bT}\right] - 1 \right\} - \left(\frac{V+I.R_S}{R_P}\right) \quad (3.10)$$

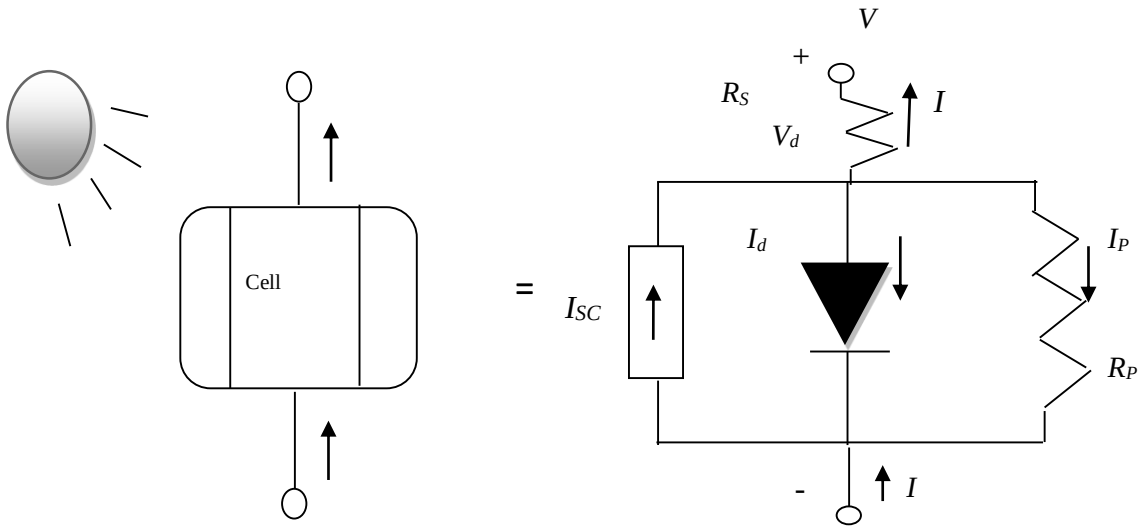

Fig. 3.13 A more complex equivalent circuit for a PV cell includes both parallel and series resistances

Rearranging, and substituting the Shockley diode eqn. (3.2) at 25°C gives

$$I = I_{SC} - I_0(e^{38.9V_d} - 1) - \frac{V_d}{R_P} \quad (3.11)$$

$$and \quad V_d = V + IR_S \quad (3.12)$$

3.2.4 Photovoltaic Module

A PV module is created by connecting numerous PV cells in series for high voltage and in parallel for high current in order to overcome the low voltage of a PV cell, which is typically approximately 0.5V [20]. Separate diodes may be required to avoid reverse currents when partial or entire shade is present, as well as at night. Monocrystalline silicon cell PN junctions may have appropriate reverse current properties, although they are not required [21]. Reverse currents waste electricity and can cause shaded cells to overheat. Solar cells lose efficiency as temperatures rise, and installers strive to ensure enough airflow behind solar panels [22]. A typical module has 36 cells in series and is often designated as a 12-V module even though it is capable of delivering much higher voltages than that [23]. Some 12-V modules include just 33 cells, which may be beneficial in some extremely simple battery charging systems, as will be

demonstrated later. Large 72-cell modules are now quite common, some of which have all of the cells wired in series, in which case they are referred to as 24-V modules. Some 72-cell modules can be field-wired to act either as 24-V modules with all 72 cells in series or as 12-V modules with two parallel strings having 36 series cells in each [25]. PV cells are grouped in larger units called PV modules which are further interconnected in series-parallel configuration to form PV arrays or PV generators [24]. The manufacturers supply PV cells in modules, consisting of N_P parallel branches, each with N_S solar cells in series, as shown in Fig. 3.14. In order to have a clear specification of which element (cell or module) the parameters in the mathematical model are regarding, the following notation is used from now on: the parameters with superscript "M" are referring to the PV module, while the parameters with superscript "C" are referring to the solar cell. Thus, the applied voltage at the module's terminals is denoted by V^M, while the total generated current by the module is denoted by I^M.

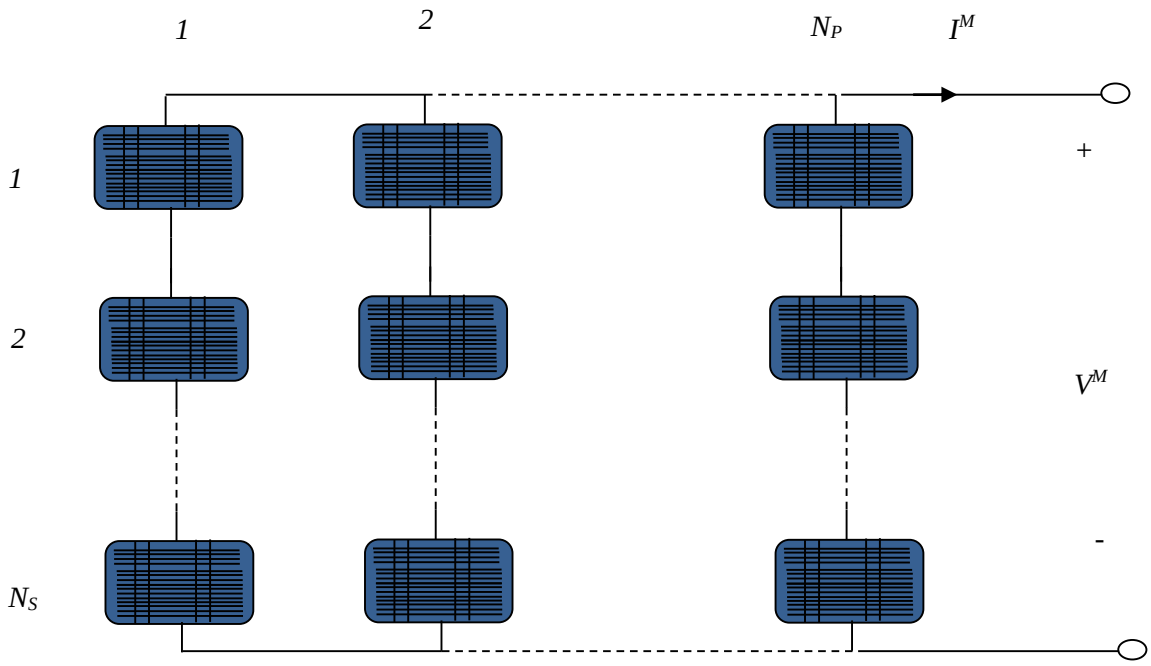

Fig. 3.14 A PV module consists of N_{PM} parallel branches, each of N_{SM} solar cells in series

The PV module's current I^M under arbitrary operating conditions can thus be described as:

$$I^M = N_p I_{SC} - N_p I_0 \left\{ \exp\left[\frac{q\left(\frac{V^M}{N_S} + I^M . {R_S}^M\right)}{n k_b T} \right] - 1 \right\} - \left(\frac{\frac{V^M}{N_S} + I^M . {R_S}^M}{{R_P}^M} \right) \quad (3.13)$$

$${R_s}^M = \frac{N_S}{N_p} R_s, \ {R_P}^M = \frac{N_p}{N_S} R_P \text{ and } V^M = N_S V \quad (3.14)$$

One can solve eqn. (3.4) for the reverse saturation current I_0 by setting *I=0* which means that no output current.

$$0 = I_{SC} - I_0 (e^{\frac{qV}{n k_b T}} - 1) \quad (3.15)$$

From eqn. (3.15) one can get that;

$$I_0 = \frac{I_{SC}}{(e^{\frac{qV}{n k_b T}} - 1)} \quad (3.16)$$

The reverse saturation current is dependent on the temperature and is given by the following eqn.

$$I_0(T) = I_0(T_{ref}) * (\frac{T}{T_{ref}})^3 * exp(\frac{qE_G}{AK}(\frac{1}{T_{ref}} - \frac{1}{T}) \quad (3.17)$$

Where $T_{ref}$is the reference temperature of the PV cell usually 298 K, $I_0(T_{ref})$is The cell reverse saturation current at reference temperature and E_G is the band gap of semiconductor used in the cell. The temperature dependence of the energy gap of the semiconductor is given by:

$$E_G(T) = E_G(0) - \frac{\alpha \times T^2}{T + \beta} \quad (3.18)$$

Where $E_G(0)$, α and β are the fitting parameters. These fitting parameters are listed for germanium, silicon and gallium arsenide in the Table 3.1.

Table 3.1 The values of fitting parameters

	Germanium	Silicons	GaAs
$E_g(0)$ [eV]	0.7437	1.166	1.519
α [eV/K]	4.77 x 10^{-4}	4.73 x 10^{-4}	5.41 x 10^{-4}
β [K]	235	636	204

The short current depends on the solar radiation and cell temperature as follows:

$$I_{SC} = \left[I_{SCr} + K_i\left(T - T_{ref}\right)\right] * G \tag{3.19}$$

Where I_{SCr} is the cell is short-circuit current at reference temperature and radiation, K_i is the short circuit current temperature coefficient, and G is the solar radiation in W/m^2. Finally; Eqn. (3.13) can be described as follows:

$$I^M = N_P I_{SC} - N_P I_0 \left\{\exp\left[\frac{q(\frac{V^M}{N_S} + I^M.{R_S}^M)}{nk_bT}\right] - 1\right\} - \left(\frac{V^M}{N_S {R_P}^M} + \frac{I^M.{R_S}^M}{{R_p}^M}\right) \tag{3.20}$$

$$I^M\{1 + \frac{{R_S}^M}{{R_p}^M}\} = N_P I_{SC} - N_P I_0 \left\{\exp\left[\frac{q(\frac{V^M}{N_S} + I^M.{R_S}^M)}{nk_bT}\right] - 1\right\} - \frac{V^M}{N_S {R_P}^M} \tag{3.21}$$

Eqn. (3.21) can be solved by Newton's method which can be described by the following eqn.

$${I^M}_{n+1} = {I^M}_n - f({I^M}_n)/\acute{f}({I^M}_n) \tag{3.22}$$

Where $\acute{f}({I^M}_n)$ is the derivative of function, ${I^M}_n$ is the present value and ${I^M}_{n+1}$ is the next value.

$$\text{Let } f(I^M) = I^M\left\{1 + \frac{{R_S}^M}{{R_p}^M}\right\} - N_P I_{SC} + N_P I_0 \left\{\exp\left[\frac{q\left(\frac{V^M}{N_S} + I^M.{R_S}^M\right)}{nk_bT}\right] - 1\right\} + \frac{V^M}{N_S {R_P}^M} \tag{3.23}$$

Then $$\acute{f}(I^M) = 1 + \frac{{R_S}^M}{{R_p}^M} + \frac{N_P I_0 q {R_S}^M}{n k_b T}\left\{\exp\left[\frac{q(\frac{V^M}{N_S} + I^M.{R_S}^M)}{n k_b T}\right]\right\} \quad (3.24)$$

The iteration can be continued until the absolute relative approximate error E_R is equal to pre-specified relative error tolerance E_S.

$$|E_R| = \left|\frac{{I^M}_{n+1} - {I^M}_n}{{I^M}_{n+1}}\right| \times 100 \quad (3.25)$$

3.2.5 Photovoltaic Array

The power that one module can produce is not sufficient to meet the requirements of home or business. Most PV arrays use an inverter to convert the DC power into alternating current that can power the motors, loads, lights etc [26] [28]. The modules in a PV array are usually first connected in series to obtain the desired voltages; the individual modules are then connected in parallel to allow the system to produce more current. The modules in a PV system are typically connected in arrays.

Fig. 3.15 illustrates the case of an array with M_P parallel branches each with M_S modules in series.

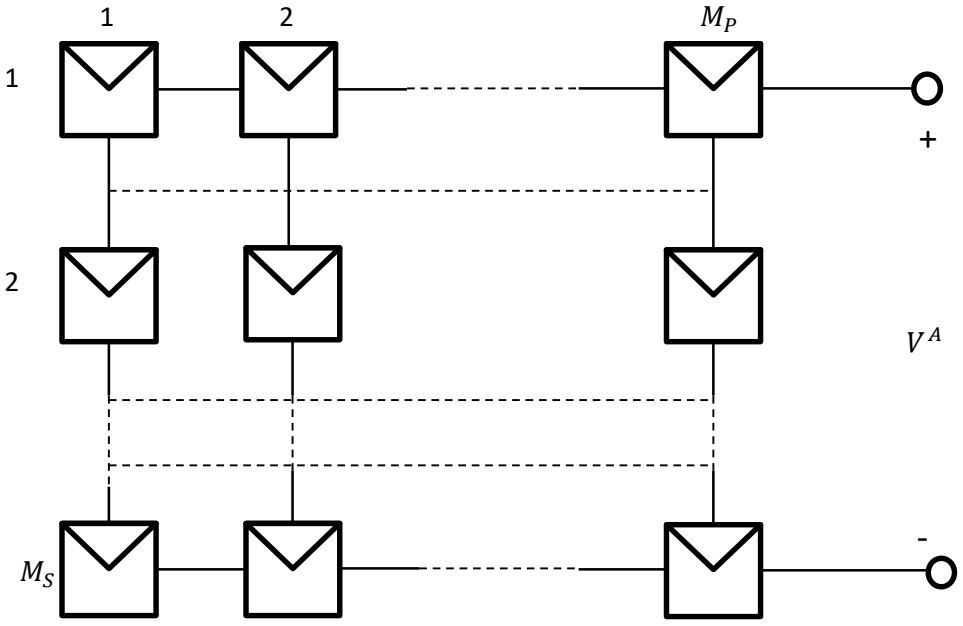

Fig. 3.15 Configuration of a PV array of M_p parallel branches and M_s series strings

The applied voltage at the array's terminals is denoted by V^A, while the total current of the array is denoted by$I^A = \sum_{i=1}^{M_P} I_i$. If it is assumed that the modules are identical and the ambient irradiation is the same on all the modules, then the array's current is $I^A = M_P I^M$.

3.3 The PV *I–V* Curve under Standard Test Conditions (STC)

Fig. 3.16 shows a voltage-current characteristic for a PV module, identifying several key parameters including the open-circuit voltage V_{OC} and the short circuit current I_{SC} [31]. Also the product of voltage and current, that is, power delivered by the module is shown. At the two ends of the voltage-current curve, the output power is zero since either current or voltage is zero at those points. The maximum power point (MPP) is that spot near the knee of the voltage-current curve at which the product of current and voltage reaches its maximum [29]. The voltage and current at the MPP are sometimes designated as V_m and I_m for the general case and designated V_R and I_R, for rated voltage and rated current, under the special circumstances that correspond to idealized test conditions.

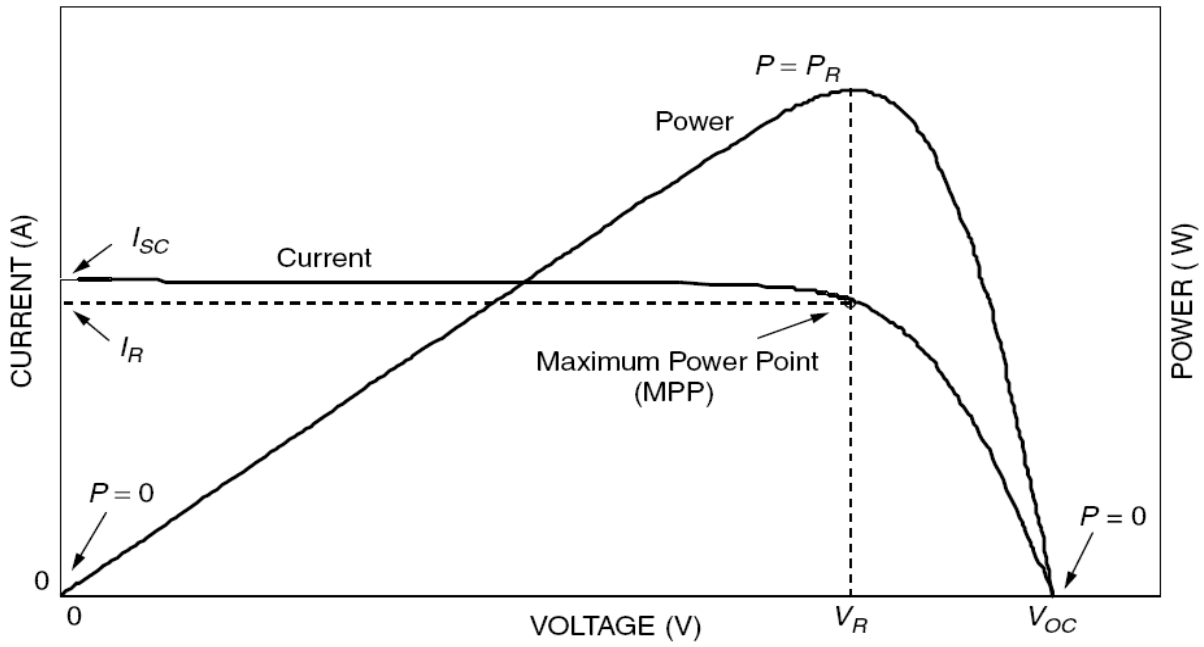

Fig. 3.16 The voltage-current curve and power output for a PV module

Another way to determine the location of the maximum power point is by imagining trying to find the biggest possible rectangle that will fit beneath the voltage-current curve [30]. As shown in Fig. 3.17, the sides of the rectangle correspond to current and voltage, so its area is power. Another quantity that is often used to characterize module performance is the *fill factor* (FF). The fill factor is the ratio of the power at the maximum power point to the product of V_{OC} and I_{SC}, so FF can be visualized as the ratio of two rectangular areas, as is suggested in Fig. 3.16. Fill factors around 70–75% for crystalline silicon solar modules are typical, while for multi junction amorphous-Si modules, it is closer to 50–60%.

$$Fill\ factor\ (FF) = \frac{power\ at\ the \max power\ point}{V_{OC}I_{SC}} = \frac{V_R I_R}{V_{OC}I_{SC}} \tag{3.26}$$

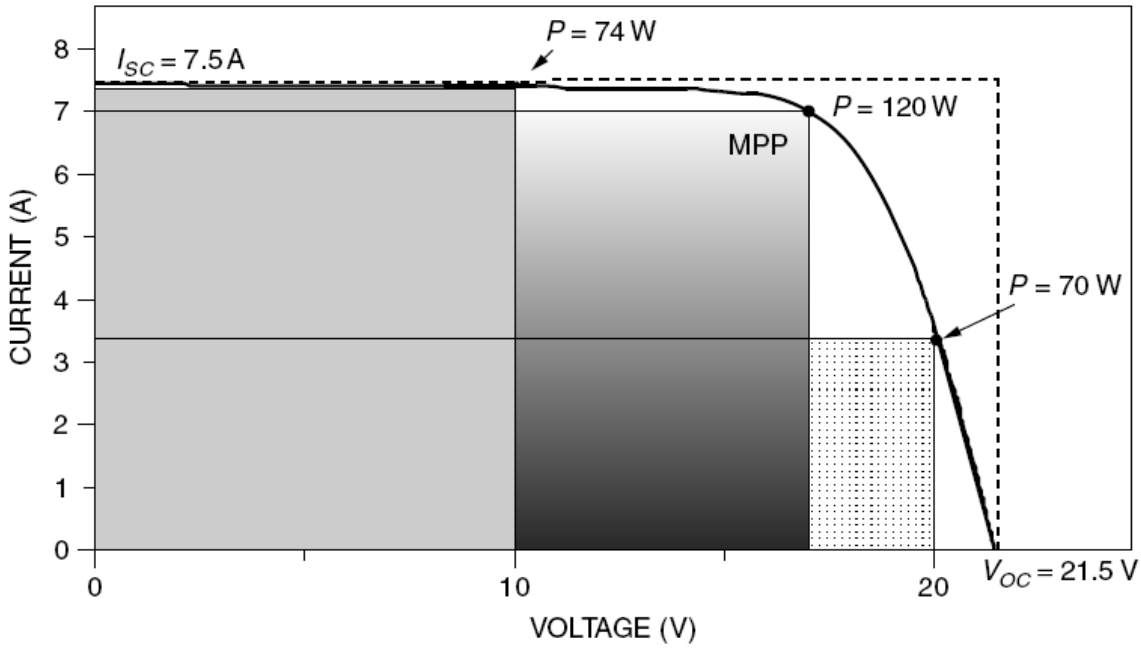

Fig. 3.17 The maximum power point corresponds to the biggest rectangle under the PV module voltage-current characteristic

3.4 Impacts of Temperature and Insolation on *I–V* Curves

Manufacturers will often provide voltage-current curves that show how the curves shift as insolation and cell temperature changes. Fig. 3.18, and 3.19, shows the Current-voltage characteristic curves under various cell temperatures and irradiance levels for the bpsx150 PV module. Since only a small fraction of the insolation hitting a module is converted to electricity and carried away, most of that incident energy is absorbed and converted to heat [32] [33]. To

help system designer's account for changes in cell performance with temperature, manufacturers often provide an indicator called the $NOCT$, which stands for nominal operating cell temperature. $NOCT$ is cell temperature in a module when ambient is 20˚C, solar irradiation is 0.8 kW/m^2, and wind speed is 1 m/s. To account for other ambient conditions, the following expression may be used [34]:

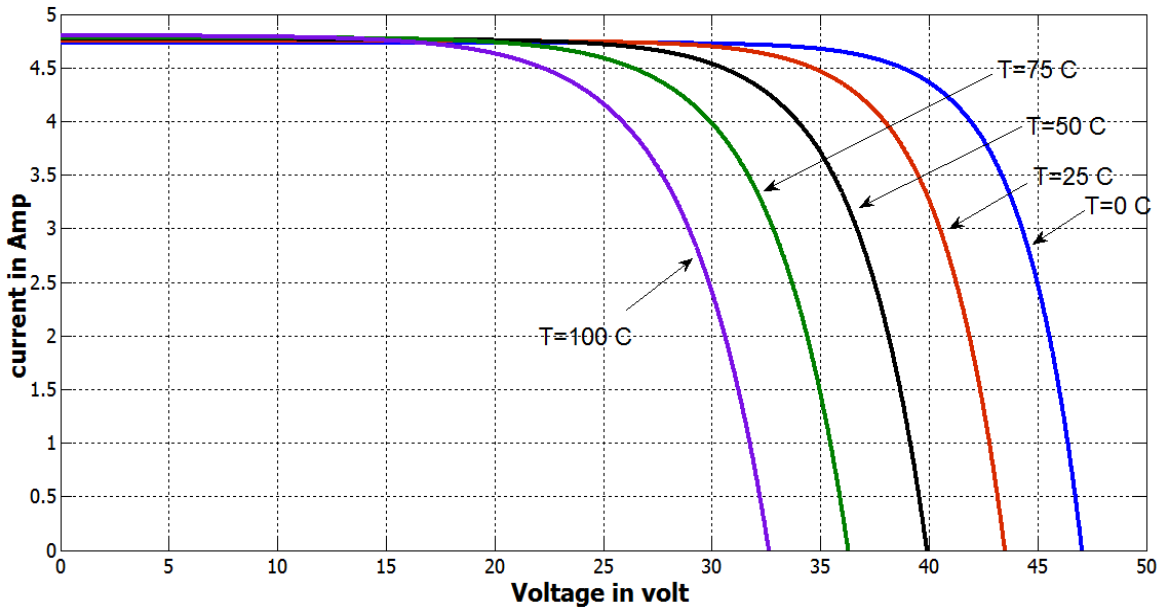

Fig. 3.18 Current-voltage characteristic curves under various cell temperatures and irradiance levels for the bpsx150 PV

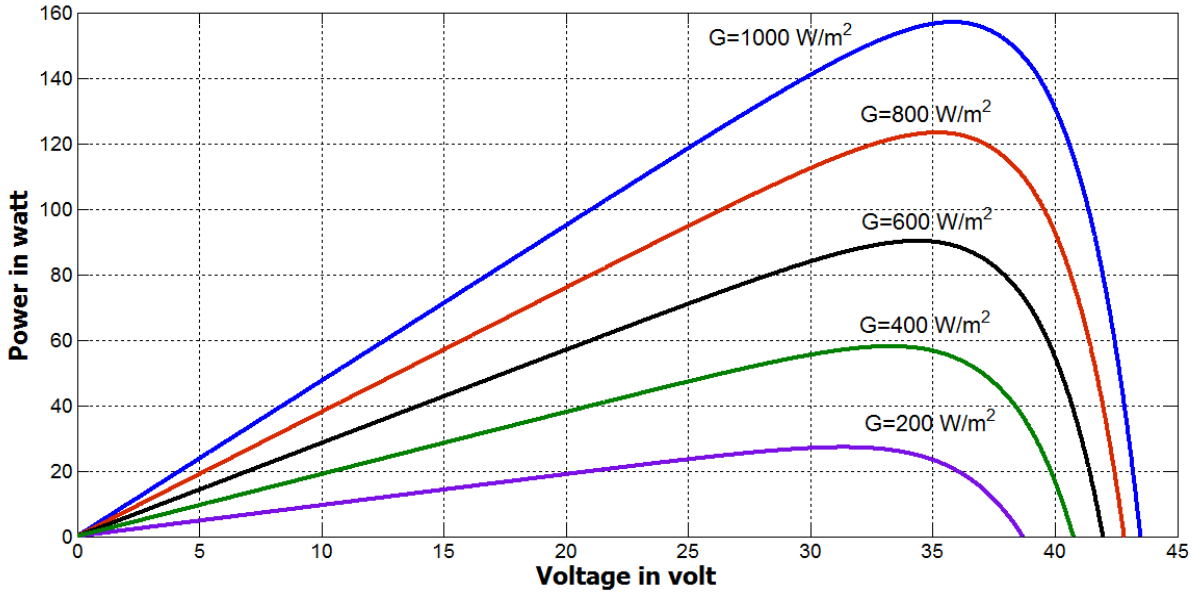

Fig. 3.19 Current-power characteristic curves under various cell temperatures and irradiance levels for the bpsx150 PV

$$T_C = T_a + \left(\frac{NOCT - 20^{\circ}}{0.8}\right) * G \tag{3.27}$$

Where T_C is cell temperature (°C), T_a is ambient temperature, and G is solar insolation (W/m^2).

3.5 PV cell

To study the modes and characteristics of PV panel, in this work, a mathematical model is used that built on the basis of an equivalent electrical equivalent circuit of a solar cell with one diode [35], as shown in Fig. 3.20.

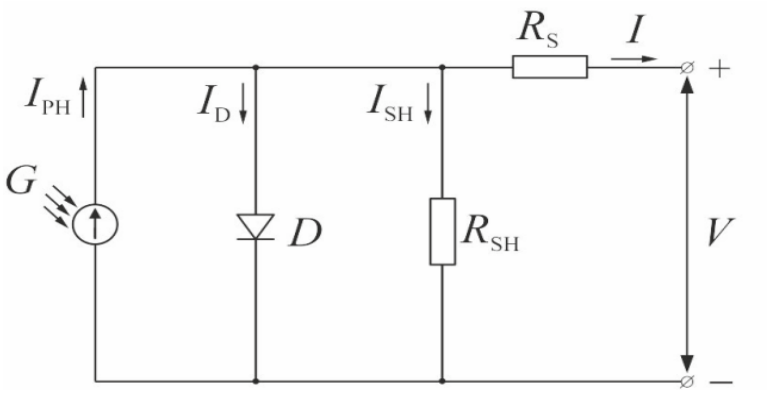

Fig. 3.20. The equivalent circuit of a solar cell

The ideal model of a solar cell consists of a current source that creates an I_{PH} photocurrent, and an ideal diode (D), the current ID through which is determined by the Shockley equation and depends on the absolute temperature (T) and voltage (V) at the output of the PV panel.

Using generally accepted assumptions, I_{PH} and the reverse current of the diode I_0 can be determined from the following expressions:

$$I_{PH} = \left[\, I_{SC_{STC}} + k_i \,.\, (T - T_{STC}) \,\right] * G \tag{3.28}$$

where I_{SC_STC} is the short circuit current of the photovoltaic converter under standard conditions; k_i is the temperature coefficient of short circuit current; T_{STC} is the cell temperature under standard conditions; G is the value of solar irradiance, W / m^2.

$$I_0 = \left[\frac{I_{SC_{STC}}}{exp\left(\frac{q.V_{OC.STC}}{A.K.T_{STC}}\right)}\right] . \left(\frac{T}{T_{STC}}\right)^3 . exp\left[\frac{q.E_G}{K.A}\left(\frac{1}{T_{STC}} - \frac{1}{T}\right)\right] \tag{3.29}$$

where $q = 1{,}602 \cdot 10^{-19}$ C; $k = 1.38 \cdot 10^{-23}$ J / ºK - Boltzmann constant; A is the diode ideality coefficient (takes values from 1 to 5); E_G- semiconductor band gap (determined by the type of SC used).

For a photovoltaic module, consisting of N_S series and N_P, parallel connected panaels, the equation of the current-voltage characteristic has the following form:

$$I = N_P \,.\, I_{PH} - N_P \,.\, I_0 \,.\left[exp\left(\frac{q(V + I.R_S)}{N_S \,.\, A \,.\, K.T}\right) - 1\right] - \frac{V + I \,.\, R_S}{R_{SH}} \qquad (3.30)$$

where I, V are the current and voltage at the terminals of the PV module; R_S and R_{SH} are equivalent series and shunt resistances of the photovoltaic module, respectively.

Equation (3.30) contains five unknown parameters (I_{PH}, I_0, A, R_S, R_{SH}), which are dependent on the surface temperature of the PV string and the intensity of solar irradiance. The technical specification provides important points of the energy characteristics of the PV panel: I_{SC} short circuit current, the analytical expression for which can be obtained from (3.30), substituting $V = 0$ into it; open circuit voltage V_{OC} corresponding to the voltage value at the PV panel terminals with an open external circuit ($I = 0$). The parameters of the operating mode for the load corresponding to the point of maximum power at which $I = I_{MPP}$, $V = V_{MPP}$ are also given.

Using the data of the technical specification of PV panel, it is possible to obtain a numerical solution of equation (3.30) and construct a dynamic mathematical model of PV. For simulation of PV modes, the PV Array standard block from the MATLAB / Simulink library, built on the basis of equations (3.28) - (3.30), was used as a PV model.

To select the parameters of the DC-converter, it is necessary to set the operating range of its input voltage, which is determined by the values of the irradiance G and temperature T_{FM} of the PV modules. Figure 3.21 shows the "family" of volt-watt characteristics of a solar battery, consisting of three Kyocera Solar KD320GX-LPB FM modules in series (the Kyocera polycrystalline module combines the highest energy efficiency with an enviable rated power and stylish design, so it is an undoubted leader in sales for several years), built on the basis of simulation results. The characteristics are built at discrete set values of G = 100, 400, 700, 1000 W / m^2 and T_{FM} = –25, 0, 25, 50ºC, which corresponds to the ranges of the external climatic

conditions under which electric power generation of photovoltaic systems is possible. The shaded area, in Fig. 3.21, defines the working range of the input voltage of the DC converter and its power.

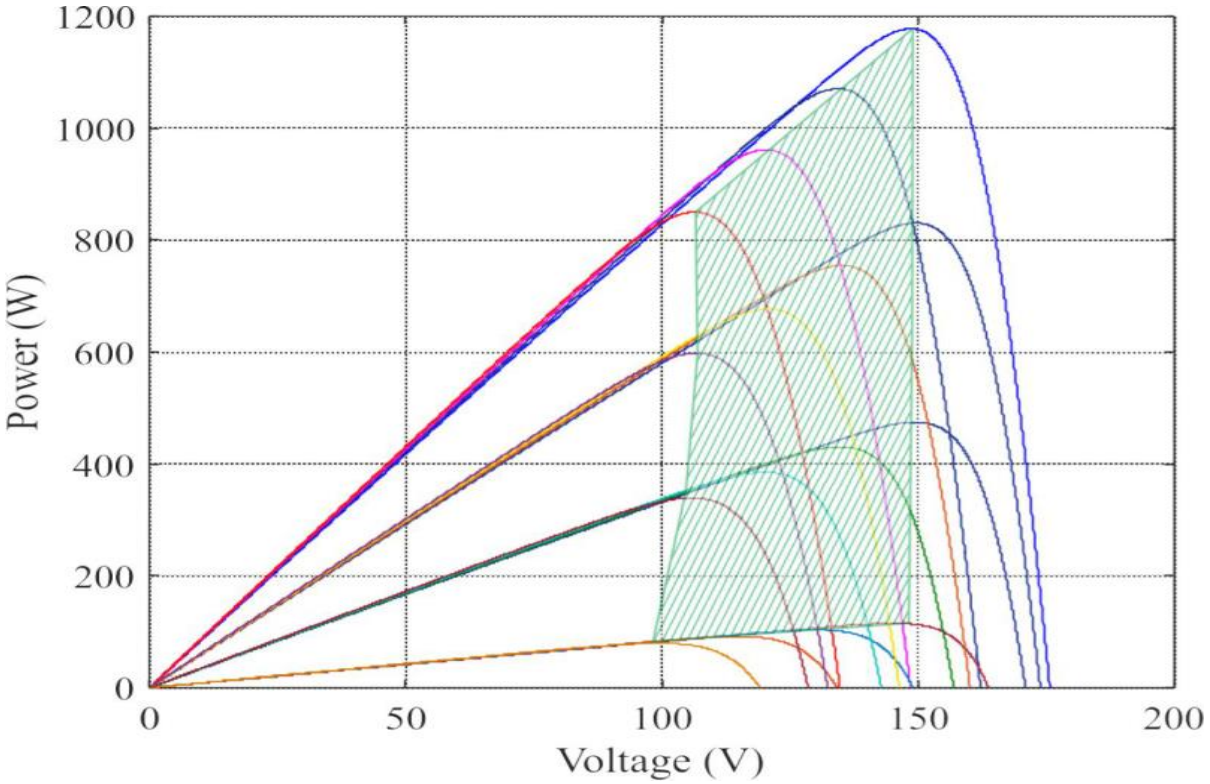

Fig. 3.21 Volt-watt characteristics of PV panel

The task of determining the operating range of input voltages and the nominal power of the DC- DC converter can be significantly simplified by solving it analytically using the technical specification of the PV panel, and also assuming that when the external climatic conditions change, the voltage in MPP changes in proportion to the open-circuit voltage, and the current in MPP changes in proportion to the photocurrent. Then, to determine V_{MPP} and I_{MPP} for arbitrary values of G and T_{FM}, the following equations can be used [14, 15]:

$$I_{MPP} = \left[I_{MPP\_STC} + K_I \,.\, (T_{PM} - T_{STC})\right] . N_{PMp} * \frac{G}{G_{STC}} \tag{3.31}$$

$$V_{MPP} = \left[V_{MPP\_STC} + K_V \,.\, (T_{PM} - I_{STC})\right] . N_{PMs} - \left[\left(I_{MPP_{STC}} - I_{MPP}\right) . R_S\right] * \frac{N_{PMs}}{N_{PMp}} \tag{3.32}$$

where V_{MPP_STC} and I_{MPP_STC} are voltage and current in MPP under standard testing conditions (G_{STC} = 1000 W / m^2, T_{STC} = 25ºC); N_{FMs} and N_{FMp} are the numbers of series-connected and parallel-connected panels in the PV string, respectively; R_S is the series resistance of the PV module. The value of R_S is determined by the expression [14]:

$$R_S = \frac{\frac{N_S .A.K.T_{STC}}{q} ln\left(1-\frac{I_{MPP\_STC}}{I_{SC\_STC}}\right)+V_{OC\_STC}-V_{MPP\_STC}}{I_{MPP\_STC}} \quad (3.33)$$

where N_S is the number of series solar cells in the module.

The above simplified approach for determining the parameters of the MPP PV mode with obvious ease of use provides a sufficiently high accuracy. A comparison of the results of calculating the voltage and current values in the MPP PV panel obtained by equations (4) - (6), with the simulation results of the characteristics of the PV btained by the numerical solution of equations (1) - (3), shows that the maximum error in the determination of V_{MPP} and I_{MPP} in the entire practical range of changes in G and T_{FM} is not more than 4%.

3.6. DC-DC buck converter

The circuit diagram of the buck converter is shown in Fig. 3.22.

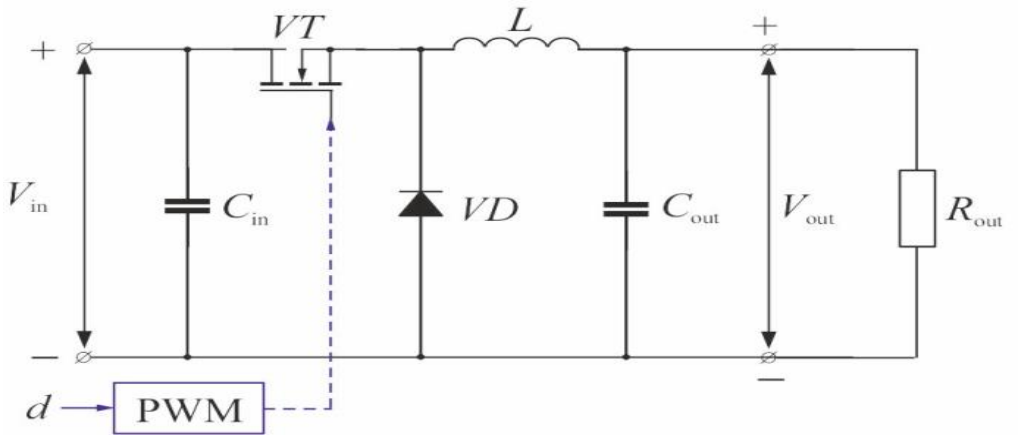

Fig. 3.22. Schematic diagram of DC-DC buckconverter

The main elements of the converter are input capacitive filter C_{in}, transistor switch *VT*, output LC-type smoothing filter on the *L* and C_{out} elements, and a discharge diode *VD*. The power supply of the converter is the PV panel, the output terminals are connected to the resistance *R*out, which simulates the output load of the PV. The transistor switch control signal

is supplied from a pulse width modulation (PWM) generator and is generated based on the values of the duty cycle *d* calculated by the MPPT controller [36] [39].

In most practical cases, the converter is designed to operate in continuous curruent mode (CCM), which ensures its better controllability and minimization of energy loss. The timing diagrams of an ideal converter for the continuous current mode of the inductor are shown in Fig. 3.23.

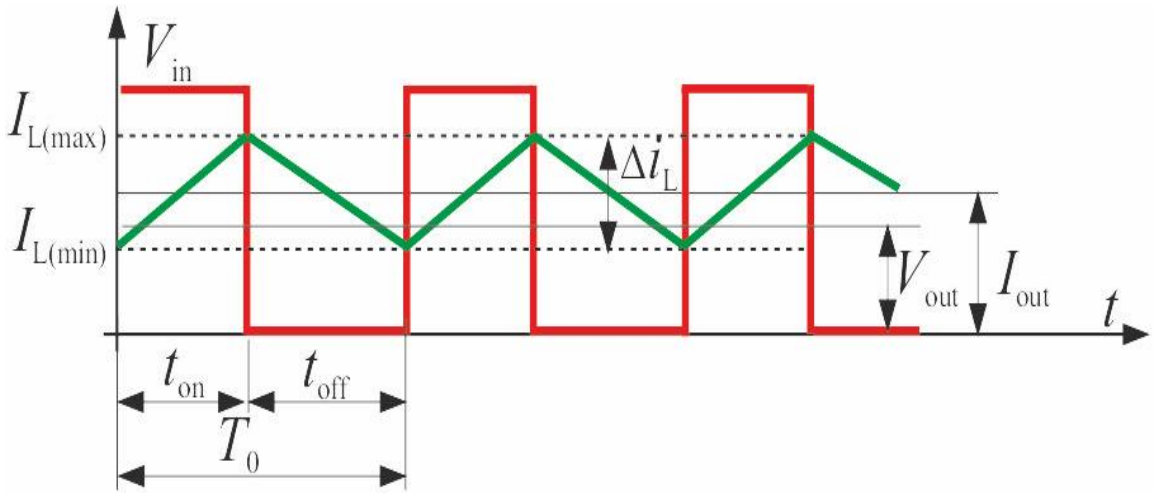

Fig. 3.23. Timing diagram of a buck converter for the continuous current mode of the inductor

If the ripples of the output voltage are neglect, from Fig. 3.23, the ripple current of the inductor can be expressed:

$$\Delta i_L = I_{in(max)} - I_{out(min)} = \frac{V_{in} - V_{out}}{L} * t_{on} = \frac{V_{out}}{L * f} * \left(1 - \frac{V_{out}}{V_{in}}\right) = \frac{V_{out} * (1 - d)}{L * f} \quad (3.34)$$

where t_{on} is the time interval of the conducting state of the key; t_{off} - pause time interval; $T_0 = 1 / f$ is the period of the pulse-width modulated pulses; f is the switching frequency; $d = t_{on} / T_o = V_{out} / V_{in}$–duty cycle or relative pulse duration.

To preserve the CCM up to the minimum load current, the following condition must be fulfilled: $\Delta i_L = 2 \cdot I_{out}$ (min). Fulfillment of this condition will provide a CCM, however, a large ripple negatively affects the saturation of the inductor core and the quality of the output voltage of the converter. Therefore, in practice, the value of current ripple is limited by the choice of

the corresponding ripple coefficient $k_{\Delta i} = \Delta i_L / I_{out}$, the value of which is usually taken within 20–50%. Then, taking into account (3.34), we obtain the condition for choosing L:

$$L \geq \frac{V_{in}}{K_{\Delta I} * f * I_{out(\min)}} * \left(1 - \frac{V_{out}}{V_{in}}\right) = \frac{R_{out(\max)} * (1-d)}{K_{\Delta I} * f} \tag{3.35}$$

The value of the ripple of the output voltage of the converter can be determined by assuming that the AC component of the current is closed only through the filter capacitor C_{out} [16]. Given that the maximum ripple current corresponds to the mode d = 0.5, from Fig. 3.23, one can express the change in charge on the output capacitor:

$$\Delta Q = \frac{1}{2} * \left(\frac{T_0}{2}\right) * \left(\frac{\Delta I_L}{2}\right) = \frac{\Delta i_L}{8 * f} \tag{3.36}$$

Taking into account that the voltage ripple and the change in the charge of the capacitance are related by the relation $\Delta V = \Delta Q / C$ from (3.34) and (3.36), the condition for choosing a filter capacitor can be expressed as:

$$C_{out} \geq \frac{V_{out} * (1-d)}{8 * L * f^2 * \Delta V_{out}} = \frac{(1-d)}{8 * L * f^2 * K_{\Delta V_{out}}} \tag{3.37}$$

where $k_{\Delta Vout} = \Delta V_{out} / V_{out}$ is the permissible ripple coefficient of the output voltage, this value can be determined by the requirements of the load (usually 1–5%).

An obligatory element of the converter is the input capacitor C_{in}, which provides smoothing of the voltage ripples of the PV panel due to the nonlinearity of its characteristics [38]. The capacitor C_{in} is selected from the condition that the ripple of the input voltage of the converter is limited to no more than $k_{\Delta Vin}$ = 1%, which will ensure the most efficient use of the energy generated by the PV panel [37]. The condition for choosing the input capacitor of a step-down voltage converter can be represented in the form of the expression:

$$C_{in} \geq \frac{V_{in} * (1-d)}{8 * L * f^2 * \Delta V_{in}} = \frac{1}{32 * L * f^2} \tag{3.38}$$

The most important task of designing voltage converters is the calculation and analysis of their dynamic characteristics. PWM voltage converters belong to nonlinear discrete automatic control systems, to determine the dynamic characteristics of which are widely used analysis

methods based on approximate averaged models of converting devices [18]. The transfer functions of the buck DC-DC converter according to the control action obtained from the linearized averaged model [19] will be written in the following form:

$$W_{\Delta d}^{\Delta V_{out}}(s) = \frac{V_{in}}{L * C_{out}} * \frac{1}{s^2 + \frac{s}{R_{out} * C_{out}} + \frac{1}{L * C_{out}}} \tag{3.39}$$

$$W_{\Delta I}^{\Delta V_{in}} = \frac{V_{in}}{L * C_{out}} * \frac{s + \frac{1}{R_{out} * C_{out}}}{s^2 + \frac{s}{R_{out} * C_{out}} + \frac{1}{L * C_{out}}} \tag{3.40}$$

Equations (12) describe the response of the output voltage and current of the converter to a change (deviation relative to the linearization point) of the duty ratio *d*. The obtained equation (12) allows us to analyze the frequency characteristics of the converter and synthesize a control system built on the basis of traditional analog controllers.

3.7 The output loads of the DC-DC converter

The nature of loads of the DC-DC voltage converter is determined by the power plant construction schema. For a PV constructed according to schema 1 (see Fig. 1), the operating modes of the DC-DC converter can be considered equivalent to the operating conditions for the load with the same active resistance. In schema 2,the load of the converter is battery bank. In schema 3, DC-DC converter is loaded on a DC bus.

When constructing the simulation model of PV system, the load of the converter was modeled as a separate functional unit (Fig. 3.24), which makes it easy to change the configuration of the system under study.

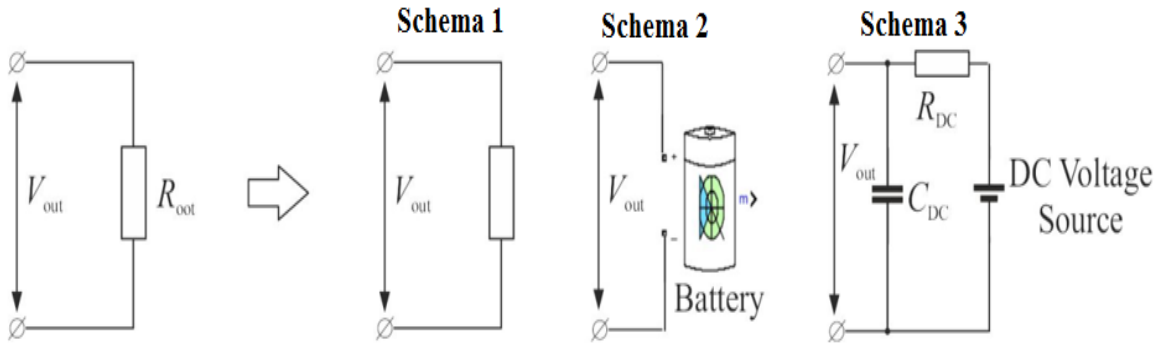

Fig. 3.24. The simulation model of the different loads of the DC-DCConverter of the photovoltaic station

The Battery standard block from the MATLAB / Simulink library is used as a dynamic model of the battery. The DC bus model is based on a C_{DC} capacitor and a DC voltage source with an internal resistance R_{DC}.

3.8 DC-DC boost converter

The modelling of the boost converter is presented in this thesis before beginning our research on the modeling of MPPT controls. This causes the output voltage of Vs to be increased compared to the input voltage of Vpv. The circuit diagram modelling the converter is shown in Figure 3.25, whereas Table 2 summarizes the values of the elements used to make this converter [40].

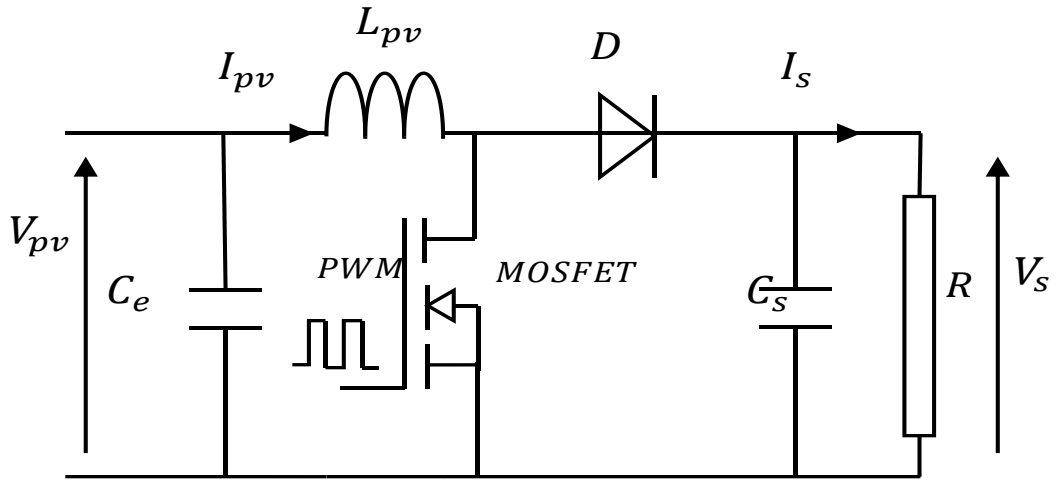

Figure. 3.25. The boost converter scheme

Table 3.2. Component values of DC/DC converter

Parameters	Value
Bobbin L_{pv}	18 mH
Intput capacitorC_e	2200 µF
Output capacitor C_s	2200 µF
Switching frequency of the MOSFT f	1 KHz
Load *R*	22 Ohm

The following equations show the process of the boosting of the voltage of the PV system:

$$V_{pv} = L_{pv}\frac{di_{L_{pv}}}{dt} + (1 - a_{pv})V_s \tag{3.41}$$

$$C_s\frac{dV_s}{dt} + \frac{V_s}{R} = (1 - a_{pv})i_{L_{pv}} \tag{3.42}$$

3.8.1 Maximum Power Point Trackers (MPPTs)

In order to achieve an optimal power transfer, from generator to load, it is imperative to maintain both the PV generator and the load at their respective optimum operating conditions. MPPT algorithms are necessary in PV applications because the MPP of a solar module varies with the irradiation and temperature so the use of MPPT algorithms is required in order to obtain the maximum output power from a solar array. Of course, the maximum power point is the target for the operating point of the PV generator and this is the main task of the MPPT circuits. When a PV module is directly coupled to a load, the PV module's operating point will be at the intersection of its V–I curve and the load line which is the V-I relationship of load as shown in Fig. 3.26.A resistive load has a straight line with a slope of $1/R_{load}$ as shown in Fig. 3.28. In other words, the impedance of load dictates the operating condition of the PV module. In general, this operating point is seldom at the PV module's MPP, thus it is not producing the maximum power.

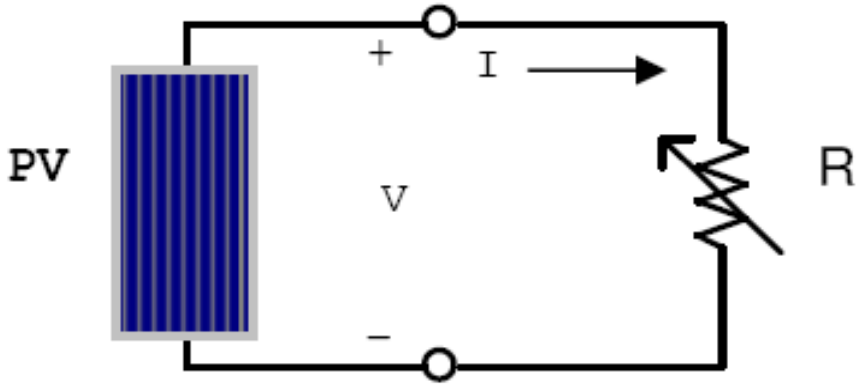

Fig. 3.26. PV module is directly connected to a (variable) resistive load

To mitigate this problem, a maximum power point tracker (MPPT) can be used to maintain the PV module's operating point at the MPP. MPPTs can extract more than 97% of the PV power when properly optimized [41]. A photovoltaic system for the stand-alone PV system applications as shown in Fig. 3.27 is a typically composed of these main components;

- PV module that converts solar energy to electric one.
- DC-DC converter that converts produced DC voltage by the PV module to a load voltage demand.
- Digital controller that drives the converter operation with MPPT capability.

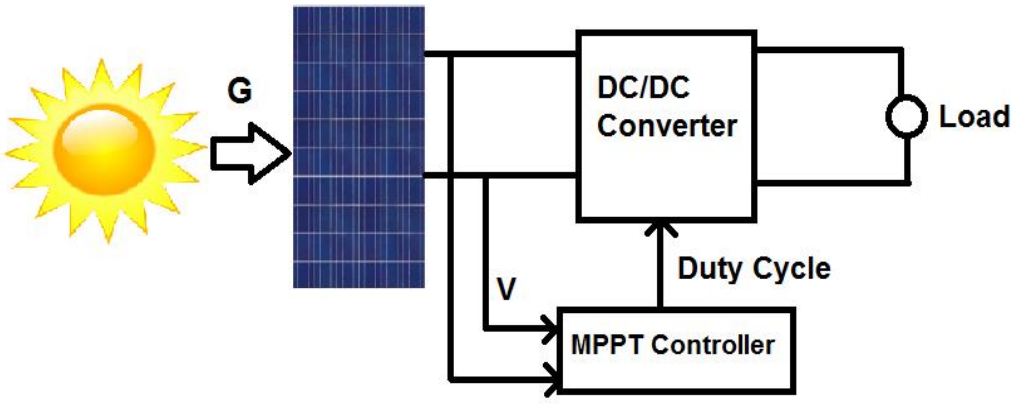

Fig. 3.27 Block diagram of the stand-alone PV system

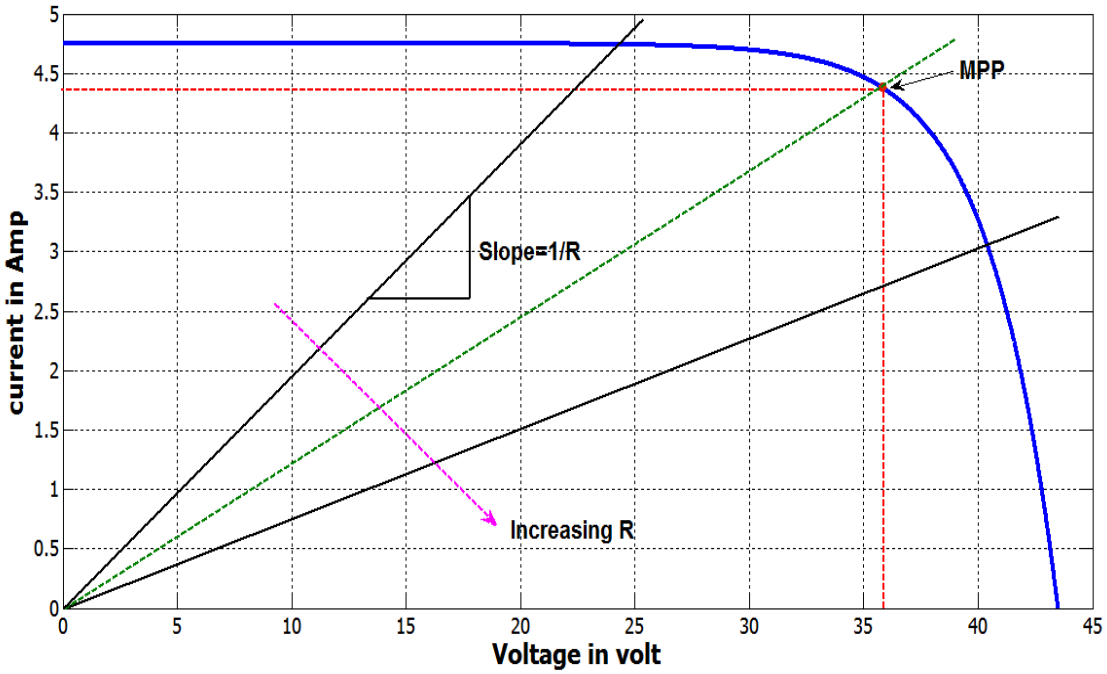

Fig. 3.28 V-I curve of PV module and various resistive loads

Maximum power point trackers are basically DC/DC converters and can be represented as shown in Fig. 3.29. The input power at the DC/DC converter is:

$$P_i = V_i I_i \tag{3.43}$$

And the power supplied by the converter at the output is:

$$P_o = V_o I_o \tag{3.44}$$

The relationship between input and output power defines the DC/DC converter efficiency, η:

$$\eta = \frac{P_o}{P_i} \tag{3.45}$$

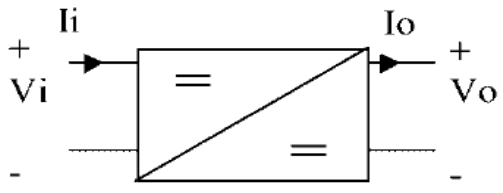

Fig. 3.29 DC/DC converter schematic diagram

In a DC/DC tracker, the input impedance of the DC/DC converter must be adapted in order to force the PV generator to work at the maximum power point. The DC/DC converter output must also be adapted to the specific load characteristics. The DC/DC converter can give a variable DC output voltage from a nominally fixed DC input voltage. Depending on the load requirements the output voltage, V_o, can be lower or higher than the input voltage, V_i. For this reason DC/DC converters can be divided into two main basic categories:

- Voltage reductors also called step-down or buck converters.
- Voltage elevators also called step-up or boost converters.

Other types of DC-DC converters are full-bridge DC-DC converters, Cúk DC-DC converters and buck-boost converters, which can be used in applications where special requirements are needed, mainly negative polarity output, output voltage higher or lower than input voltage or DC motor drives [42] [43]. In the past few years power electronics has produced high performance converters, which can be used in PV applications.

3.9 The improved Particle Swarm Optimization (IPSO)

The PSO is based on the continuous movement of particles in a possible solution space, while each particle in the search space is characterized by two variables: the coordinate and the speed of movement.

The modified PSO algorithm is described by the following system of equations:

$$v_i^{k+1} = v_i^k . w + c_1 . r_1 . \left[Ppbest_i - x_i^k \right] + c_2 . r_2 . \left[Pgbest - x_i^k \right] \qquad (3.46)$$

$$v_i^{k+1} = x_i^k + v_i^k; \qquad i = 1, 2, \ldots\ldots, N; \qquad K = 1, 2, \ldots\ldots, K_{max}$$

Where c_1 and c_2 are the acceleration constants. r_1 and r_2 are random values in the range [0, 1]. *i* denotes the order number of the particle, and *k* denotes the number of the current iteration value. *N* is the number of the particles. k_{max} denotes the maximum number of iterations, and *w* denotes the coefficient of inertia.

The measured voltage and current are provided to the PV panels and the proposed model calculates the maximum power. The value of *d* is updated by Δ*d* with the speed of the particle v_i^k after a certain sampling time *ts*, and the PV system output power is considered to be the fitness function $P_{PV.}$

In this study, the technique that was named by constriction factor based PSO (CFPSO), the convergence of the algorithm is ensured by using a special constriction coefficient *CF*, the numerical values of which are demonstrated by the following equation:

$$CF = \frac{2}{\left|2 - \phi - \sqrt{\phi^2 - 4\,\phi}\right|} \; ; where \;\; \phi = c_1 + c_2 , \;\; \phi > 4 \tag{3.47}$$

The new coordinates of the particle (i.e., the duty cycle *d* of the DC-DC converter) at each iteration of the algorithm are calculated by the equation:

$$d_i^{k+1} = d_i^k + CF \begin{bmatrix} d_i^k + c_1 . r_1 . (Ppbest_i - d_i^k) \\ + c_1 . r_1 . (Pgbest - d_i^k) \end{bmatrix} \tag{3.48}$$

The application of CFPSO algorithm guarantees the convergence of the algorithm for any values of c_1 and c_2, which greatly simplifies the task of determining their optimal values. The results of [6] confirms the possibility of using CFPSO for extracting the MPP of the PV system. Furthermore, preliminary studies have shown that the highest efficiency of the CFPSO algorithm in tracking the MPP is observed at the following numerical values c_1=c_2=2.5, which corresponds to *CF* = 0.382. The principle operation of IPSO is shown in figure 3.30.

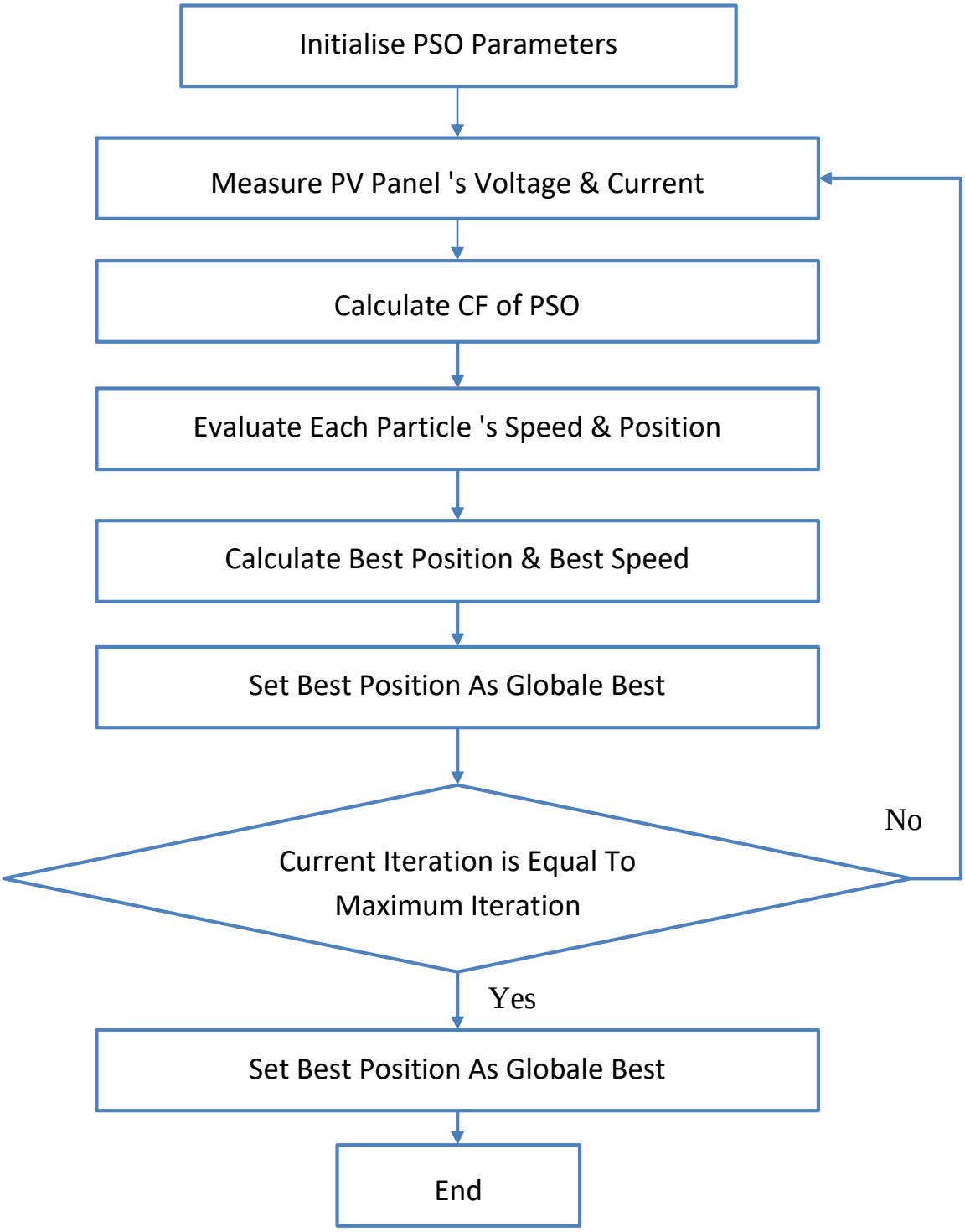

Figure 3.30. The steps of executing the improved particle swarm optimization

3.10 Incremental conductance (IC)

The principle of operation of the increment conductance (IC) algorithm is based on the equality of the instantaneous conductivity of the PV panel and the derivative of the conductivity at the maximum power point [44] [46]. Mathematical relations explaining the operation of the IC algorithm can be easily obtained by differentiating the power *P* of the solar battery with respect to voltage *V*, taking into account the fact that the derivative at the maximum power point vanishes:

$$\frac{dP}{dV} = \frac{d(V.I)}{dV} = I + Vd\left(\frac{dI}{dV}\right) = 0 \tag{3.49}$$

Equation (3.46) can be represented as:

$$\frac{dI}{dV} = -\frac{I}{V} \tag{3.50}$$

Expression (3.47) implies two important relationships that allow to determine the position of the operating point of the PV on its voltage-power characteristics relative to the point of maximum power:

$$\begin{cases} \frac{dI}{dV} = -\frac{I}{V} \ \left(\frac{dP}{dV} > 0\right) & -Left\ of\ MPPT; \\ \frac{dI}{dV} = -\frac{I}{V} \ \left(\frac{dP}{dV} > 0\right) & -Right\ of\ MPPT; \end{cases} \tag{3.51}$$

Taking into account relations (3.48), the operation of the IC algorithm can be represented in the form of a block diagram shown in Fig. 3.31 In the PV simulation model,

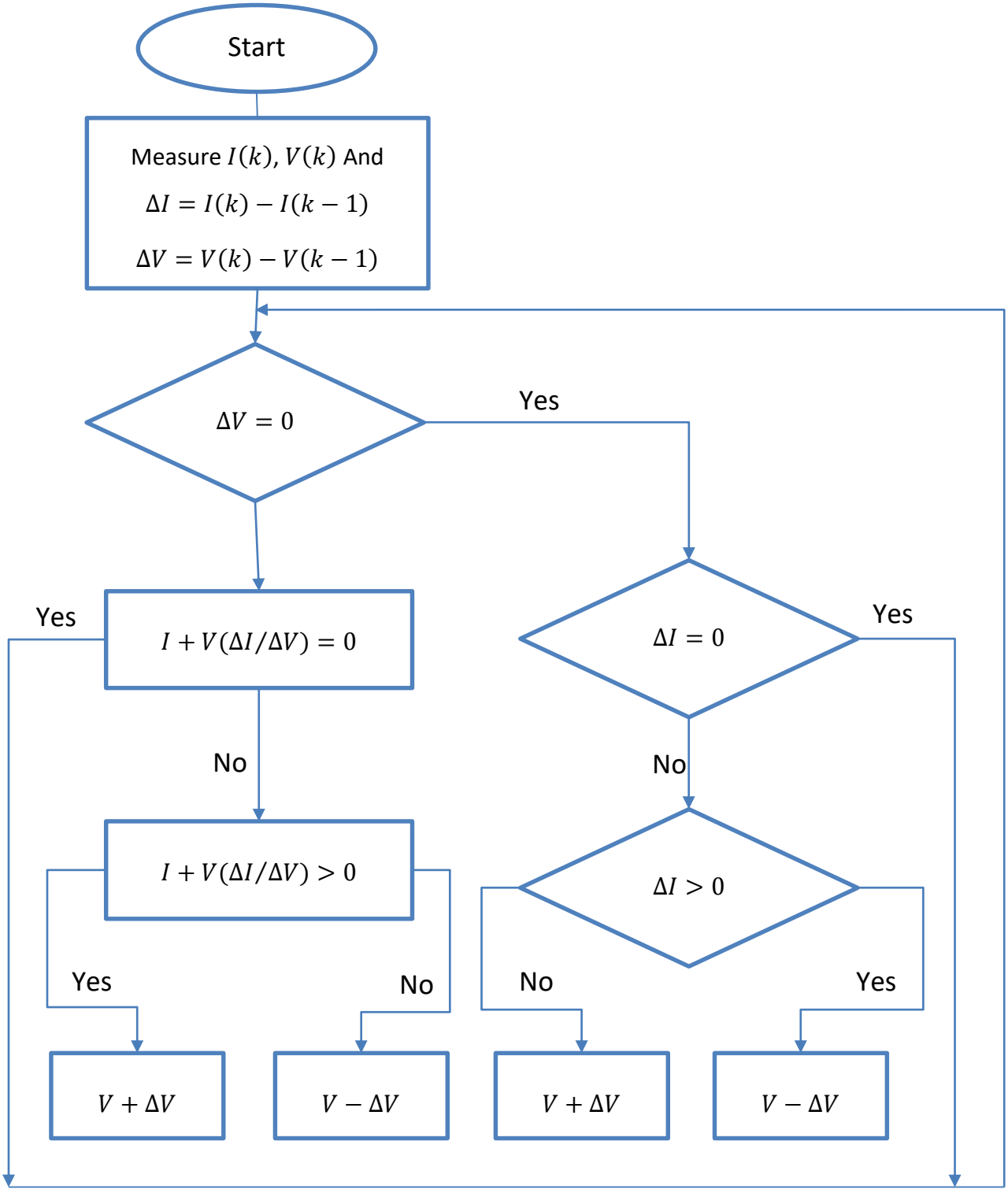

Figure 3.31. Flowchart for the incremental conductance algorithm

3.11 Perturb-and-observe

The perturb and observe (P&O) algorithm is the most commonly used in practice because of its easiness of implementation [45]. Fig. 4.1 shows the flowchart of this algorithm. The most basic form of the P&O algorithm operates as follows. Consider Fig. 3.33, which shows a family of PV array power curves as a function of voltage, P–V curves, at different irradiance, G levels, for uniform irradiance and constant temperature. As previously described, these curves have global maxima at the MPP. Assume the PV array to be operating at point A in Fig. 3.30, which is far from the MPP.

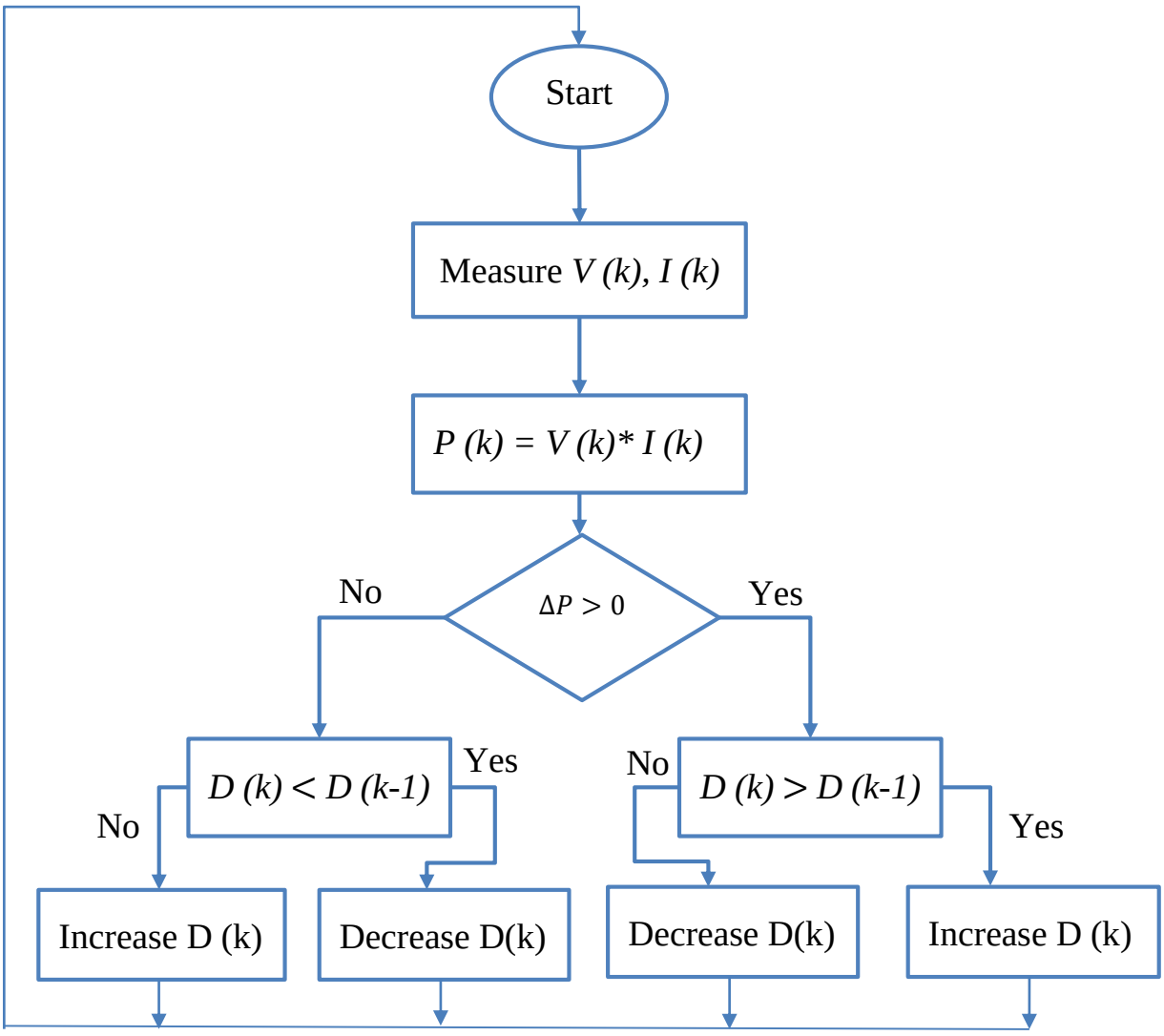

Fig. 3.32 Flowchart of the P&O algorithm

In the P&O algorithm, the operating voltage of the PV array is perturbed by a small increment, and the resulting change in power, ΔP, is measured. If ΔP is positive, then the perturbation of the operating voltage moved the PV array's operating point closer to the MPP. Thus, further voltage perturbations in the same direction (that is, with the same algebraic sign) should move the operating point toward the MPP. If ΔP is negative, the system operating point has moved away from the MPP, and the algebraic sign of the perturbation should be reversed to move back toward the MPP. Fig. 3.34 shows the previous stated cases for the P&O algorithm. The advantages of this algorithm, as stated before, are simplicity and easiness of implementation.

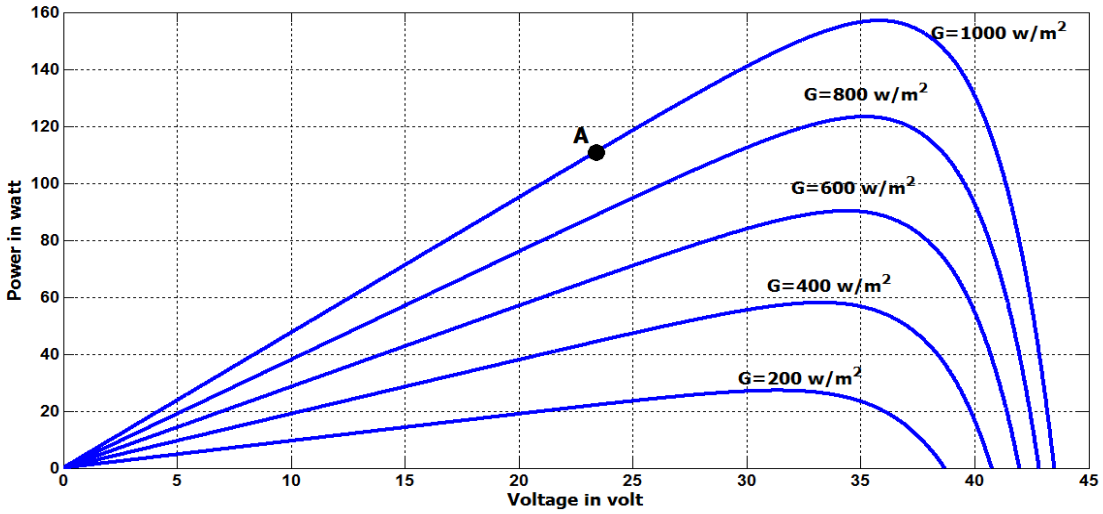

Fig. 3.33 Photovoltaic array power–voltage relationship

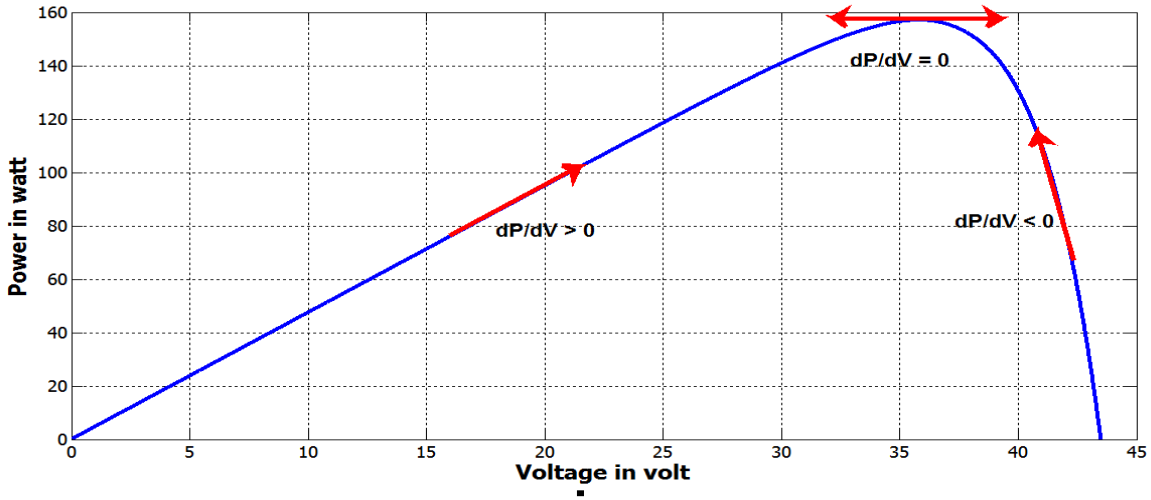

Fig. 3.34 The P&O algorithm modes for the PV module at G=1000 W/m^2 and temperature 25^{o}C

However, P&O has limitations that reduce its MPPT efficiency. One such limitation is that as the amount of sunlight decreases, the P–V curve flattens out, as seen in Fig. 3.33. This makes it difficult for the MPPT to determine the location of the MPP, owing to the small change in power with respect to the perturbation of voltage [47]. Another fundamental drawback of P&O is that it cannot determine when it has actually reached the MPP [48] [49]. Instead, it oscillates around the MPP, changing the sign of the perturbation after each ΔP measurement. Also, it has been shown that P&O can exhibit erratic behavior under rapidly changing irradiance levels. Consider the case in which the irradiance is such that it generates P–V curve 1 in Fig. 3.35. The MPPT is oscillating around the MPP from point B to A to C to A and so on.

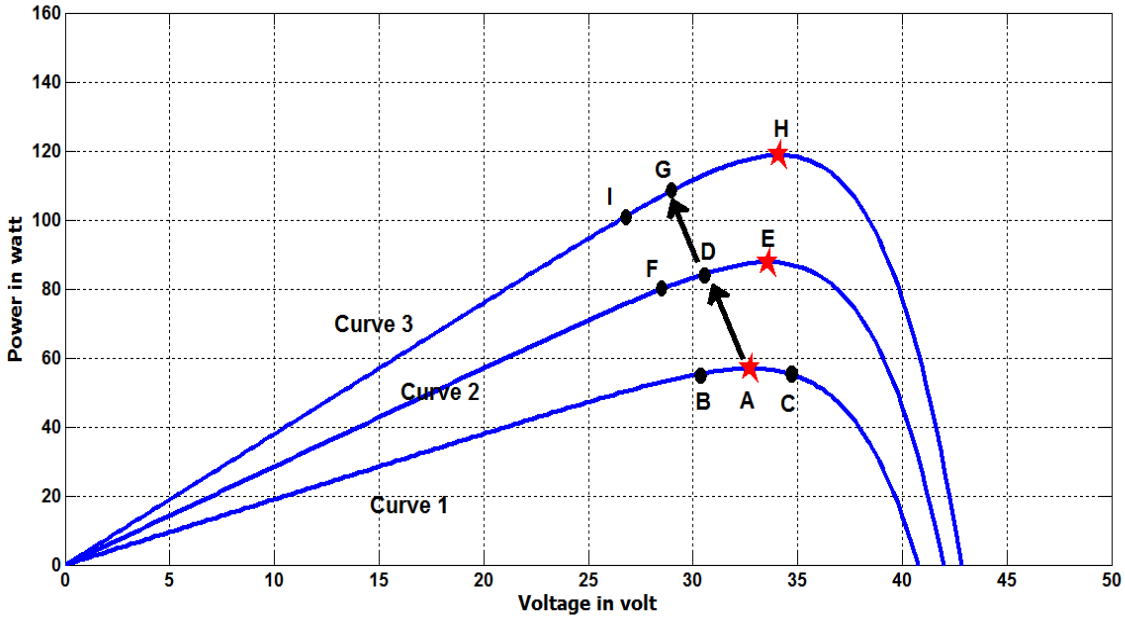

Fig. 3.35 Illustration of erratic behavior of P&O under rapidly increasing irradiance

Then, assume the irradiance increases and the P–V curve of the array moves to curve 2. If, during the rapid increase in solar irradiance and output power, the MPPT was perturbing the operating point from point A to point B, the MPPT would actually move from A to D. As seen in Fig. 3.35, this result in a positive ΔP and the MPPT will continue perturbing in the same direction, toward point F. If the irradiance is still rapidly increasing, the PV power curve will move to G on curve 3 instead of to F on curve 2. Again the MPPT will see a positive ΔP and will assume it is moving towards the MPP, continuing to perturb to point I. From points A to D to G to I the MPPT is continually moving away from the MPP, decreasing the efficiency of the

P&O algorithm. This situation can occur on partly cloudy days, when MPP tracking is most difficult, owing to the frequent movement of the MPP.

The main task of designing digital MPPT controllers is to determine the clock frequency f_d of the change in the duty cycle of the DC-DC converter.

It is advisable to select the value of f_d from the condition of stable operation of the control system, which is ensured if the transient process in the converter, caused by a change in the control action or external conditions, ends in the time $t_s = 1 / f_d$.

The time constant of the step-down DC-DC converter τ can be approximately found from the equation:

$$\tau = \frac{L}{R_{out}} . \tag{3.52}$$

According to that the duration of any transient process is up to 5 of τ, it is recommended to use the expression to determine the optimal value of t_s:

$$t_s \geq 5 \cdot \tau . \tag{3.53}$$

The choice of the value of t_s according to condition (3.9) will ensure maximum performance of the MPPT controller and at the same time stable operation in MPP.

For determining the parameters of the MPPT controller, the load nature of the DC-DC converter must be considered. For PV constructed according to schema 1, the value of the equivalent electrical load is uniquely determined by this expression:

$$R_{out} = R_{load} . \tag{3.54}$$

In PV, according to schema 2 and 3, the voltage at the converter output is stabilized. Neglecting the change in voltage on the battery bank clamps from the value of its charge and without taking into account the states of the DC bus, the value of the equivalent resistance of the DC-DC converter can be determined through the output power. For an ideal converter with a stabilized output voltage, the equivalent output resistance is determined by the formulas:

$$R_{out(\min)} = \frac{{V_{out}}^2}{P_{MPP(max)}}; \qquad R_{out(\max)} = \frac{{V_{out}}^2}{P_{MPP(min)}}, \tag{3.55}$$

where P_{MPP} (max), P_{MPP} (min) are the values of the maximum and minimum powers generated by the PV module.

Since the converter time constant is inversely proportional to R_{out}, it is necessary to substitute the minimum value of the equivalent resistance determined by (19) into equation (16).

An important parameter of the digital MPPT controller is the value of the change in the operating cycle of the converter Δd during the sampling time ts. A large Δd value shortens the MPP search time, but this reduces the tracking accuracy and can also lead to an oscillatory mode near MPP. It can be approximately assumed that the magnitude of the step in changing the output power of the PV panelΔP linearly depends on the value of Δd. With this assumption, to determine the optimal value of Δd, you can use the equation:

$$\Delta d = \frac{\varepsilon}{100}\,(d_{max} - d_{max}) \tag{3.56}$$

Where ε is the permissible relative error (%); dmin, dmax are the minimum and maximum values of the duty cycle, respectively. The results of the studies showed that a good compromise between the speed and accuracy of tracking MPP provides the value ε = 1%, which was used in the computational experiments.

3.12 MPPT by using fuzzy logic

In recent years, fuzzy logic control has been widely used in maximum power point tracking (MPP) systems [50]–[47], this control does not require the exact knowledge of the model to be regulated. However, a good knowledge of the behavior of the system is required for the development of such a regulator.

The implementation of a fuzzy controller is carried out in three steps: fuzzification, inference and defuzzification (Figure 3.36).

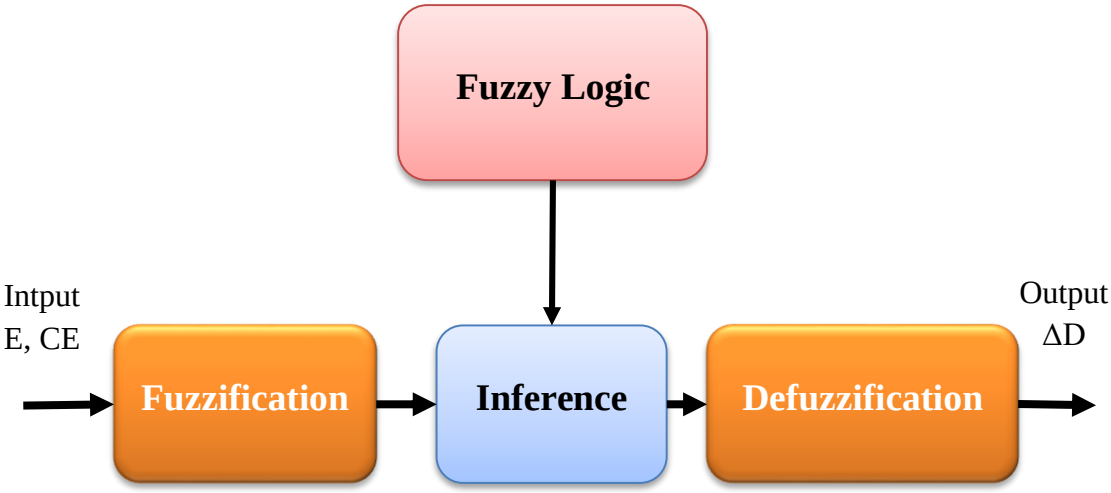

Figure. 3.36. Principle of the Fuzzy Controller

3.12.1. Fuzzification

Controls are selected depending on the satisfaction of two control variables in the proposed input; they are the E error and the change in CE error in the k-test. We display the E and CE variants in the following form:

$$E(k) = \frac{P(k)-P(k-1)}{V(k)-V(k-1)} \tag{3.57}$$

$$CE(k) = E(k) - E(k-1) \tag{3.58}$$

Where:

P(k) the power and V(k) voltage of PV module. The change in duty cycle ratio (ΔD) of the DC-DC Boost Converter is used as the output of the controller. Therefore, the control is done by changing this duty cycle ratio according to the slope E(k) in order to track the operation point optimal where the slope is zero

The input variables of the fuzzy controller E, CE are converted to seven the linguistic variables NB (negative big), NM (Negative Medium), NS (negative small), ZO (zero), PS (positive small), PM (Positive Medium), PB (positive big) using basic fuzzy subset. Figures 3.37, 3.38 and 3.39 shows the membership grades of seven basic fuzzy subsets for input and output variables. Which can adapt shape up to appropriate system [51], [52]

The main goal of the rules are to bring the operation point of PV module to the Maximum Power Point (MPPT) by increasing or decreasing the duty cycle ratio of DC-DC boost Converter depending on the position of the operation point from the MPPT.

3.12.2. Inference method

A rule is applied to fuzzy input by the inference engine to determine the fuzzy output. Therefore, the real input value must be fuzzified , before the rule can be evaluated to obtain an appropriate linguistic value. The fuzzy controller rule table shows in figure 2, where all the matrix entries are fuzzy sets of the error E and the change of error CE and the change of duty cycle ratio ΔD to boost converter. the fuzzy logic controller output is converted from a linguistics variables to a numerical variables. Since the DC-DC boost converter require a precise control signal D at its entry, This the operation is called defuzzification [50],[53], [54].

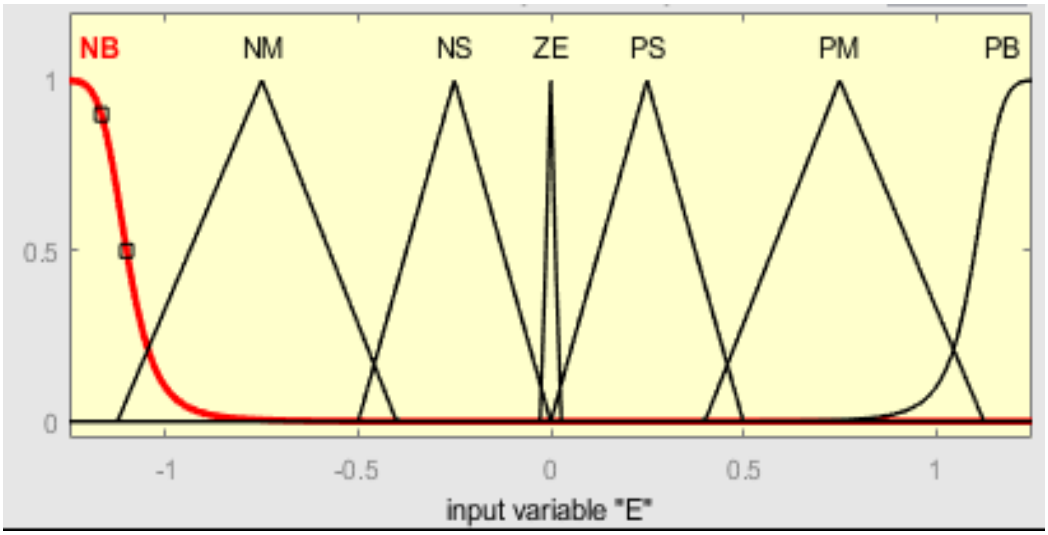

Figure. 3.37. Membership function for Input E

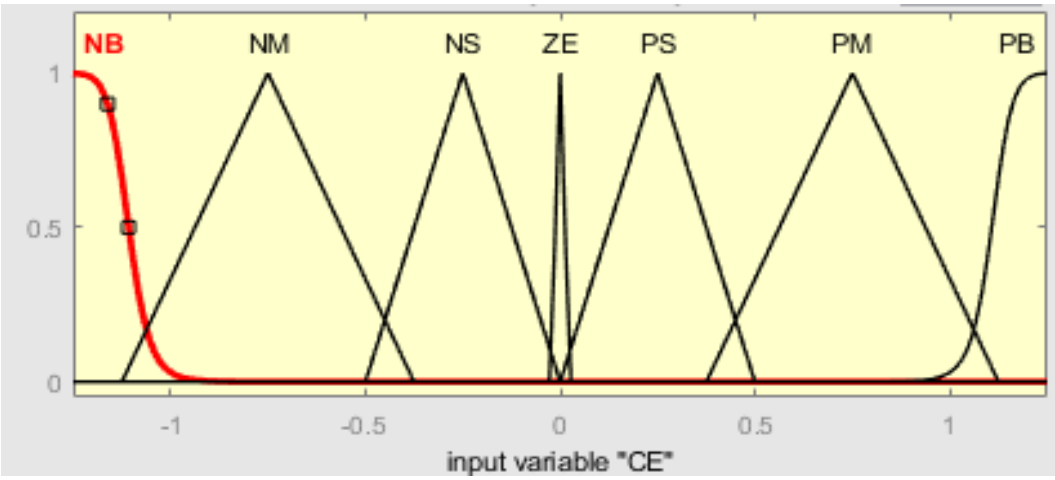

Figure. 3. 38. Membership function for Input CE

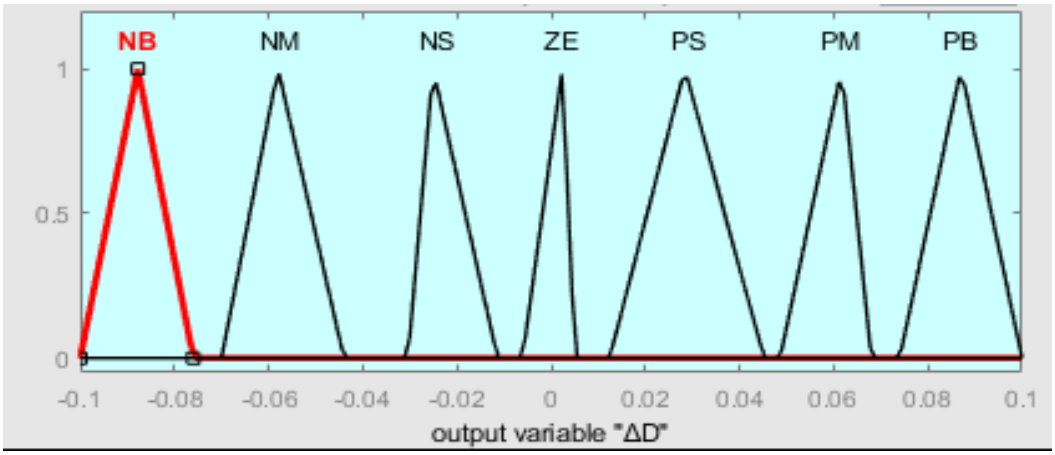

Figure. 3.39. Membership function for Output ΔD

The rule Table 3 contains 49 rules of fuzzy controller.

Table. 3.3, The rule contains 49 rules of fuzzy controller.

CE / E	NB	NM	NS	ZE	PS	PM	PB
NB	NB	NB	NB	NB	NM	NS	ZE
NM	NB	NB	NB	NM	NS	ZE	PS
NS	NB	NM	NM	NS	ZE	PS	PM
ZE	NB	NM	NS	ZE	PS	PM	PB
PS	NM	NS	ZE	PS	PB	PB	NS
PM	NS	ZE	PS	PM	PB	PB	ZE
PB	PB	ZE	PS	PM	PB	PB	PB

3.12.3. Defuzzification

Defuzzification is the process of obtaining a single number from the output with can, defined by two algorithms; the max criterion method (MCM) and center of area (COA) .

$$\Delta D = \frac{\sum_{j=1}^{n} \mu(\Delta D_j).\Delta D_j}{\sum_{j=1}^{n} \mu(\Delta D_j)} \tag{3.59}$$

the actual duty cycle ratio D is calculated as follows:

$$D(k) = D(k-1) + S_{\Delta D}\Delta D(k) \tag{3.60}$$

Fig. 11 shows the FLC output surface using Matlab/Simulink simulation, which represent the relationship between the FLC inputs (E , CE) and output (ΔD) used.

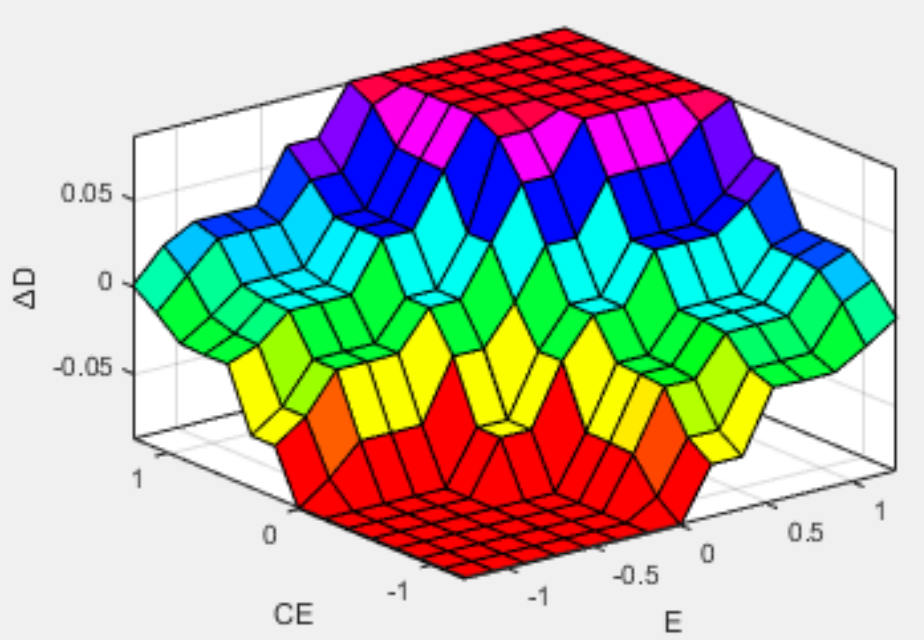

Figure. 3.40. Fuzzy control output surface.

3.13 Conclusion

In this chapter, the mathematical model development for the component parts of the proposed PV system are discussed. The component parts are: PV array, a DC-DC converter operating under the control of the MPPT point search controller. For a PV constructed according to schema 1 (see Fig. 3.24), the operating modes of the DC-DC converter can be considered equivalent to the operating conditions for the load with the same active resistance. In schema 2, the load of the converter is battery bank. In schema 3, DC-DC converter is loaded on a DC bus.

The chapter begins with the physical structure of PV cells along with the fundamental concept and principles of converting the solar energy to electrical energy. The modeling of equivalent electrical circuit of PV cell presented and discussed. The model is implemented using MATLAB to study the PV characteristics. Furthermore, the low output power of the single cell is discussed and how to connect number of cells in series and parallel to form a PV panel and array to meet the desired load power. The effect of temperature and solar radiation on the I-V and P-V characteristics of PV cell also discusses this chapter to show the importance of MPPT in the PV system.

This chapter introduces and investigates various DC-DC converters used in the MPPT algorithms of PV systems. As the PV system is proposed in this work is a stand-alone system therefore, the focus was on the Buck converter. The electrical circuit of this converter was presented and operating concept of this convert was thoroughly discussed. And then followed by a proposed three MPPT controllers: novel improved particle swarm optimization (IPSO), the conventional incremental conductance algorithm (P&O) and perturb and observe (IC) algorithm. To verify the functionality and benefits of the proposed MPPT techniques.

References

[1] S. Munisekhar, G. V. Marutheswar, P. Sujatha, K.R. Vadivelu, "A novel approach for the fastest MPPT tracking Algorithm for a PV array fed BLDC motor driven air conditioning system," Indonesian Journal of Electrical Engineering and Computer Science, vol. 18, pp. 622-628, 2020.

[2] Guohui Zeng, Xiubin Zhang, Junhao Ying,Changan Ji, " A Novel Intelligent Fuzzy Controller for MPPT in Grid-connected Photovoltaic Systems", Proc. of the 5th WSEAS/IASME Int. Conf. on Electric Power Systems, High Voltages, Electric Machines, Tenerife, Spain, December 16-18, 2005, pp. 515-519.

[3] M.S. Aït Cheikh, C. Larbes, G.F. Tchoketch Kebir and A. Zerguerras, " Maximum power point tracking using a fuzzy logic control scheme", Revue des Energies Renouvelables, Vol. 10, No 3, 2007, pp. 387 – 395.

[4] A. Jäger-Waldau, European Commission, and Joint Research Centre, {PV} status report 2018 study. 2018.

[5] N. A. Kamarzaman and C. W. Tan, "A comprehensive review of maximum power point tracking algorithms for photovoltaic systems," Renew. Sustain. Energy Rev., vol. 37, pp. 585–598, Sep. 2014.

[6] S. G. Obukhov, I. A. Plotnikov, and S. K. Sheryazov, "Methods of effective use of solar power system," in 2016 2nd International Conference on Industrial Engineering, Applications and Manufacturing (ICIEAM), 2016, pp. 1–6

[7] M. A. Husain, A. Tariq, S. Hameed, M. S. Bin Arif, and A. Jain, "Comparative assessment of maximum power point tracking procedures for photovoltaic systems," Green Energy Environ., vol. 2, no. 1, pp. 5–17, Jan. 2017

[8] G. Shankar and V. Mukherjee, "MPP detection of a partially shaded PV array by continuous GA and hybrid PSO," Ain Shams Eng. J., vol. 6, no. 2, pp. 471–479, Jun. 2015

[9] S. G. Obukhov, I. A. Plotnikov, and S. K. Sheryazov, "Methods of effective use of solar power system," in 2016 2nd International Conference on Industrial Engineering, Applications and Manufacturing (ICIEAM), 2016, pp. 1–6

[10] Mirhassaniet SM, Golroodbari SZ, Golroodbari SM, Mekhilef S. An improved particle swarm optimization based maximum power point tracking strategy with variable sampling time. Electr Power Energy Syst 2015; 64:761–70

[11] Rezk H, Fathy A. Simulation of global MPPT based on teaching–learning-based optimization technique for partially shaded PV system. Electr Eng 2016. http://dx.doi.org/10.1007/s00202-016-0449-3, (Oct)

[12] Ahmed J, Salam Z. A Maximum Power Point Tracking (MPPT) for PV system using Cuckoo Search with partial shading capability. Appl Energy 2014;119:118–30

[13] Kofinas P, Dounis AI, Papadakis G, Assimakopoulos MN. An Intelligent MPPT controller based on direct neural control for partially shaded PV system. Energy Build 2015; 90:51–64

[14] Sarvi, M., Ahmadi, S., Abdi, S., 2015. A PSO-based maximum power point tracking for photovoltaic systems under environmental and partially shaded conditions. Prog. Photovoltaics Res. Appl. 23, 201–214. https://doi.org/10.1002/pip.2416

[15] Karami, N., Moubayed, N., Outbib, R., 2017. General review and classification of different MPPT Techniques. Renew. Sustain. Energy Rev. https://doi.org/10.1016/j.rser.2016.09.132

[16] http://en.wikipedia.org/wiki/Solar_panel

[17] Manwell, J.F., & McGowan, J.G., "Lead acid battery storage model for hybrid energy systems", Solar Energy, 50(5), 1993, pp. 399-405.

[18] « International Energy Agency ». [En ligne]. Disponible sur: http://www.iea.org/. [Consulté le: 21-mai-2018].

[19] K. Ramalingam et C. Indulkar, « Chapter 3 - Solar Energy and Photovoltaic Technology », in Distributed Generation Systems, Butterworth-Heinemann, 2017, p. 69-147.

[20] A. H. Ali, H. S. Hamad and A. A. Abdulrazzaq, "Performance Investigation of Grid Connected Photovoltaic System Modeling Based on MATLAB Simulation," International Journal of Electrical and Computer Engineering (IJECE), vol. 8, no. 6, pp. 4847-4854, 2018.

[21] L. Fialho, R. Melicio, V. M. F. Mendes, J. Figueiredo, et M. Collares-Pereira, « Effect of Shading on Series Solar Modules: Simulation and Experimental Results », Procedia Technol., vol. 17, p. 295-302, janv. 2014.

[22] L. Bun, « Détection et localisation de défauts dans un système photovoltaïque », Thèse de Doctorat, GRENOBLE, 2011.

[23] H. M. Abd Alhussain, N. Yasin, "Modeling and simulation of solar PV module for comparison of two MPPT algorithms (P&O & INC) in MATLAB/Simulink,'' Indonesian Journal of Electrical Engineering and Computer Science (IJEECS), vol. 18, 2020.

[24] F. Martínez-Moreno, J. Muñoz, et E. Lorenzo, « Experimental model to estimate shading losses on PV arrays », Sol. Energy Mater. Sol. Cells, vol. 94, no 12, p. 2298-2303, déc. 2010.

[25] O. Bingöl et B. Özkaya, « Analysis and comparison of different PV array configurations under partial shading conditions », Sol. Energy, vol. 160, p. 336-343, janv. 2018.

[26] S. Skouri, A. Ben Haj Ali, S. Bouadila, M. Ben Salah, et S. Ben Nasrallah, « Design and construction of sun tracking systems for solar parabolic concentrator displacement », Renew. Sustain. Energy Rev., vol. 60, p. 1419-1429, juill. 2016.

[27] B. Das, A. Jamatia, A. Chakraborti, P. R. Kasari, et M. Bhowmik, « New Perturb and Observe MPPT algorithm and its validation using data From PV module », Int. J. Adv. Eng. Technol., vol. 4, no 1, p. 579-591, 2012.

[28] G. A. Madrigal, K. G. Cuevas, V. Hora, K. M. Jimenez, J. N. Manato, M. J. Porlaje, B. Fortaleza, "Fuzzy logic-based maximum power point tracking solar battery charge controller with backup stand-by AC generator," Indonesian Journal of Electrical Engineering and Computer Science (IJEECS), vol. 16, pp.136–146, 2019.

[29] M. A. Elgendy, B. Zahawi, et D. J. Atkinson, « Assessment of Perturb and Observe MPPT Algorithm Implementation Techniques for PV Pumping Applications », IEEE Trans. Sustain. Energy, vol. 3, no 1, p. 21-33, janv. 2012.

[30] J. Kivimaki, S. Kolesnik, M. Sitbon, T. Suntio, et A. Kuperman, « Design Guidelines for Multiloop Perturbative Maximum Power Point Tracking Algorithms », IEEE Trans. Power Electron., vol. 33, no 2, p. 1284-1293, févr. 2018.

[31] T. C. C. Saibabu et J. S. Kumari, « Modeling and Simulation of PV Array and its Performance Enhancement Using MPPT (P&O) Technique », Int. J. Comput. Sci. Commun. Netw., vol. 1, no 1, p. 9-16, oct. 2011.

[32] R. Subha, S. Himavathi, "Active power control of a photovoltaic system without energy storage using neural networkbased estimator and modified P&O algorithm," IET Generation, Transmission & Distributionn, vol. 12, pp. 927-934, 2018.

[33] N. Adhikari, "Design of solar photovoltaic energy generation system for off grid applications," Int. J. of Renewable Energy Technology, vol. 9, pp. 198 – 207, 2018.

[34] N. Femia, G. Petrone, G. Spagnuolo, et M. Vitelli, « Optimizing sampling rate of P&O MPPT technique », in 35th Annual IEEE Power Electronics Specialists Conference, Aachen, Germany, 2004, p. 1945-1949.

[35] N. S. D'Souza, L. A. C. Lopes, et X. Liu, « Comparative study of variable size perturbation and observation maximum power point trackers for PV systems », Electr. Power Syst. Res., vol. 80, no 3, p. 296-305, mars 2010.

[36] E. Irmak and N. Güler, "A model predictive control-based hybrid MPPT method for boost converters," International Journal of Electronics, Taylor & Francis, 2019.

[37] M. A. Sahnoun, H. M. R. Ugalde, J.-C. Carmona, et J. Gomand, « Maximum Power point Tracking Using P&O Control Optimized by a Neural Network Approach: A Good Compromise between Accuracy and Complexity », Energy Procedia, vol. 42, p. 650-659, 2013.

[38] K. L. Lian, J. H. Jhang, et I. S. Tian, « A Maximum Power Point Tracking Method Based on Perturb-and-Observe Combined With Particle Swarm Optimization », IEEE J. Photovolt., vol. 4, no 2, p. 626-633, mars 2014

[39] H. M. El-Helw, A. Magdy, et M. I. Marei, « A Hybrid Maximum Power Point Tracking Technique for Partially Shaded Photovoltaic Arrays », IEEE Access, vol. 5, p. 11900-11908, 2017.

[40] Z. Xuesong, S. Daichun, M. Youjie, et C. Deshu, « The simulation and design for MPPT of PV system Based on Incremental Conductance Method », in International Conference on Information Engineering (WASE 2010), Beidaihe, Hebei, China, 2010, p. 314-317.

[41] K. H. Hussein, « Maximum photovoltaic power tracking: an algorithm for rapidly changing atmospheric conditions », IEE Proc. - Gener. Transm. Distrib., vol. 142, no 1, p. 59, 1995.

[42] J. Kouta, A. El-Ali, N. Moubayed, et R. Outbib, « Improving the incremental conductance control method of a solar energy conversion system », Renew. Energy Power Qual. J., vol. 1, no 06, p. 273-276, mars 2008.

[43] A. Safari et S. Mekhilef, « Simulation and Hardware Implementation of Incremental Conductance MPPT With Direct Control Method Using Cuk Converter », IEEE Trans. Ind. Electron., vol. 58, no 4, p. 1154-1161, avr. 2011.

[44] Fangrui Liu, Shanxu Duan, Fei Liu, Bangyin Liu, et Yong Kang, « A Variable Step Size INC MPPT Method for PV Systems », IEEE Trans. Ind. Electron., vol. 55, no 7, p. 2622-2628, juill. 2008.

[45] B. Liu, S. Duan, F. Liu, et P. Xu, « Analysis and Improvement of Maximum Power Point Tracking Algorithm Based on Incremental Conductance Method for Photovoltaic Array », in PEDS 2007, Bangkok, Thailand, 2007, p. 637-641.

[46] K. S. Tey et S. Mekhilef, « Modified incremental conductance MPPT algorithm to mitigate inaccurate responses under fast-changing solar irradiation level », Sol. Energy, vol. 101, p. 333-342, mars 2014.

[47] D. Menniti, A. Burgio, N. Sorrentino, A. Pinnarelli, et G. Brusco, « An incremental conductance method with variable step size for MPPT: Design and implementation », in 10th International Conference on Electrical Power Quality and Utilisation EPQU 2009, Lodz, Poland, 2009.

[48] N. E. Zakzouk, B. W. Williams, A. A. Helal, M. A. Elsaharty, et A. K. Abdelsalam, « Improved performance low-cost incremental conductance PV MPPT technique », IET Renew. Power Gener., vol. 10, no 4, p. 561-574, avr. 2016.

[49] I. Houssamo, F. Locment, et M. Sechilariu, « Maximum power tracking for photovoltaic power system: Development and experimental comparison of two algorithms », Renew. Energy, vol. 35, no 10, p. 2381-2387, oct. 2010.

[50] S. Motahhir, A. El Hammoumi, and A. El Ghzizal, "Photovoltaic system with quantitative comparative between an improved MPPT and existing INC and P&O methods under fast varying of solar irradiation," Energy Reports, vol. 4, pp. 341–350, 2018.

[51] M. Rolevski, Z. Zecevic, MPPT controller based on the neural network model of the photovoltaic panel. In Proceedings of the 2020 24th International Conference on Information Technology (IT), Zabljak, Montenegro, 18–22, pp. 1–4, February 2020.

[52] S. Qin, M. Wang, T. Chen, et X. Yao, « Comparative analysis of incremental conductance and perturb-and-observation methods to implement MPPT in photovoltaic system », présenté à 2011 International Conference on Electrical and Control Engineering, Yichang, China, 2011, p. 5792-5795.

[53] T. Noguchi, « Short-Current Pulse-Based Maximum-Power-Point Tracking Method for Multiple Photovoltaic-and-Converter Module System », IEEE Trans. Ind. Electron., vol. 49, no 1, p. 7, 2002.

[54] P. Bhatnagar et R. K. Nema, « Maximum power point tracking control techniques: State-of-the-art in photovoltaic applications », Renew. Sustain. Energy Rev., vol. 23, p. 224-241, juill. 2013.

Chapter (4)

Data Analysis

4.1 Introduction

This chapter presents a method for selecting the parameters of the main components of an autonomous photovoltaic (PV) stations and methods Of Data Collection to ensure the most efficient conversion and use of solar energy. The main energy characteristics are analyzed and the mathematical models of the components of an autonomous PV system are developed to study the modes of tracking the maximum power point (MPP). The necessary conditions for matching the parameters of the PV and the DC-DC buck converter are evaluated to track the MPP. This work aims to create an original method and algorithm for calculating and selecting parameters of the main elements of a PV stations. The optimal value of the sampling time of the MPP controller is obtained for different schemes of the PV system. A practical example is considered for selecting the parameters of a DC-DC buck converter and a digital MPP of an autonomous PV station. The simulation of dynamic modes of an autonomous photovoltaic (PV) station is performed in the MATLAB/SIMULINK software package. The simulation results of dynamic operations of the PV system show that the voltage converter and the MPP controller with the selected parameters according to the proposed method provide reliable and effective tracking of the MPP in all different connections of the PV systems.

4.2 Methods Of Data Collection

Equations (3.28) - (3.30) determine the form of the current-voltage characteristics of the PV panel, which depend on the level of illumination G and the surface temperature T. Fig. 4.1 shows the I-V characteristics of the PV panel for different levels of solar irradiance and temperature.

On each of the $I - V$ characteristics, there is a single point (in Fig. 4.1 designated as A and B), corresponding to certain values of the current I_{MPP} and voltage V_{MPP}, at which the PV panel will generate the maximum power P_{MPP}.

These voltage and current values determine the equivalent PV panel resistance at the maximum power point:

$$R_{MPP} = \frac{V_{MPP}}{I_{MPP}}. \tag{4.1}$$

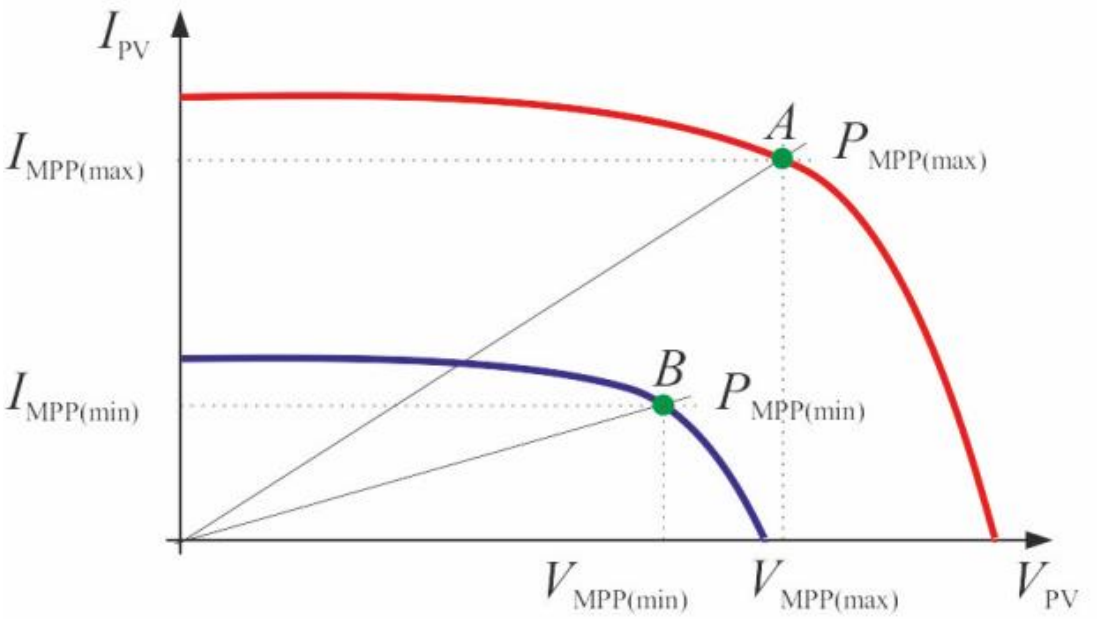

Fig. 4.1. Volt-current characteristic of PV panel under different solar irradiance and temperature conditions

The maximum power with PV panel is ensured when the equivalent output resistance of the PV module in MPP R_{MPP} and the equivalent input resistance of the converter R_{in} are equal. The value of R_{in} depends on the converter topology, its load R_{out} and the duty cycle value d (duty cycle).When searching for MPP, controller changes the value of d so that the condition is satisfied: $R_{MPP} = R_{in}$. If we neglect the losses in the step-down DC-converter, an important practical relation is derived from the condition of equality of its input and output power:

$$\frac{V_{MPP}^2}{R_{MPP}} = \frac{V_{out}^2}{R_{out}} = \frac{\left(V_{MPP} \cdot d\right)^2}{R_{out}} \Rightarrow d = \sqrt{\frac{R_{out}}{R_{MPP}}} \,. \tag{4.2}$$

Since the value of d cannot be greater than 1, it follows from (4.2) that the output resistance of the buck converter must be less than the minimum equivalent resistance of the PV panel in MPP in order to ensure the PV module in MPP in all possible operating modes:

$$R_{out} < R_{MPP(min)} \,. \tag{4.3}$$

When designing the converter for PV system; built according to schemes 2 and 3, this condition is transformed into the choice of the rational value of the nominal output voltage of the converter according to the condition, where:

$$V_{out} < V_{MPP(min)} . \quad (4.4)$$

A characteristic feature of PV panel is the direct dependence of I_{MPP} and the inverse dependence of V_{MPP} on the surface temperature of the module, with the temperature coefficient of voltage k_V in absolute value far exceeding the temperature coefficient of current k_I. Analysis of the V-P characteristics PV panel (see Fig. 4.1) shows that, for designing a converter, it is necessary to determine the current and voltage values in MPP for four nodes at various combinations of *G* and *T*. Characteristics of the PV panel nodes and their corresponding indicators modes are given in table. 4.1.

Table 4.1 Key points the solar panels of a photovoltaic station

Solarirradiance (G)	Temperature (T)	Indicators	Mode
min	min	$R_{MPP(max)}$, $I_{MPP(min)}$	Maximum resistance
min	max	$P_{MPP(min)}$, $V_{MPP(min)}$	Minimum power
max	min	$P_{MPP(max)}$, $V_{MPP(max)}$	Maximum power
max	max	$R_{MPP(min)}$, $I_{MPP(max)}$	Minumum resistance

The minimum and maximum values of *G* and *T* are determined in accordance with the location and operating conditions of the PV panel. In the present studies, the ranges of the radiation and temperature changes, characteristic for the operating conditions of photovoltaic power plants in the northern latitudes are determined as follows: G_{min} = 100 W / m^2, G_{max} = 1000 W / m^2, T_{min} = - 25ºC, T_{max} = + 50ºC.

The values of currents, voltages and power at the nodal points of the PV panel are easily determined by equations (3.31) - (3.33). The values of equivalent resistances are calculated by equation (4.3). To determine the limiting values of the duty cycle of the buck converter, equation (4.2) is used.

4.3 Method of calculation and selection of parameters of basic elements of the PV system

Based on the analysis of the energy characteristics of the main elements of the PV system, a methodology has been developed for calculating and selecting their optimal parameters, presented in the form of a flowchart shown in Fig. 4.2.

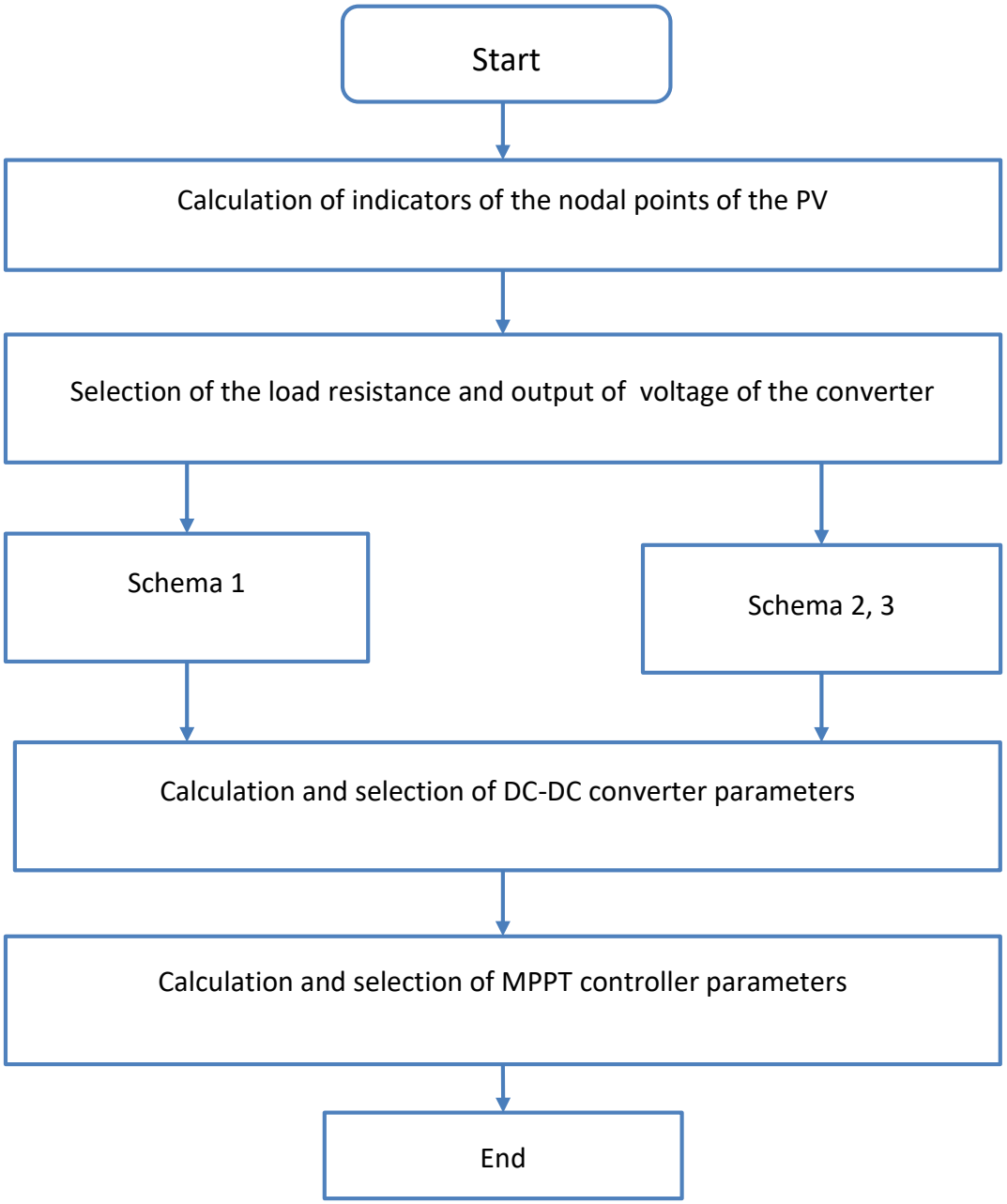

Fig. 4.2. Flowchart for calculating and selecting optimal parameters of the main elements of an Autonomous photovoltaic station

When using the proposed method it is necessary to consider features of modes of DC-DC-converter for loads of different nature. This feature can be noted when operating on a load in the form of a constant resistance (Schema 1), an increase in *d* values leads to an increase in the output power of the converter, while in power systems with a stabilized output voltage of the converter (Schema 2, 3), an increase in *d* causes a decrease in the output power. Accordingly, when calculating the parameters of the DC-DC converter for circuit 1 in equations (3.25) and (3.37), the minimum duty cycle *d*min must be used, for circuits 2 and 3, $d_{\max}$ must be used in equation (8), and in equation (3.37) - $d_{\min}$.

4.4 Reliability And Validity

To test the proposed methodology, we considered two different PV systems a practical example of calculating and selecting the parameters of a DC-DC converter and a digital MPPT controller of an autonomous PV system. The first system consisting of three series-connected Kyocera Solar KD320GX-LPB, the main technical characteristics are given in Tab. 4.2, and the second system composed of 36 monocrystalline silicon cells connected in serer having a maximum power is 50 W under standard conditions with $G = 1000\ W/m^2$ and $T = 25\ ^\circ$ C (298°K),A = 1.3, N_s=36, N_P =1; T_{ref} = 298°K(25°C), E_g = 1.12eV, R_{sh} = 1000Ω, R_s = 0.1Ω, the main technical characteristics are given in Tab. 4.3,

Table 4.2 ,Electrical parameters of the Kyocera Solar KD320GX-LPB PV module

Parameter	Value
Open-circuit voltage, V_{OC}, V	49,5
Short circuit current, ISC, A	8,6
Voltage at PMPP , VMPPV	40,1
Current at PMPP, IMPPA	7,99
Maximum power, PMPPW	320,4
Oopen circuit voltage coefficient VOC, kV V/ºC	-0,1832
Short circuit current coefficient ISC, kI A/ºC	0,00328
Number of cells connected in series, NS	80

Table 4.2 , Electrical Characteristics 50M (36) PV module

Parameters	Value
Maximum power	50W
Voltage at P_{max} (V_{max})	17.98V
Current at P_{max} (I_{max})	2.78A
Short Circuit current (I_{sc})	3.04A
Open circuit voltage (V_{oc})	21.87V
Temperature coefficient Ki	(0.065±0.15)A/°C

For completeness of the analysis, three possible options for constructing autonomous PV were considered; schemes 1-3. For each circuit, simulation models of PVstation based on the mathematical models of the components presented above were developed and implemented in the MATLAB / Simulink software environment. To increase the reliability of the results and evaluate the efficiency of energy conversion in the FES simulation model, the non-ideality of the converter elements - the active resistance of the inductor and the equivalent internal resistance of the capacitors, as well as the static characteristics of the transistor and diode - voltage drop and resistance in the conducting state are taken into account.

The parameters of the DC-DC converter and MPPT controller were calculated and selected by the proposed method in accordance with the block diagram shown in Fig. 4.2. In the FES simulation model for circuit 2, a lead-acid battery with a nominal capacity of 200 A.h is adopted as an energy storage device, the DC bus model in circuit 3 was built on the basis of a 300 μF capacitor and an active resistance of 0.01 Ohms. The frequency of the PWM generator (*f*) in all computational experiments was taken equal to 25 kHz.

The parameters of the DC-DC converter and MPPT controller, selected as a result of calculation by the proposed method, are given in table. 4.4.

Table 4.4 Results of calculation and selection of parameters of the main components of an autonomous photovoltaic station

Parameter	Value	
	Schema 1	Schema 2, 3
R_s, Ohm	0,487	0,487
R_{out},Ohm	10	–
V_{out},V	–	48
d_{min}	0,24	0,33
d_{max}	0,87	0,50
L, μH	800	1500
C_{out}, μF	20	10
C_{in}, μF	20	10
t_s, s	0,0004	0,004
Δd	0,005	0,0015

The calculation results show that the inertia of a DC-DC converter, designed to operate as a part of autonomous photovoltaics, which is constructed according to schemes 2 and 3 is an order of magnitude higher than that of a similar converter operating on an active load. In addition, from the table. 4.3 it is obvious that for a DC-DC converter with a stabilized output voltage, the working range of the duty cycle changes significantly, which determines the high rigidity of its adjustment characteristics, and accordingly, increases the requirements for accuracy and quality of regulation of the control system.

All simulations in this study have been performed using a Matlab/Simulink tool Fig.4.3 illustrates the simulation model of the PV system using the Matlab platform.

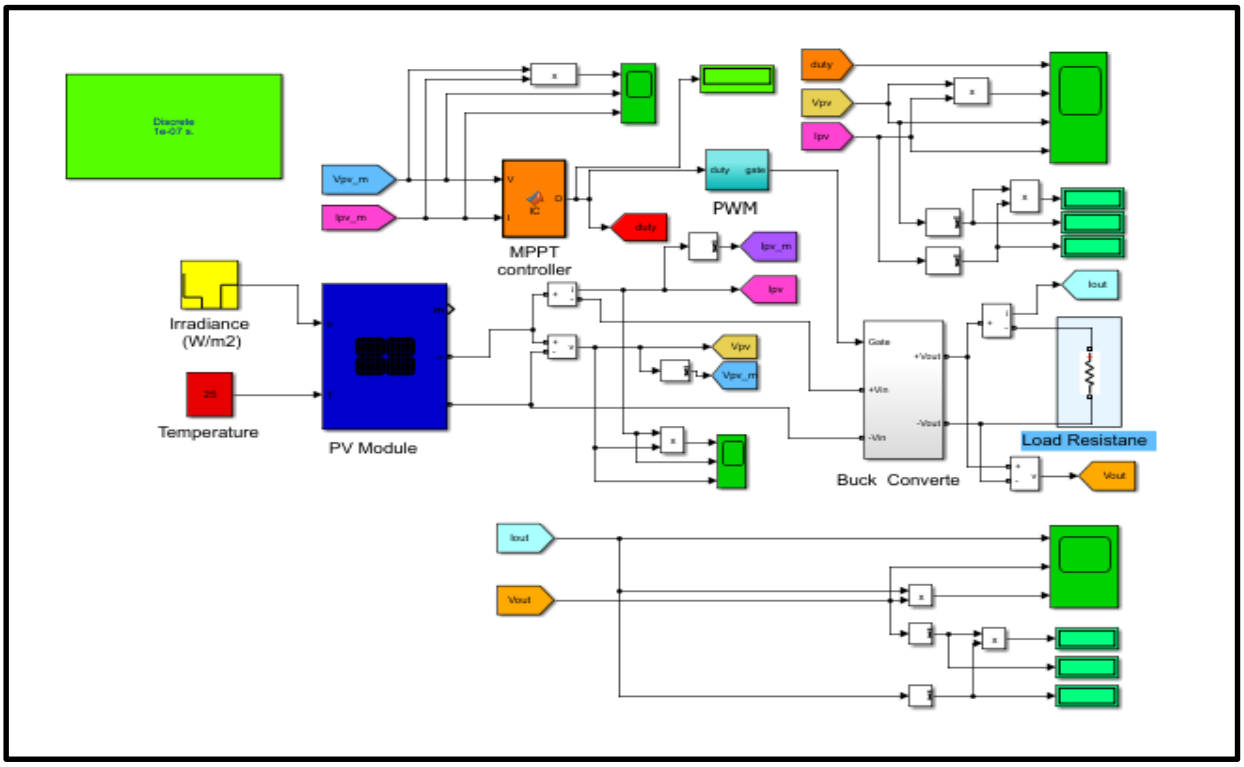

Figure 4.3. Matlab/Simulink of the proposed PV system with a resistive load.

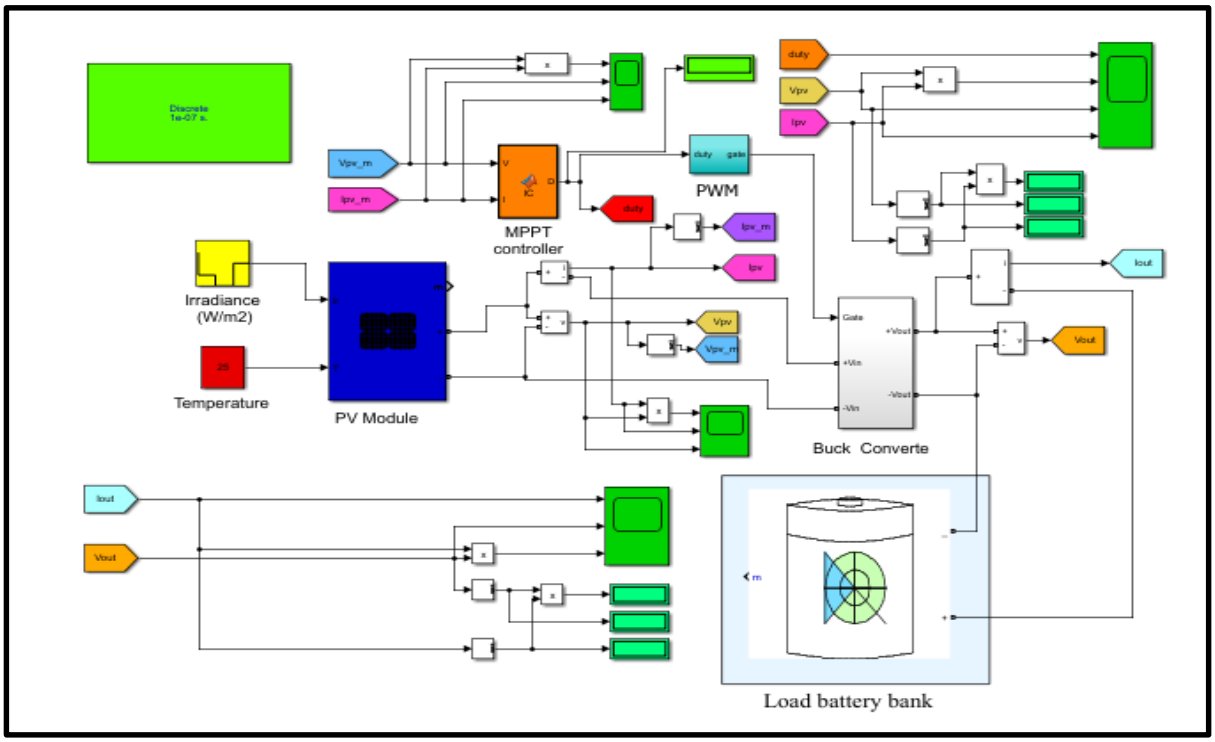

Figure 4.4. Matlab/Simulink of the proposed PV system with the battery bank.

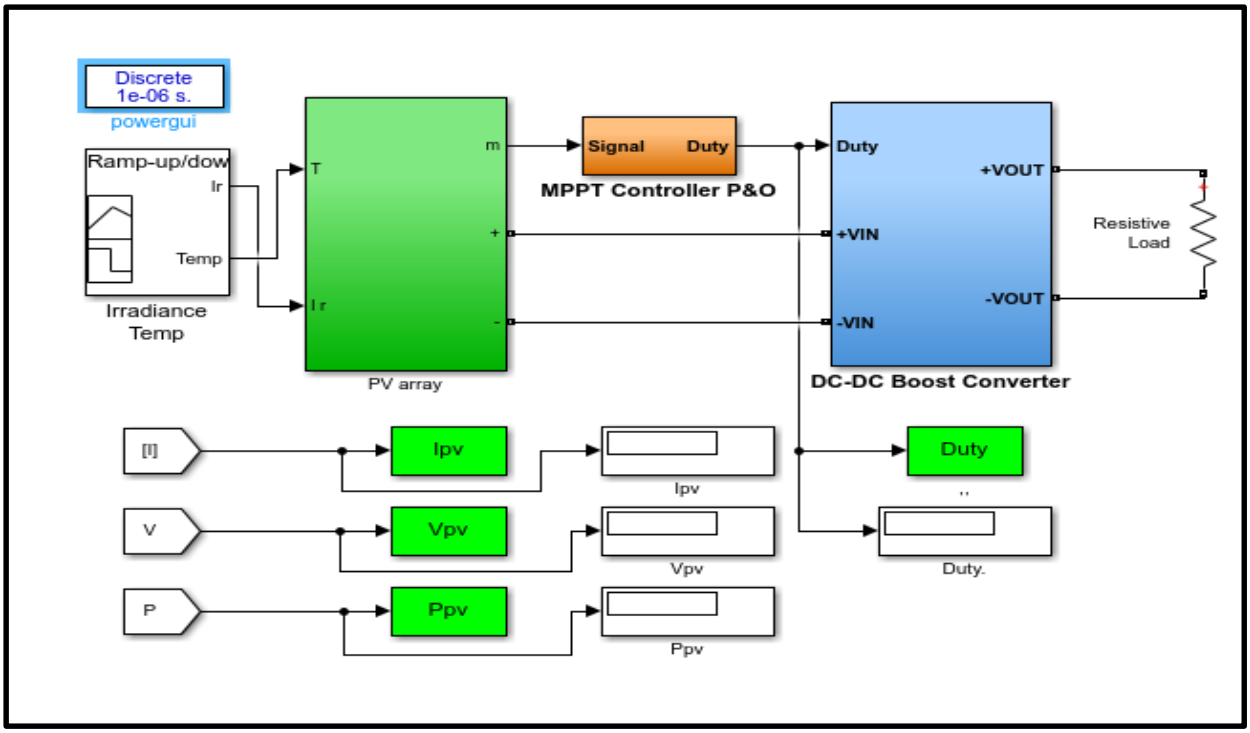

Figure 4.5: Simulink model of PV system with MPPT tracking.

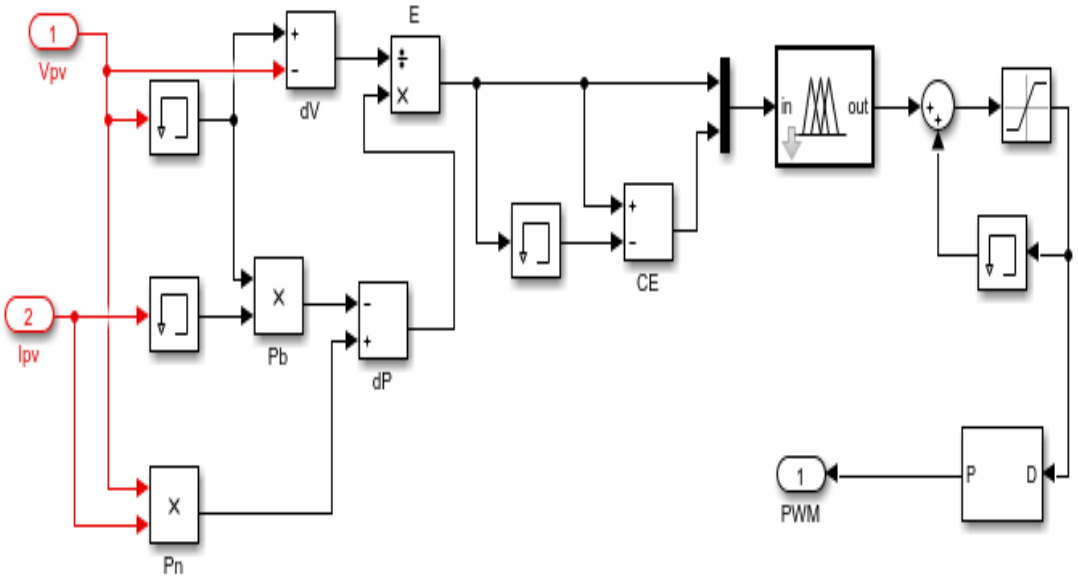

Figure. 4.6. Block diagram of fuzzy MPPT algorithm.

4.5 Conclusions

The research presents an original methodology for calculating and choosing optimal parameters for the main elements of an autonomous PV systems; a buck DC-DC converter and a MPPT controller. The parameters of the converter are selected on the basis of calculation and analysis of the possible range of voltage changes at the point of maximum power under various lighting conditions and temperatures. The parameters of the digital MPPT controller are selected based on the calculated value of the converter time constant and the nature of its electrical load. The research considers three main options for constructing autonomous PV, for each of which design features are established. The proposed method has been tested on a specific example, its adequacy is confirmed by the results of the simulation of dynamic modes of an autonomous PV for all three considered topologies.

Chapter (5)

Results and Discussion

5.1 Introduction

This chapter present how the SIMULINK models of the proposed PV power systems are implemented, to test and verify the functionality of the proposed MPPT controls. In this thesis, two different PV systems are implemented in MATLAB/SIMULINK environment. The first system is implemented with a resistive load and battery bank with DC-DC buck converter to evaluate the effectiveness and the advantages of the proposed novel improved particle swarm optimization (IPSO) a comparison with the conventional incremental conductance algorithm (IC) and perturb and observe (P&O) algorithm . The second PV system is also simulated in MATLAB, but by using fuzzy logic control (FLC) and compared to the conventional (P&O) algorithm with DC-DC boost converter to demonstrate the feasibility and performance of the proposed controller based on MPPT of PV system. Furthermore, a comparison has been carried out between the proposed controllers by way of simulation results.

5.2 Results of simulation

5.2.1 Results of simulation with DC-DC buck converter

5.2.1.1 Tracking The MPPT by IC

Fig. 5.1 shows the results of modeling the operating modes of the FES with a sudden change in the lighting conditions of the SB for circuits 1 and 2 (the results for circuit 3 are not given, since they are almost identical to circuit 2). When carrying out this computational experiment, the lighting conditions of the SB change after 0.05 s of model time and correspond to the following successive values of solar radiation: G = 800; 400; 200; 600; 1000 W / m2. The surface temperature of the PM is assumed unchanged - 25ºC.

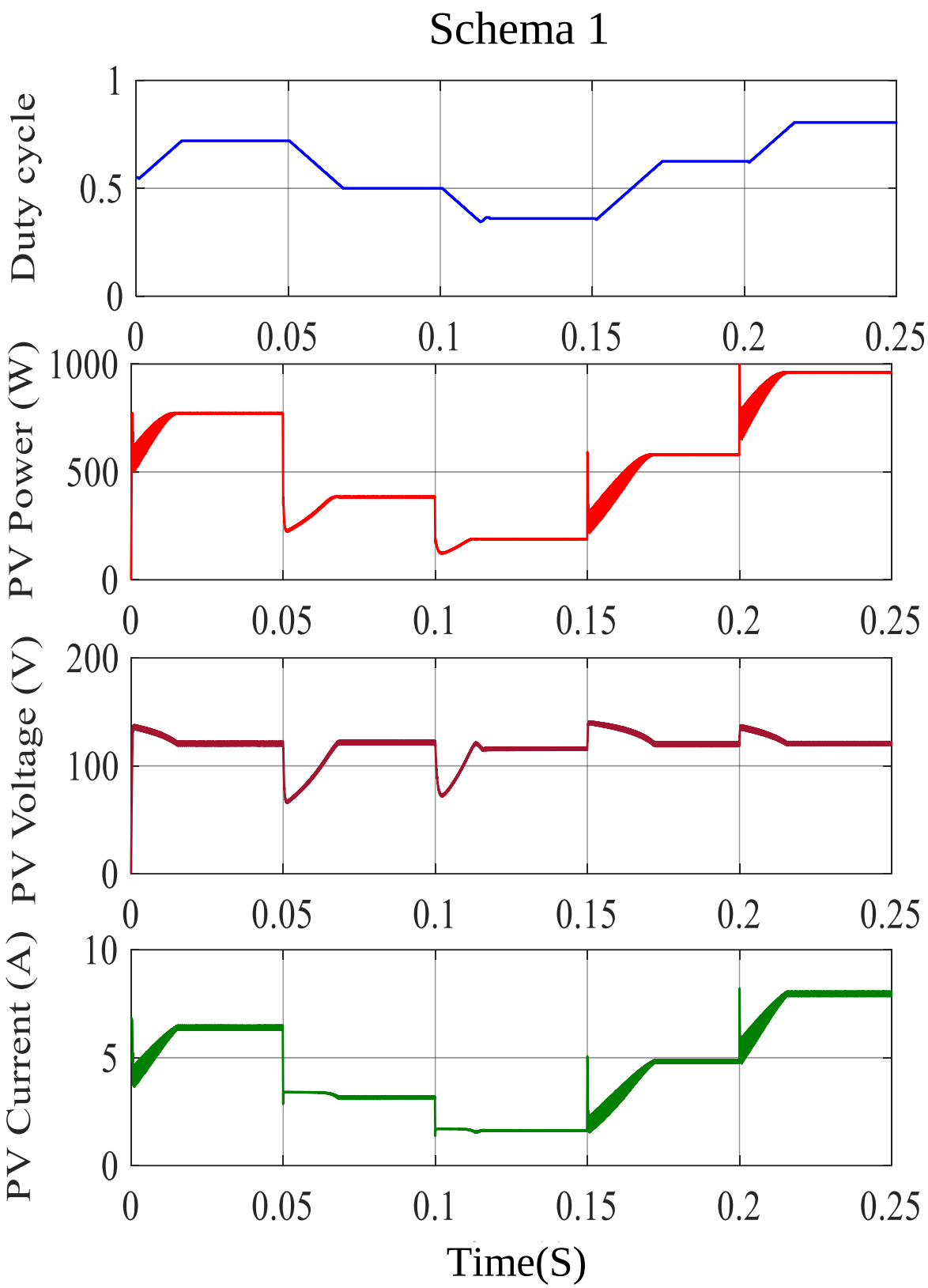

Fig. 5.1. Results of simulation of photovoltaic station modes under changing lighting conditions with a resistive load

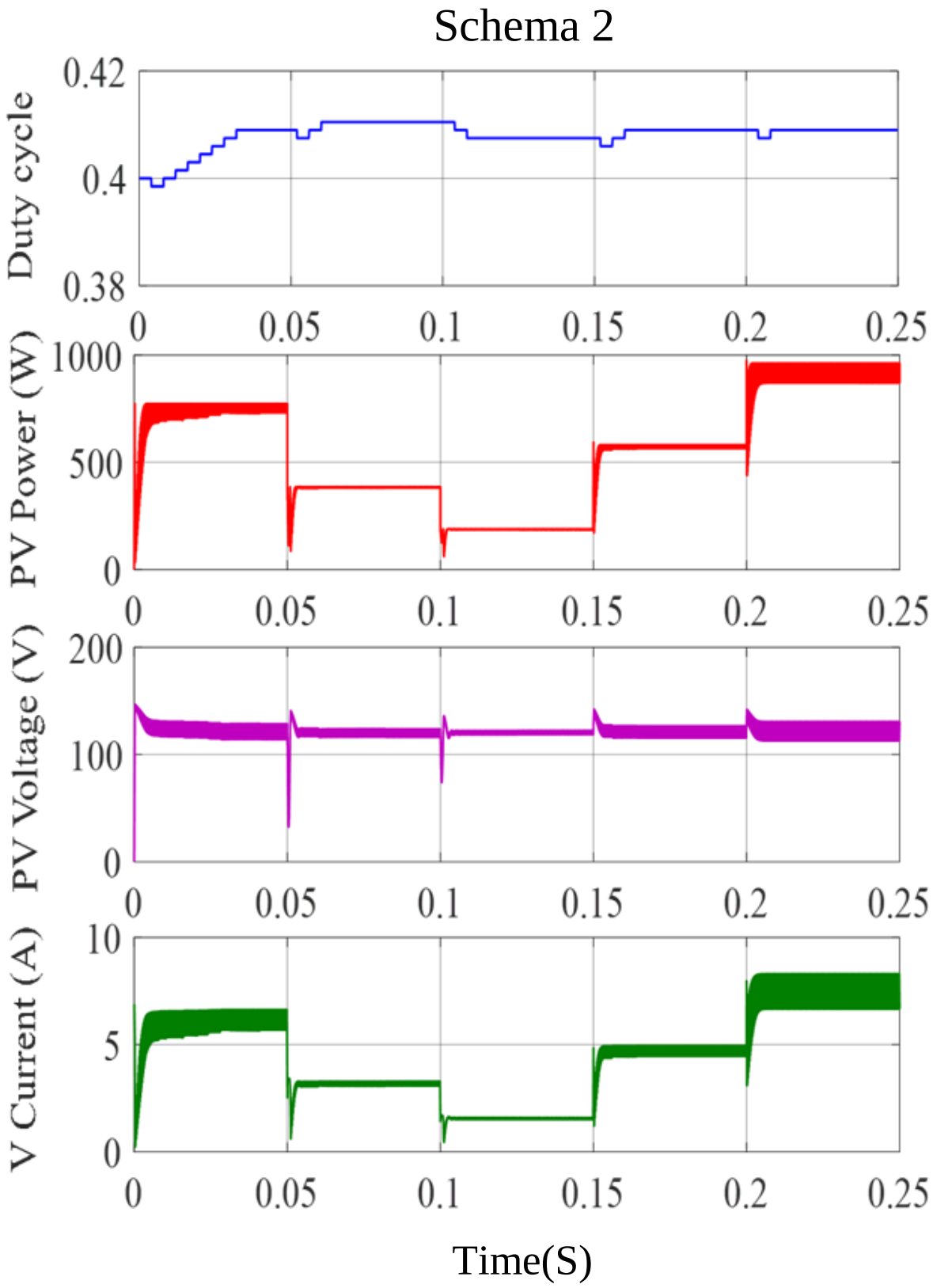

Fig. 5.2. Results of simulation of photovoltaic station modes under changing lighting conditions by solar panels with battery bank

During the computational experiments, the values of the duty cycle d (duty cycle), output power (PV Power), voltage (PV Voltage) and current (PV Current) of solar batteries, as well as the parameters of the electric energy consumed by the load were recorded.

The simulation results presented in Fig. 10 prove that the DC-DC converter and the MPPT controller with the selected parameter values provide reliable and efficient MPP tracking in all 5 test variants of the illumination change. The tracking accuracy of the maximum power point in scheme 1 is at least 99.6%, in scheme 2 it is at least 98.2%, and the efficiency of the DC-DC converter in all the considered modes did not fall below 93.2%. The operating ranges for changing the energy characteristics of the main elements of the PV system (current, voltage, power) correspond to the calculated values obtained during their design. With correctly selected parameters of the converter and MPPT controller, the MPP tracking time does not exceed 0.03 s, which is obvious from Fig. 5.1.

5.2.1.2 Tracking The MPPT by IPSO

The details simulations results of a PV system with MPPT controller based on IPSO algorithm for schemes 1 and 2 is shown in Fig.5.2.

When carrying out these experiments, a modified version of the PSO algorithm with variable values of the coefficients of inertia and acceleration (IPSO) is used. The number of particles is taken to be $N = 4$, the maximum number of iterations is $k\max = 32$.

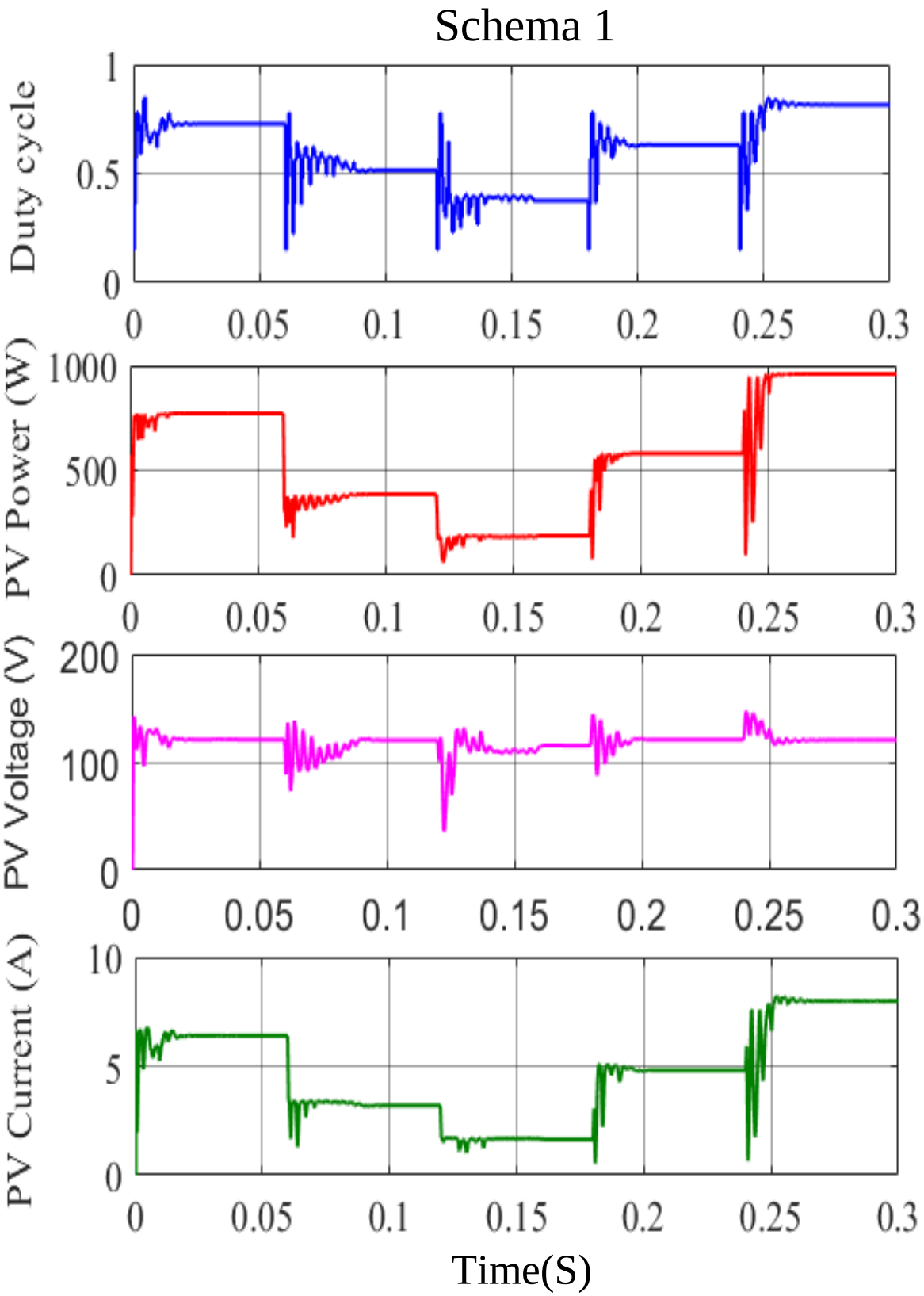

Figure 5.3. The performance of IPSO controller with a resistive load

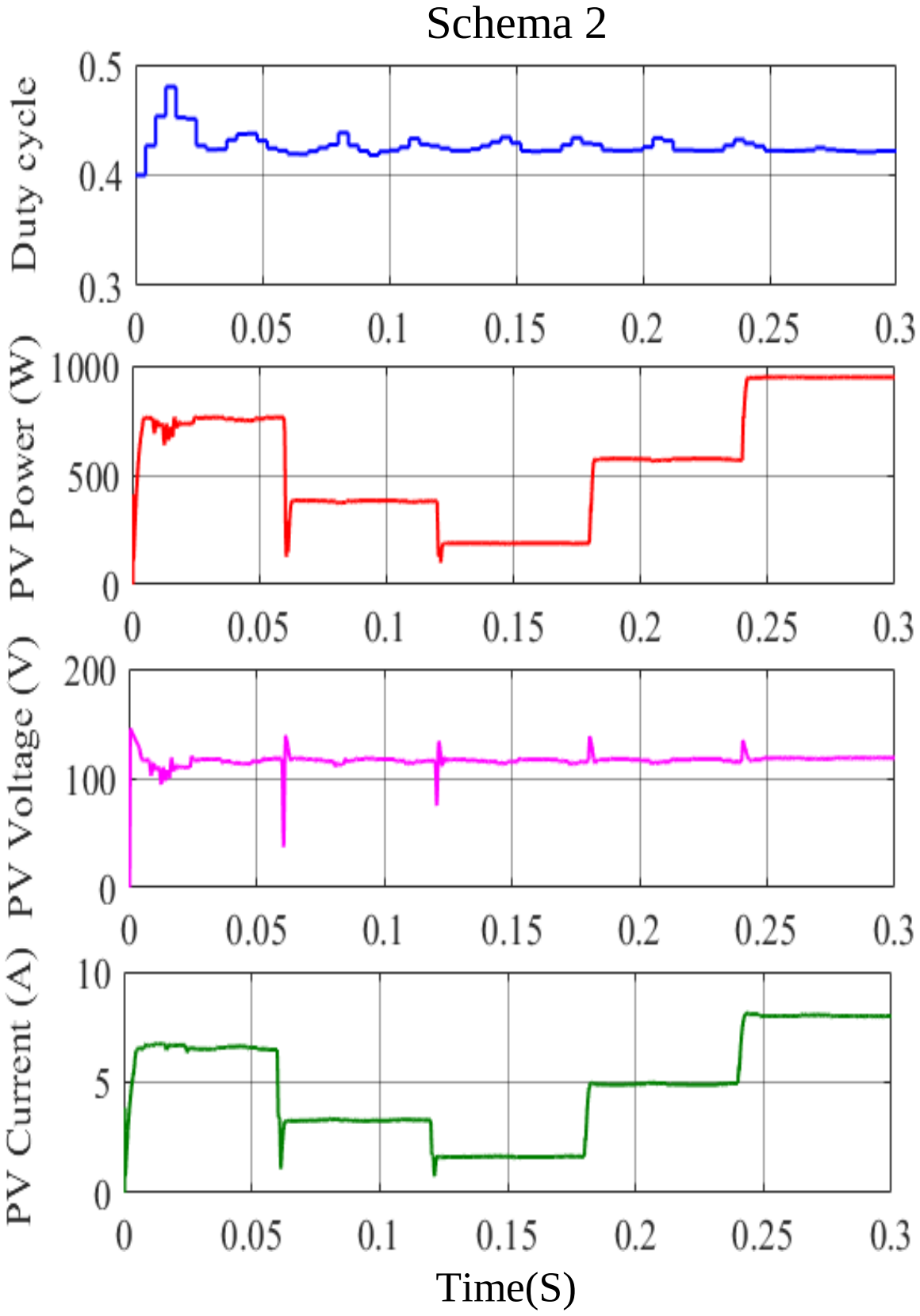

Figure 5.4. The performance of IPSO controller with battery bank

The tracking accuracy of the maximum power point based on IPSO in scheme 1 is at least 99.78%, in scheme 2 it is at least 98.2%, and the efficiency of the DC-DC converter in all the considered modes did not fall below 99.93%.

5.2.1.3 Tracking The MPPT by P&O

An interesting feature of the dynamic modes of an autonomous PV is as follows: despite the fact that circuit 2 has a much greater inertia than circuit 1, the transients in it, caused by a sudden change in the illumination of the PV panel, end much faster. This is explained by the fact that a change in the value of solar irradiance insignificantly affects the voltage in the MPP PV (see Fig. 5.1), and in circuits with a stabilized output voltage of the converter, the value of the duty cycle *d* remains practically unchanged, which ensures a quick end of the transient process. The value of *d* depends much more strongly on the surface temperature of the photovoltaic modules, which cannot change instantly or with a high gradient commensurate with the time constant of the DC-DC converter, and this dependence is not critical. When a DC-DC converter operates on an active resistance, the value of its output voltage changes in proportion to the supply voltage, which requires a change in the value of *d* within a fairly wide range.

Fig. 5.3 shows the results that simulated the operation modes of the P&O based tracker of PV system under changing the solar irradiance of the solar panels under the partial condition

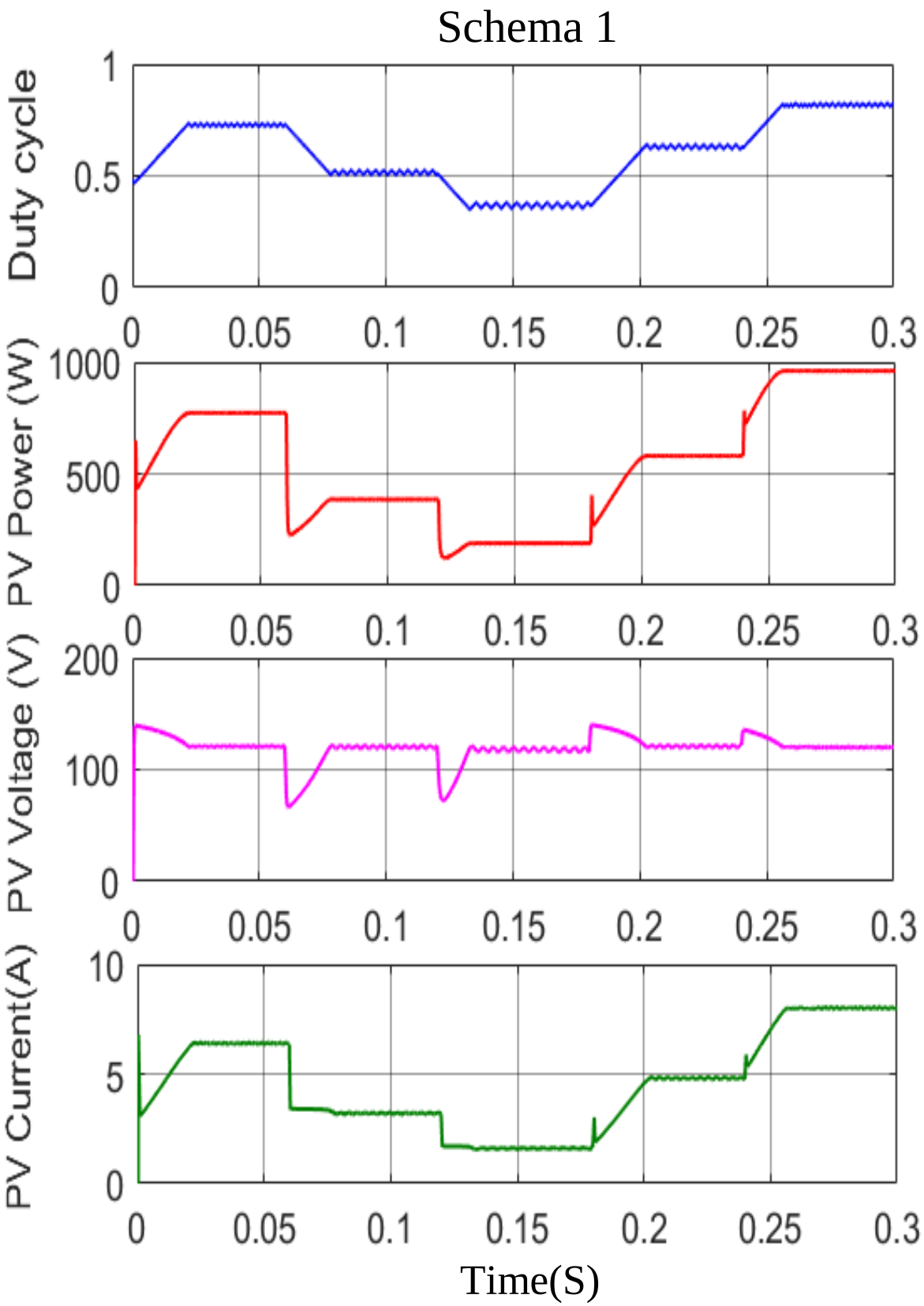

Figure 5.5. The performance of P&O algorithm with a resistive load

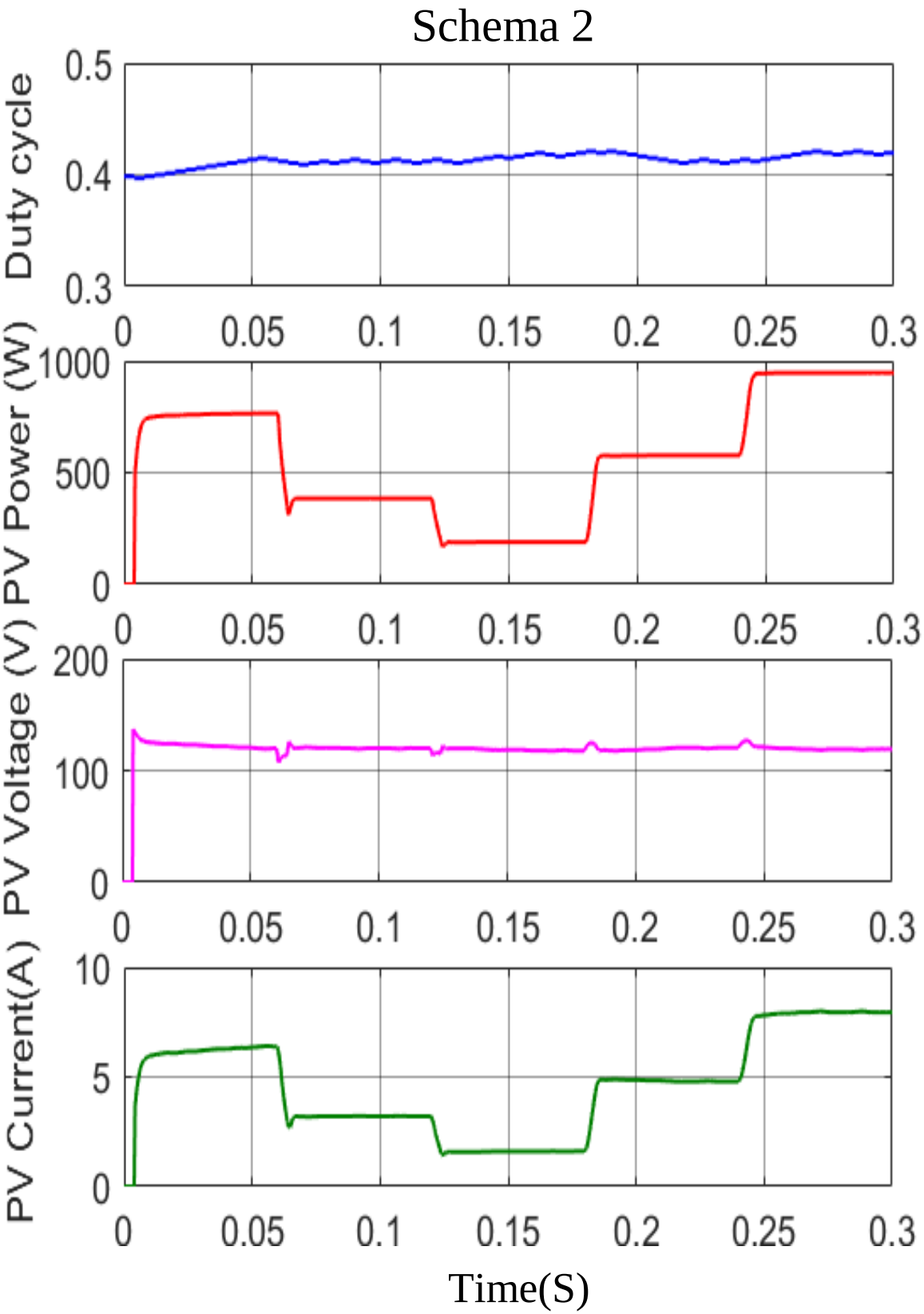

Figure 5.6. The performance of P&O algorithm with battery bank

5.2.1.4 Comprehensive comparison between IPSO,IC, and P&O

A comparison between different studied MPPT techniques is listed in Table 5.1. From this table, one must see the superiority of IPSO-based tracker over the IC algorithm.

Table 5.1 Comparison between IPSO, IC, and P&O**.**

Test number	scheme 1						scheme 2					
	IC		PSO		P&O		IC		PSO		P&O	
	η, %	t_{MPP}, s	η, %	t_{MPP}, s	η, %	t_{MPP}, s	η, %	t_{MPP}, s	η, %	t_{MPP}, c	η, %	t_{MPP}, s
1	99.93	0.015	99.94	0.04	99.93	0.037	99.81	0.028	99.93	0.052	99.90	0.045
2	99.92	0.014	99.97	0.03	99.94	0.028	99.66	0.016	99.97	0.062	99.94	0.053
3	99.73	0.010	99.78	0.02	99.76	0.018	99.41	0.012	99.96	0.049	99.95	0.035
4	99.91	0.020	99.91	0.03	99.91	0.025	99.62	0.018	99.98	0.061	99.96	0.052
5	99.95	0.012	99.99	0.03	99.98	0.029	98.72	0.010	99.99	0.056	99.97	0.049
Average value	**99.88**	**0.0142**	**99.92**	**0.03**	**99.90**	**0.027**	**99.44**	**0.016**	**99.97**	**0.056**	**99.94**	**0.047**

5.2.2 Results of simulation with DC-DC boost converter:

Figures 7 to 12. Shows the different output results of the photovoltaic generator simulated using P&O and FL under (G=1000W/m² and T=25°C). Figure 7 shown the Output power of the PV generator for the different simulated algorithms. Where it takes 0.042 s for the traditional Perturb and Observe (P&O) algorithm to obey the MPP with a major power swing of (50.41-52.39W). Whilst for the fuzzy logic controller method it takes 0.035 s just and without power oscillation at standard conditions (E=1000W/m² and T=25°C)

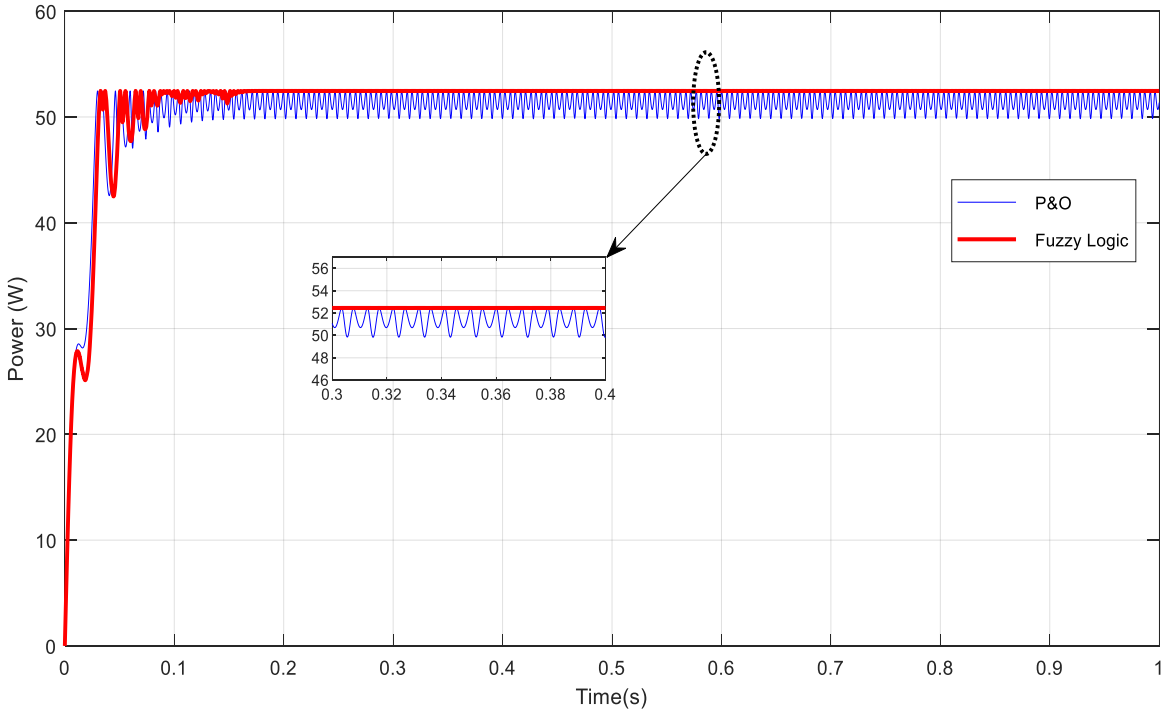

Figure 5.7. Output power at the standard condition with Fuzzy Logic controller (FLC) and conventional P&O

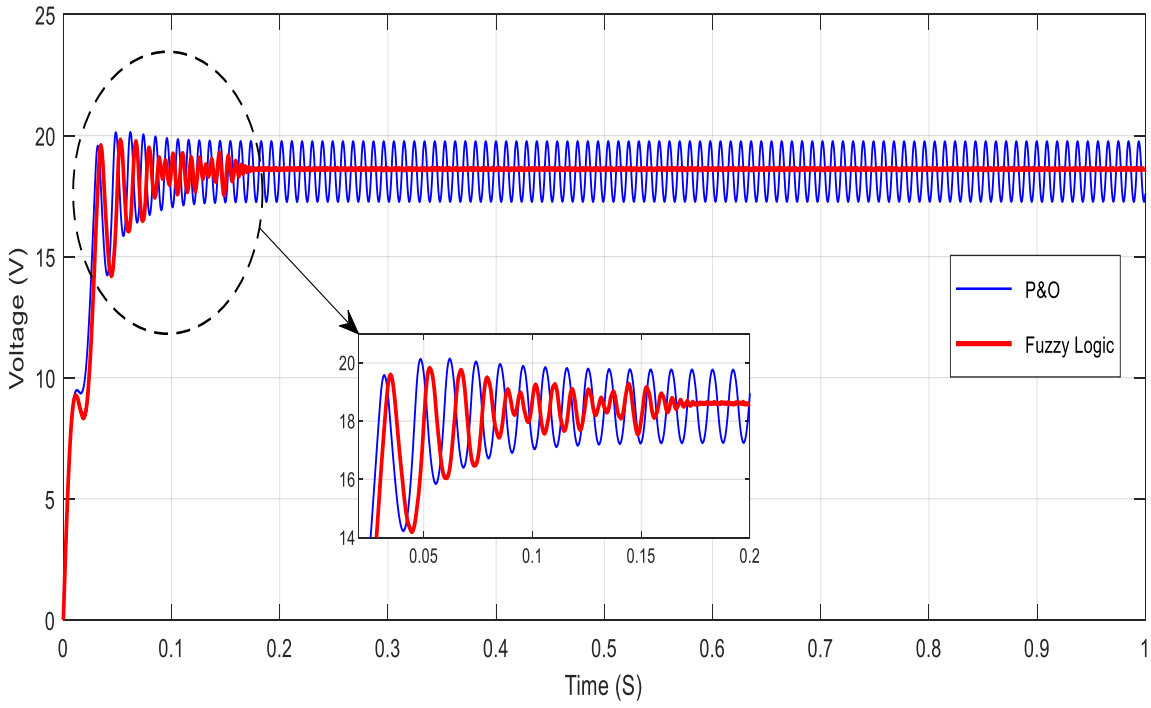

Figure 5.8. Output current at the standard condition with Fuzzy Logic controller (FLC) and conventional P&O

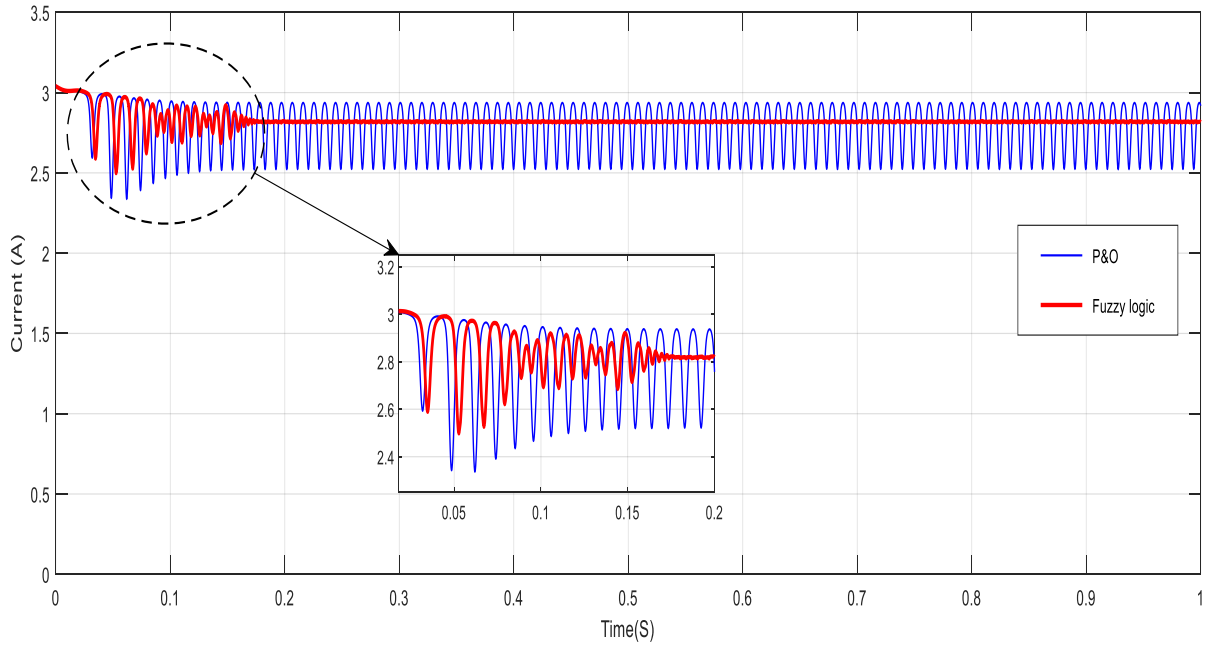

Figure 5.9. Output voltage at the standard condition with Fuzzy Logic controller (FLC) and conventional P&O

Figure 10 shows the results of the PV generator for many solar irradiance values (800W/m²,900W/m² and 1000W/m²) at fixed temperature of 25°C. To examine the system. Where we observe the fuzzy logic controller has better response time, much more accurate tracking and less oscillation at each step compared to the classical P&O controller.

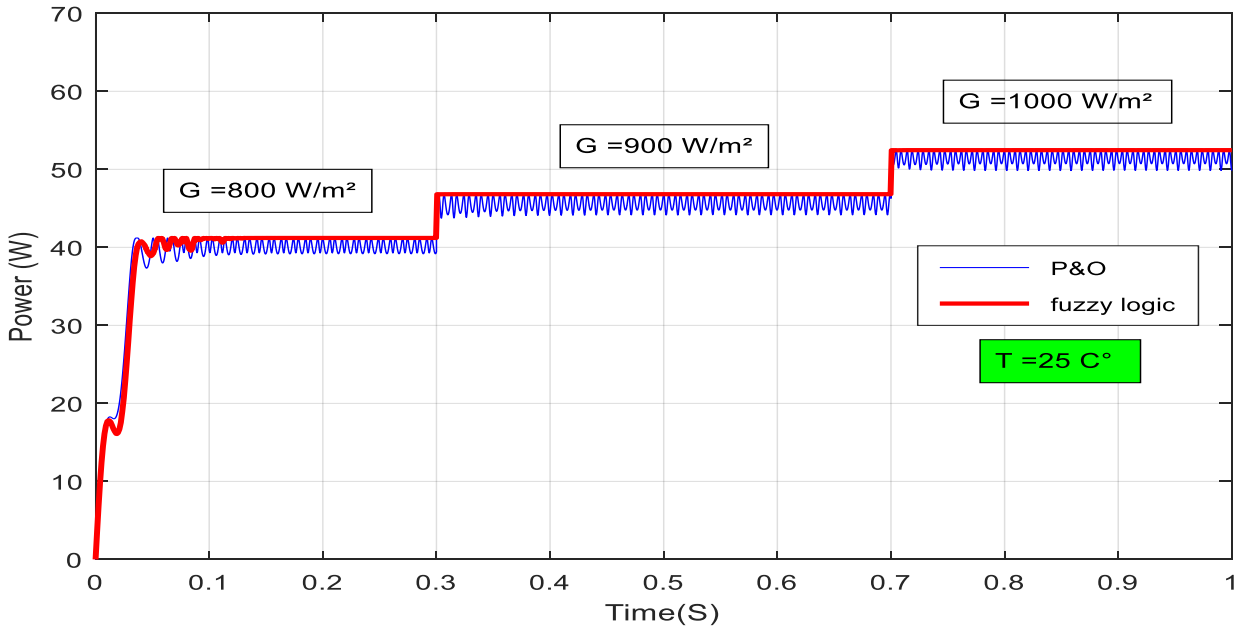

Figure 5.10. Output power at the different irradiance values and fixed temperature of 25°C with Fuzzy Logic controller (FLC) and conventional P&O

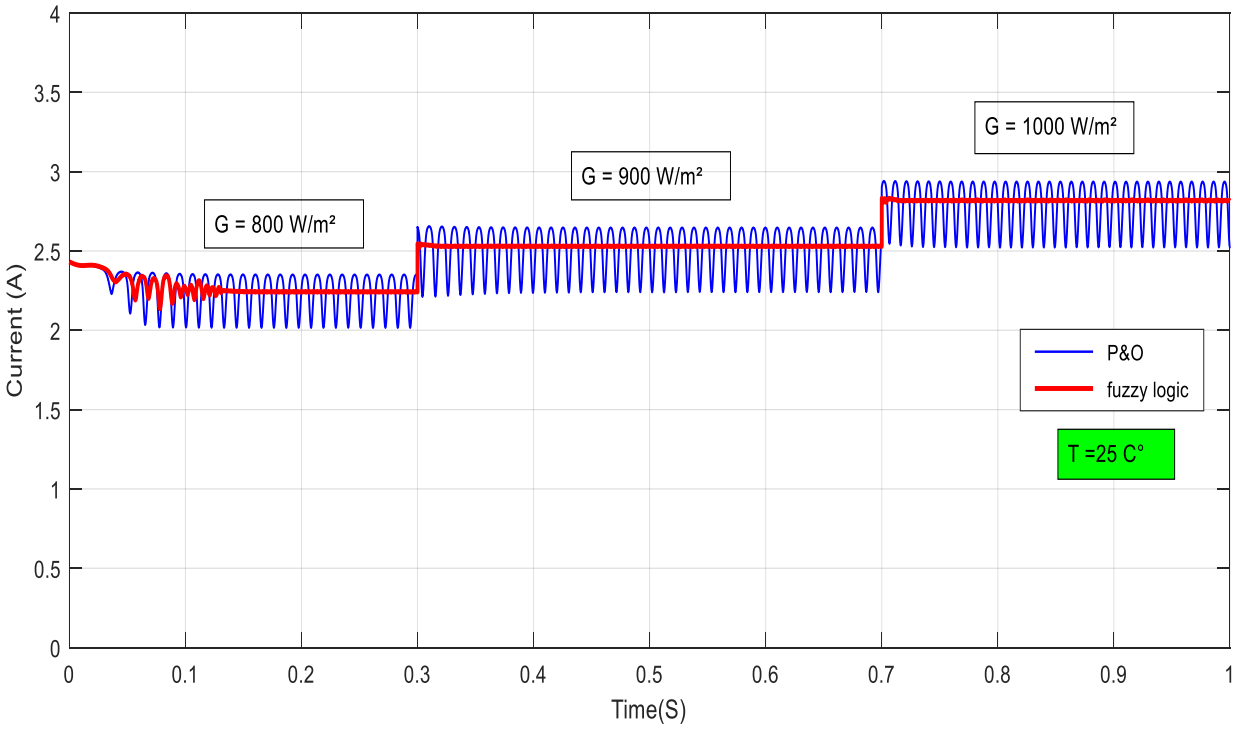

Figure 5.11. Output power at the different irradiance values and fixed temperature of 25°C with Fuzzy Logic controller (FLC) and conventional P&O

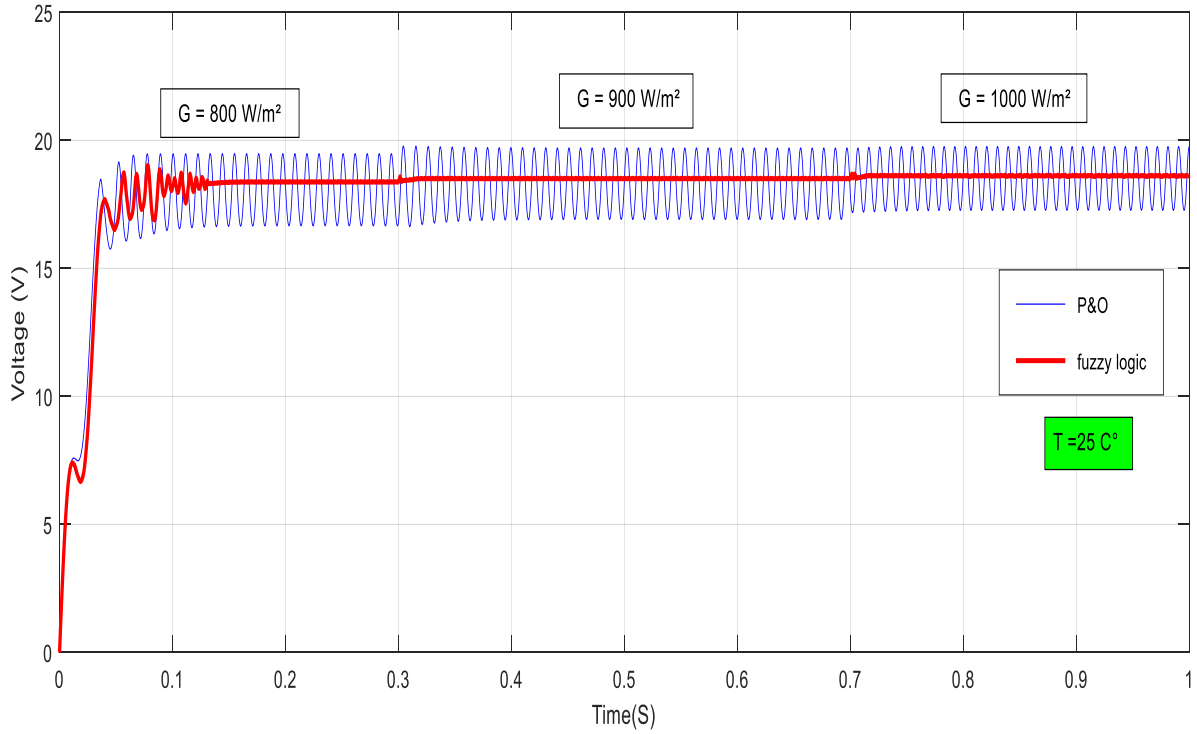

Figure 5.12. Output voltages at the different irradiance values and fixed temperature of 25°C with Fuzzy Logic controller (FLC) and conventional P&O

5.2.2.1 Comprehensive comparison between Fuzzy Logic (FLC), and P&O

Fuzzy Logic control is developed for maximsation of PV array. We study the MPPT technology based on P&O and comparted to FLC. The controller of the fuzzy logic showed fast response and successfully control of tracking the maximum power point (MPPT) considering the effect of atmospheric changes. more than, the MPPT technology based on fuzzy logic control achieves good and more accurate results, more flexibility and eliminates the fluctuations in the power compared to MPPT technology based on P&O. The table 5.2. summarize The different performance results of the photovoltaic generator simulated using the fuzzy controller and the Perturb and Observe (P&O) algorithm.

Table 5.2 Comparison between FLC and P&O**.**

MPPT method	E=1000W/m², and T=25°C	
	Efficiency (%)	Response time(s)
FLC	98.02	0.033
P&O	97.99	0.042

5.2 Conclusion

This chapter presents the performance for three control strategies applied of the proposed PV power systems are implemented. The theoretical background is described, and the advantages and disadvantages of each application are studied through analyses and a series of simulations. A comprehensive comparison and evaluation are implemented for the four methods from several aspects such as algorithm complexity, steady state performance. From the first system, one must see the superiority of IPSO-based tracker over conventional incremental conductance algorithm (IC) and perturb and observe (P&O) algorithm. Where results show that the IPSO-based tracker method can provides best steady state and dynamic performance compared to the conventional controllers, and from second PV system, we conclude that the MPPT using the fuzzy logic technique takes a fast response and can improve the performance of the PV system compared to the P&O.

Chapter (6)

Conclusions

6.1 Conclusions

In this research, a stand-alone photovoltaic system is presented to provide the electric power to the consumers in isolation from the central electrical network with a clean and sustainable source of energy. The main focuses of this research was how to improve the total system efficiency by proposes a method for selecting the parameters of the main components of an autonomous photovoltaic (PV) stations to ensure the most efficient conversion and implementing an efficient MPPT techniques to transfer the maximum available power to the load especially under rapidly changing atmospheric conditions.

The thesis reviewed and discussed some existing MPPT controller methods, including P&O method, INC, particle swarm optimisation (PSO), fuzzy logic and neural network, , etc., and showed their ability to track the MPP under rapidly changing weather conditions. It illustrated the advantages and disadvantages of each individual MPPT technique tracking performance. Based on the outcome of this evaluation, three proposed MPPT techniques were identified which substantially address the disadvantages that most MPPT techniques suffer from.

The three more efficient MPPT controllers proposed were analysed and developed in more depth using new system simulations to clearly show improvements. In this thesis, we performed the MPPT process in the PV system using the proposed novel improved particle swarm optimization (IPSO) and compare it with the conventional incremental conductance algorithm (IC) and perturb and observe (P&O) algorithm. To test and verify the results obtained, simulation modeling of the dynamic regimes of the PV was used in the MATLAB / Simulink® software package. The novel improved particle swarm optimization (IPSO) was shown to have a faster dynamic response and virtually eliminates the steady state oscillation around the MPP there by; it improves the MPPT efficiency of the PV system. The design and results of the novel improved particle swarm optimization (IPSO) technique were presented and explained.

The simulation results were presented in order to show the benefits of MPPT and evaluate the performance and functionality of the proposed MPPT techniques. The simulations were performed using MATLAB/SIMULINK. A model of the complete PV systems was presented and discussed along with how all of the masked components have been combined to form this system. A more detailed SIMULINK model of each component was also presented, starting with the PV solar panels, buck converter, DC load and MPPT controllers, and then each component masked within a subsystem.

the simulation results were divided into two parts: in the first part the PV system is implemented with a resistive load and battery bank with DC-DC buck converter to evaluate the effectiveness and the advantages of the proposed novel improved particle swarm optimization (IPSO) a comparison with the conventional incremental conductance algorithm (IC) and perturb and observe (P&O) algorithm. The simulation results prove that the DC-DC converter and the MPPT controller with the selected parameter values provide reliable and efficient MPP tracking in all maximum power point tracking techniques with changing solar irradiation conditions. As the simulation results clearly showed that, the the proposed novel improved particle swarm optimization (IPSO) algorithms has the ability to improve both the steady-state and dynamic performance of tracking the MPP and thereby increasing the total efficiency of the PV system. The second part the PV system is also simulated in MATLAB, but by using fuzzy logic control (FLC) and compared to the conventional (P&O) algorithm with DC-DC boost converter to demonstrate the feasibility and performance of the proposed controller based on MPPT of PV system.

In the last step of simulation evaluation, the performance of the three proposed IPSO, P&O and IC MPPT methods were compared under rabidly changing irradiation levels. The results validate that the all of three proposed MPPT techniques can significantly increase the efficiency and the performance of the PV system. The highest system efficiency was shown to be achieved by the IPSO, followed by the P&O, and then the IC method with values of 99.97%, 99.94% and 99.88%, respectively. As comparison figures were presented with a table summarising the performance of the proposed MPPT techniques and the efficiency improvement of the PV system gained by each technique.

6.2 Contributions

The major contributions of this thesis are:

1) this thesis proposes a method for selecting the parameters of the main components of an autonomous photovoltaic (PV) stations to ensure the most efficient conversion and use of solar energy, by create an original method and algorithm for calculating and selecting parameters of the main elements of a PV stations. The optimal value of the sampling time of the MPP controller is obtained for different schemes of the PV system.
2) the proposed novel improved particle swarm optimization (IPSO)MPPT method. The measured voltage and current are provided to the PV panels and the proposed model calculates the maximum power. The value of d is updated by Δd with the speed of the particle after a certain sampling time ts, and the PV system output power is considered to be the fitness function PPV. In this study, the technique that was named by constriction factor based PSO (CFPSO), the convergence of the algorithm is ensured by using a special constriction coefficient CF, the numerical values of which are demonstrated by the following equation:

$$CF = \frac{2}{\left|2-\varphi-\sqrt{\varphi^2-4\cdot\varphi}\right|}, \text{ where } \quad \varphi=c_1+c_2, \ \varphi>4$$

The application of CFPSO algorithm guarantees the convergence of the algorithm for any values of c1 and c2, which greatly simplifies the task of determining their optimal values. The results of [6] confirms the possibility of using CFPSO for extracting the MPP of the PV system. Furthermore, preliminary studies have shown that the highest efficiency of the CFPSO algorithm in tracking the MPP is observed at the following numerical values c1=c2=2.5, which corresponds to CF = 0.382. The principle operation of IPSO is shown in figure 3.28.

6.2 Future work

In the current PV system, the buck converter is used as an interface to enable the MPPT process. Future research could investigate some other converters such as boost, cuk and buck-boost along with the proposed MPPT techniques to improve flexibility in the choice and configuration of PV array connection.

In this work, The main energy characteristics are analyzed and the mathematical models of the components of an autonomous PV system are developed to study the modes of tracking the maximum power point (MPP). simulation models were developed and used to compare the performance of the proposed MPPT techniques. However, practical hardware tests at a representative power level and under the typical climatic conditions of an application need to be conducted to verify the simulation results. The simulation results achieved in this work will hopefully incentivise future investigations involving building prototype models to test experimentally the developed MPPT techniques for the PV system.

Implementation in Arduino of MPPT Using the proposed novel improved particle swarm optimization (IPSO) Algorithm and conventional methods P&O, IC in an autonomous PV system.